Exploring the regulation and function of the human guanine nucleotide exchange factor Ect2 (epithelial cell transforming protein 2) in cytokinesis

Dissertation
der Fakultät für Biologie
der Ludwig-Maximilians-Universität
München

Vorgelegt von
Ravindra B. Chalamalasetty

Martinsried / München 2006

Dissertation eingereicht am 02, February, 2006
Tag der mündlichen Prüfung : 08, March, 2006

Erstgutachter: Prof. Dr. Erich A. Nigg
Zweitgutachter: Prof.Dr. Stefan Jentsch

Hiermit erkläre ich, dass ich die vorliegende Dissertation selbständig und ohne unerlaubte Hilfe angefertigt habe. Sämtliche Experimente sind von mir selbst durchgeführt worden, falls nicht explizit auf dritte verwiesen wird. Ich versichere, daß ich weder versucht habe, eine Dissertation oder Teile einer Dissertation an einer anderen Stelle einzureichen, noch eine Doktorprüfung durchzuführen.

München, den 24-01-2006

Table of contents

Acknowledgements

Firstly, I am thankful to Prof. Erich Nigg for giving me the opportunity to work in his department and for reviewing this manuscript. I enjoyed the opportunity of having access to scientific and technical resources within the department and the institute. I thank him for giving me the opportunity to be part of wonderful international scientific atmosphere in the department.

I am also greatly indebted to Dr. Herman Silljé for being my supervisor. His continuous assistance in the form of open discussions, technical advice and brain storming exercises always encouraged me to perform more than I could possibly imagine. His guidance and suggestions are of immense help to me to learn more and carry out my PhD here.

In particular, I would like to express my gratitude to Dr.Francis Barr for stimulating discussions and Dr.Roman Körner and Dr.Marjaana Nousiainen for helping and teaching me to perform MALDI-TOF mass spectrometry.

My special appreciation to Alison Dalfovo for her continuous help in dealing with official documents. I would like to acknowledge Elena Nigg for technical assistance and support throughout my stay here. I would also like to express thanks to all the members of the Department of Cell Biology for their contributions and helping me to find my way and work here (special thanks to Xiumin, Xuiling, Andreas Schmidt, Stefan Huemmer, Christoph Baumann, Thomas Mayer, Claudia Szalma, Marianne Siebert and Klaus Weber for helping me in one way or the other).

In addition, I would like to thank my colleagues, Herman silljé, Robert, Anja Hanisch and Jorge for critically reviewing this manuscript and giving me helpful suggestions and comments. I would like to acknowledge Anna for her advice and helping me with the formatting and organization of my thesis. I would like to thank Eunice for all her help and support in and outside the lab and for being a ‘wonderful friend’ all these years that we spent in this department and I also would like to acknowledge her for discussions on the collaborative projects. I would also like to thank Anja Wehner for friendly atmosphere at our work-bench and for helping me to pick up the stable cell line

clones. I am grateful to all my colleagues for the wonderful time that I spent in and outside the lab. My special thanks to Dr.Anja Schmidt from Prof.Alan Hall's laboratory for helping me with GEF activity assays.

In particular, I would like to thank Martina, Guido and Giulia for their continuous support, suggestions and helping me all throughout my stay here.

I would like to thank my friends Suresh, Sudarshan, Kasturi Prasad and Rajneesh for their continuous support and sharing my experiences. I especially would like to thank Aditya, Naidu, Sridhar and Avinash for all the wonderful time that I had spent with them during the end of my thesis work here in Munich and for all the traditional gourmet Indian food that I miss here.

Finally, I am greatly indebted to my parents and brother, without whose support and help I would not have been able to do my thesis work here.

I dedicate this thesis work to my parents

Summary

Cytokinesis is the process that divides the cytoplasm of a parent cell into two. In animal cells, cytokinesis requires the formation of the central spindle and the contractile ring structures. The onset of cytokinesis is marked during anaphase with the specification of the division site, followed by cleavage furrow formation and ingression, midbody formation and abscission. The astral microtubules that originate from the centrosomes and the anti-parallel microtubules of the central spindle are proposed to determine the site of cleavage furrow formation (Bringmann and Hyman, 2005). The acto-myosin based contractile ring assembles at the division site and constricts the cytoplasm which is supported by the fusion of membrane vesicles to the ingressing plasma membrane. All these processes together result in the formation of two daughter cells.

The small GTPase RhoA is one of the most upstream regulators of contractile ring assembly at the cortex. Rho proteins are activated by GEF's (guanine nucleotide exchange factors) and one GEF that is required for cytokinesis is Ect2 (epithelial cell transforming protein2) (Tatsumoto *et al.*, 1999).

The *Drosophila pebble (pbl)* gene product is the founding member of the Ect2 protein family and has been shown to be required for cytokinesis (Lehner, 1992). In mammals, Ect2 was originally identified as a transforming protein in an expression cloning assay (Miki *et al.*, 1993) and subsequently shown to be essential for cytokinesis. In this study, we have explored the temporal and spatial mechanisms that regulate Ect2 function. In agreement with previous studies, we show that Ect2 is a cell cycle regulated protein and is phosphorylated during mitosis. We identify a number of potentially interesting endogenous phosphorylation sites in Ect2, including potential Plk1 and Cdk1 sites. Although we have not been able to determine the function of these phosphorylation sites, their strong conservation among different species implies that they accomplish evolutionarily conserved roles.The identification of these phosphorylation sites sets the stage for future functional analyses.

In complementary studies, we have shown that the central spindle and cell cortex localizations of Ect2 are facilitated by the BRCT and PH domains, respectively. The

targeting of Ect2 to the central spindle is mediated by the MKlp1/MgcRacGAP and MKlp2/Aurora-B complexes. Of the two complexes, we show that Ect2 interacts and colocalizes only with the MKlp1/MgcRacGAP complex in telophase and propose that this interaction is mediated by a phosphorylation dependent docking mechanism that targets Ect2 to the central spindle. Interestingly, the displacement of Ect2 from the central spindle did not prevent cytokinesis, suggesting that localized GEF activity is not absolutely essential for cleavage furrow ingression and cytokinesis.

In the second part of this thesis, we have explored the role of Ect2 during cytokinesis and show that, in Ect2 depleted cells, levels of RhoA and Citron kinase are diminished at the cleavage site, concomitant with the impairment of cleavage furrow formation and ingression. Additionally, overexpression of appropriate amino-terminal Ect2 fragments in cells also hinders cytokinesis. In these cells, RhoA and Citron kinase localize to the cortex and cleavage furrow ingression occurs, but, the subsequent abscission fails. Taken together, these results suggest that proper function of Ect2 is not only important for cleavage furrow ingression, but also for cell abscission. Finally, we investigate the overexpression phenotypes of different Ect2 truncation mutants. We show that abscission failure correlates with the persistence of amino-terminal Ect2 fragments at striking ring-like structures surrounding the midbody, indicating that completion of cell division requires the displacement of Ect2 from the contractile ring and its re-import into the reforming cell nucleus. Collectively, our data indicate that multiple mechanisms cooperate to regulate Ect2 in a spatial-temporal manner.

1.0 Introduction

1.1 Overview of the cell cycle

The 'cell theory' states that all organisms are composed of similar units of organization, called cells. This was formally articulated in 1839 by Schleiden and Schwann and has ever since remained as the foundation of modern cell biology. The correct interpretation for the formation of cells was first phrased by Rudolph Virchow in the form of a powerful dictum, 'Omnis cellula e cellula', which means that each cell can only arise from a pre-existing cell (Virchow, 1854). Cells are generated by means of cell division and, whereas in bacteria and yeast a single round of cell division is enough to give rise to a new complete organism, in higher eukaryotes more complex rounds of cell division occur for various purposes such as replenishing old cells, growth of an organism or wound healing. The detailed mechanisms of cell division vary from organism to organism, but the most fundamental and conserved aspect of cell division is to pass on the genetic information to the newly formed daughter cell. In order to accomplish this, the genetic material of the existing cell is first duplicated and then equally segregated between the two daughter cells during the process of division so that each cell retains a single copy of the genetic material.

The eukaryotic cell cycle is divided into four phases: G1 (*Gap phase1*), S (*Synthesis phase*), G2 (*Gap phase2*) and M (*Mitosis and cytokinesis*) phase (Fig. 1). DNA synthesis occurs in S phase, which lasts about half of the time of the mammalian cell cycle. In M phase, a series of events take place beginning with nuclear envelope breakdown, chromosome condensation, chromosome alignment, sister chromatid segregation and reformation of the new nuclei in the daughter cells. Apart from DNA synthesis and chromosome segregation, the cell has to increase its mass and double its organelles. This occurs primarily during G1 phase (between M phase and S phase) and G2 phase (between S phase and M phase). The length of G1 phase varies depending on external conditions and signals from other cells. For example, if the conditions are

unfavourable for continued proliferation, cells delay progression through G1 phase and may even enter into a resting phase termed G0. However, if the conditions are favourable, cells complete G1 phase passing through a point called *start* in yeast or *restriction point* in mammalian cells after which cells are committed to S phase.

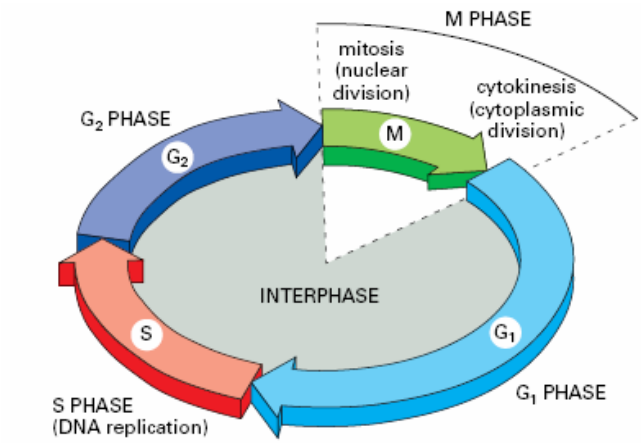

Figure 1. Schematic illustration of different phases of the cell cycle. Interphase is divided into G_1, S and G_2 phases. M phase is further divided into mitosis (nuclear division) and cytokinesis (cytoplasmic division). Image adapted from Alberts et al*, Molecular Biology of the Cell, fourth edition, 2002.*

1.1.1 An overview of mitosis

M phase is the most remarkable event of the cell cycle. Although it lasts only about 1 hour in human somatic cells, essential steps of the cell cycle like equal segregation of genetic and cytoplasmic material occur during this phase. All important steps of mitosis were already described more than 100 years ago by the German anatomist, Walther Flemming (Flemming, 1882)(more reading in (Paweletz, 2001)). In brief, mitosis is divided into prophase, prometaphase, metaphase, anaphase and telophase (Fig. 2). During prophase, the interphase chromatin compresses to form condensed chromosomes. The previously duplicated centrosomes, the major microtubule-organizing centres (MTOC) in animal cells, increase the nucleation of highly dynamic MTs (microtubules) resulting in spindle aster formation (Doxsey, 2001; Meraldi and Nigg, 2002; Paoletti and Bornens, 1997). During prometaphase, MTs are captured by dense proteinaceous material called

kinetochores situated on the centromeres of the mitotic chromosomes. The capture of MTs emanating from opposite poles to sister chromatids is essential for the congression of chromosomes to an equatorial plane termed the metaphase plate. This results in the formation of the characteristic bipolar mitotic spindle. A surveillance mechanism, the spindle checkpoint, ensures that chromosome segregation can only occur when all chromosomes have attached to MTs in a bipolar manner (Rieder *et al.*, 1995; Rudner and Murray, 1996; Wells, 1996). Sister chromatids are held together by a protein complex consisting of cohesin proteins (Hagstrom and Meyer, 2003). Sudden loss of cohesin between sister chromatids marks the onset of anaphase-A, during which sister chromatids are pulled towards the poles by shortening of kinetochore MTs (Hauf *et al.*, 2001; Page and Hieter, 1999). Then, the poles move towards the cell cortex during anaphase-B assisting further sister chromatid separation. During anaphase, the mitotic spindle is transformed into a centrally located structure consisting of non-kinetochore, anti-parallel MTs called the central spindle (Burgess and Chang, 2005; Glotzer, 2001). During telophase and cytokinesis, chromatin de-condensation begins and the nuclear envelope reforms.

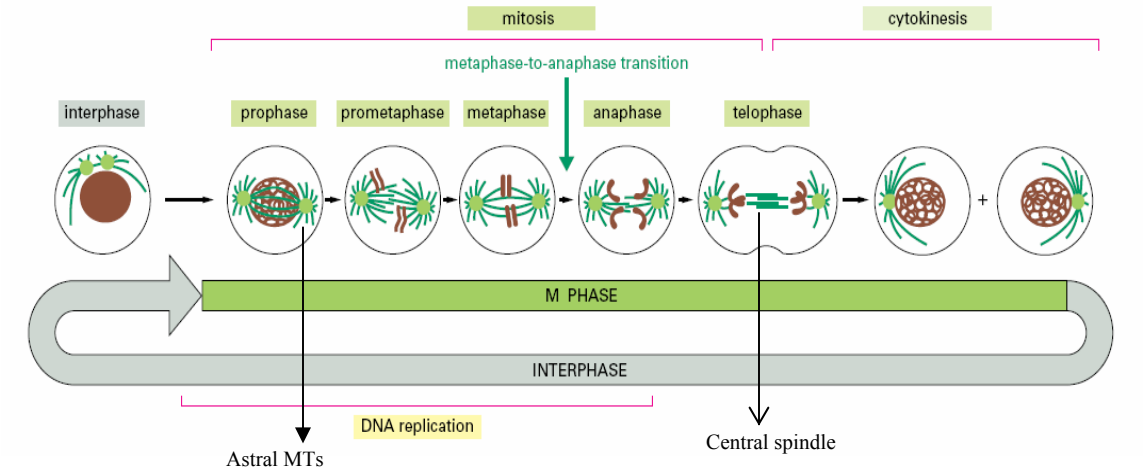

Figure 2. M phase progression in animal somatic cells.
Schematic representation of different stages of mitosis and cytokinesis. Mitosis is broadly divided into prophase, prometaphase, metaphase, anaphase and telophase. Cytokinesis is intimately linked to mitosis. The colours shown here are brown for DNA, light green for centrosomes and dark green for MTs. Image adapted from Alberts et al*, Molecular Biology of the Cell, fourth edition, 2002.*

1.1.2 An overview of cytokinesis

Cytokinesis is the process of partitioning cellular contents such as chromosomes, cytoplasm and organelles into two daughter cells (Fig. 2). Cytokinesis is intimately linked to mitosis. Cytokinesis begins at the onset of anaphase-A with the specification of the cleavage site. The mitotic spindle plays a key role in determining the site of cleavage furrow formation which generally occurs equatorially in animal cells. The cleavage furrow contains actin, myosin and other proteins that are organized into a contractile ring-like structure called the actomyosin ring. Upon ingression, the cleavage furrow constricts the components of the central spindle into a focussed structure called the midbody. In the final cytokinetic event called abscission, the furrow seals generating two separated cells. A more detailed discussion of cytokinesis follows in the next chapter.

1.1.3 Regulation of M phase progression

Progression through different mitotic stages is predominantly regulated by two post-translational mechanisms: protein phosphorylation and proteolysis. These two mechanisms are interdependent as the proteolytic machinery is controlled by phosphorylation and many mitotic kinases are downregulated by degradation (Nigg, 2001).

Out of a handful of known mitotic kinases, Cdk1 (Cyclin dependent kinase1) is considered as the master kinase involved in the regulation of mitotic progression (Morgan, 1997; Murray, 2004; Nigg, 1995). In general, the Cdks (Cyclin dependent kinases) are a family of heterodimeric serine/threonine protein kinases each consisting of a catalytic Cdk subunit and an activating cyclin subunit (Hunt, 1991; Nigg, 1995; Pines, 1993a). The levels of cyclin subunits are extensively controlled by regulated proteolysis (Evans *et al.*, 1983). The destruction of mitotic cyclins is important for the onset of telophase, as well as for the preparation for the next cell cycle (King *et al.*, 1996). Moreover, each Cdk catalytic subunit binds to only a subset of cyclins facilitating the controlled and cyclin regulated progression of the cell cycle. For example, Cdk2 interacts

with cyclin E at the beginning of S phase to induce the initiation of DNA synthesis, and then binds cyclin A throughout S phase (Morgan, 1997). Cdk1 interacts with cyclin A and contributes to the preparation for mitosis (Edgar and Lehner, 1996; Nigg, 1995), and then with cyclin B to form the Cdk1-cyclin B complex for the initiation of mitosis (Pines, 1993b).

Cdks are regulated by several processes. When first synthesized, the catalytic Cdk1 subunit has no detectable activity. Furthermore, the Cdk1/cyclin A/B complex is only partially active because the Cdk1 subunit is subject to negative regulation by phosphorylation on two inhibitory residues in the ATP-binding site (threonine 14 and tyrosine 15) due to the activity of the kinases Wee1 and Myt1, respectively (Endicott *et al.*, 1994). Inactivation of the Cdk1/cyclin B complex by phosphorylation on tyrosine 15 is important for the control of initiation of mitosis (Gould and Nurse, 1989). The Cdk1-cyclin A/B complex is activated by the dephosphorylation of these two residues by the dual-specificity phosphatase Cdc25C (Coleman and Dunphy, 1994). Moreover, complete activation of the Cdk1 kinase is accomplished by phosphorylation of threonine 161on the T-loop of Cdk1 (Nigg, 1996) by the Cdk-activating kinase (CAK) (Harper and Adams, 2001). This results in additional conformational change of Cdk1 to open the catalytic center for substrates (Russo *et al.*, 1996). Once activated, the Cdk1-cyclin A/B complex phosphorylates numerous substrates, such as nuclear lamins for nuclear envelope breakdown (Nigg, 1995), microtubule-binding proteins for spindle assembly (Andersen, 1999), Golgi matrix proteins for Golgi fragmentation (Lowe *et al.*, 1998)and condensins for chromosome condensation (Kimura *et al.*, 1998). Furthermore, the activity of the Cdk1-cyclin A/B complexes is tightly regulated by the anaphase-promoting complex/cyclosome (APC/C), a core component of the mitotic ubiquitin-dependent proteolytic machinery (Peters, 2002). The timely degradation of cyclin B by APC/C results in the inactivation of Cdk1, and consequently Cdk1 substrates are dephosphorylated by counteracting phosphatases. Then cells exit mitosis with the decondensation of chromosomes and reformation of the nuclear envelope.

Another mitotic kinase termed polo-like kinase1 (Plk1) is named after the *Drosophila polo* gene. The Plk family of protein kinases is conserved in all eukaryotes and bear a catalytic domain at the amino-terminus and a conserved motif, called the polo-

box domain (PBD), in the carboxyl-terminal region (Nigg, 2001). The PBD has been shown to constitute a phosphopeptide binding domain and to interact with a number of proteins only after these have been phosphorylated on specific sites (Elia *et al.*, 2003). The PBD targets Plk1 to several mitotic structures including spindle poles, kinetochores, and to the central spindle structures, the midzone and the midbody (Hanisch *et al.*, 2005; Seong *et al.*, 2002). Plk1 is a critical cell cycle regulator and its depletion in human cells results in a prometaphase-like arrest (van Vugt *et al.*, 2004). Plk1 is required for centrosome maturation, bipolar spindle formation and chromosome congression (Hanisch *et al.*, 2005; Lane and Nigg, 1996). Evidence for the requirement of Plk1 in cytokinesis comes from studies in *Drosophila* (Carmena *et al.*, 1998) and yeast (Ohkura *et al.*, 1995; Song and Lee, 2001). In *Drosophila*, polo1 allele mutants are viable although the spermatocytes of these mutants have cytokinesis defects.

Aurora kinases were first identified in *Drosophila,* in a screen for genes that regulate the structure and function of the mitotic spindle (Fig.3). Of these, Aurora-A was found to be associated predominantly with the centrosomes from prophase to telophase (Berdnik and Knoblich, 2002). It has been shown that the activity of Aurora-A correlates with the maturation of mitotic centrosomes. The foremost function of Aurora-A is to assist in the maturation of duplicated centrosomes by recruiting proteins such as γ-tubulin (Berdnik and Knoblich, 2002), D-TACC *(Drosophila*-Transforming, Acidic, Coiled Coil containing protein*)* (Giet *et al.*, 2002)*,* SPD-2 (Kemp *et al.*, 2004), centrosomin (Hannak *et al.*, 2001; Terada *et al.*, 2003) and chTOG (colonic and hepatic tumour overexpressed protein) and, consequently, to participate in spindle assembly and stability.

Another Aurora family member, Aurora-B, localizes to kinetochores from prophase to metaphase, and to the central spindle and midbody in anaphase and telophase (Carmena and Earnshaw, 2003), and is therefore called a chromosomal passenger protein (Adams *et al.*, 2000; Kaitna *et al.*, 2000) (Fig.3). In mammalian cells, Aurora-B is part of a larger complex comprising INCENP, survivin and Borealin (Gassmann *et al.*, 2004; Sampath *et al.*, 2004). INCENP is a substrate of Aurora-B and binding of Aurora-B to INCENP activates the Aurora-B kinase activity (Bishop and Schumacher, 2002; Honda *et al.*, 2003; Yasui *et al.*, 2004). Aurora-B is required for spindle checkpoint signaling as depletion of Aurora-B or inhibition of Aurora-B results in the inhibition of spindle-

checkpoint function (Giet and Glover, 2001). Moreover, the Aurora-B kinase is required for central spindle formation and cytokinesis (Giet and Glover, 2001). A number of substrates of Aurora-B have been discovered including CENP-A required for chromosome condensation (Zeitlin *et al.*, 2001), MCAK (mitotic centromere associated kinesin) required for correcting the improper attachment of MTs to kinetochores (Andrews *et al.*, 2004; Lan *et al.*, 2004), MgcRacGAP, a GTPase activating protein required for cytokinesis (Hirose *et al.*, 2001; Minoshima *et al.*, 2003) and MKlp1 (mitotic kinesin-like protein) which is also required for cytokinesis (Guse *et al.*, 2005). These data demonstrate that Aurora kinases have multiple roles during mitosis.

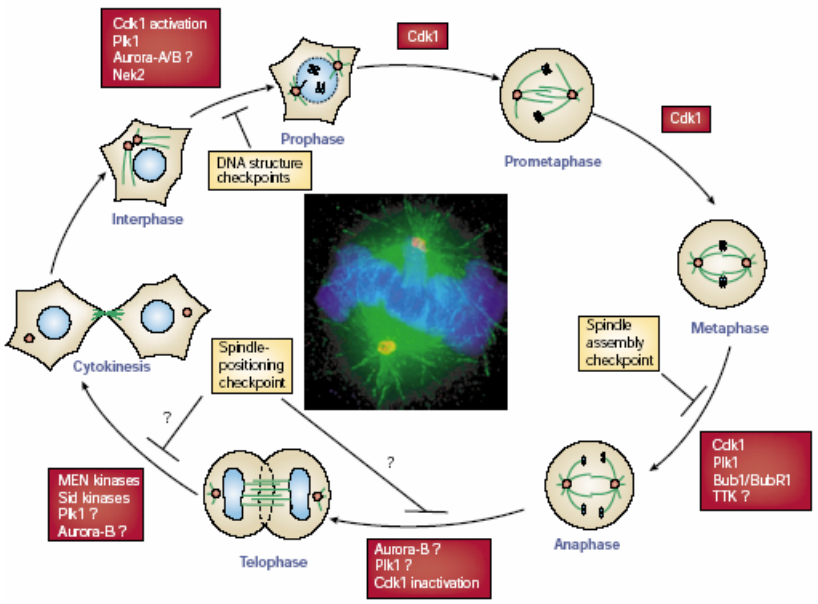

Figure 3. Role of mitotic kinases at different stages of mitosis. Image adapted from Nigg, Nature Reviews, Molecular Cell Biology, Volume 2, January, 2001.

1.2 Cytokinesis

1.2.1 Cytokinesis in yeasts and plants

Although the basic concepts of cell division are conserved among eukaryotes, the exact processes involved in cytokinesis vary in different organisms (Balasubramanian *et al.*, 2004). This is partially due to the different structural organization of cells from different organisms, like animals, plants and yeasts. Yeast genetics have been a powerful tool to investigate cell division, and the observations made in yeast and plants will be briefly discussed before elaborating animal cytokinesis in more detail.

In the budding yeast, *Saccharomyces cerevisiae,* the division plane is determined in late G1 and reflects the position of the previous division site (bud scar) (Fig. 4A). Whereas haploid cells undergo axial budding in which the bud forms adjacent to the previous bud, in diploid cells a bipolar budding pattern can be observed in which the new bud forms opposite to the previous bud. These two different ways of division site determination are thought to be mediated by axial-specific (Bud3p, Bud4p, Axl1p) and bipolar-specific (Bud8p, Bud9p) cortical landmarks (Casamayor and Snyder, 2002; Chant, 1999; Lord *et al.*, 2002). These landmark proteins interact with the Rsr1p GTPase module which controls polarized growth and organizes the actin cytoskeleton and septin ring at the bud neck. Septins are a family of GTP binding proteins that can assemble into filamentous structures and form a ring-like structure at the budneck. Septins are conserved from yeast to human, but are absent in plants (Gladfelter *et al.*, 2001; Longtine and Bi, 2003; Trimble, 1999). In budding yeast, septins are essential for cytokinesis and are involved in bud-site selection (Casamayor and Snyder, 2002; Chant, 1999; Harkins *et al.*, 2001). Surprisingly, however, the actomyosin ring is not absolutely essential for cytokinesis in budding yeast, in clear contrast to animal cells (Sanders and Field, 1994).

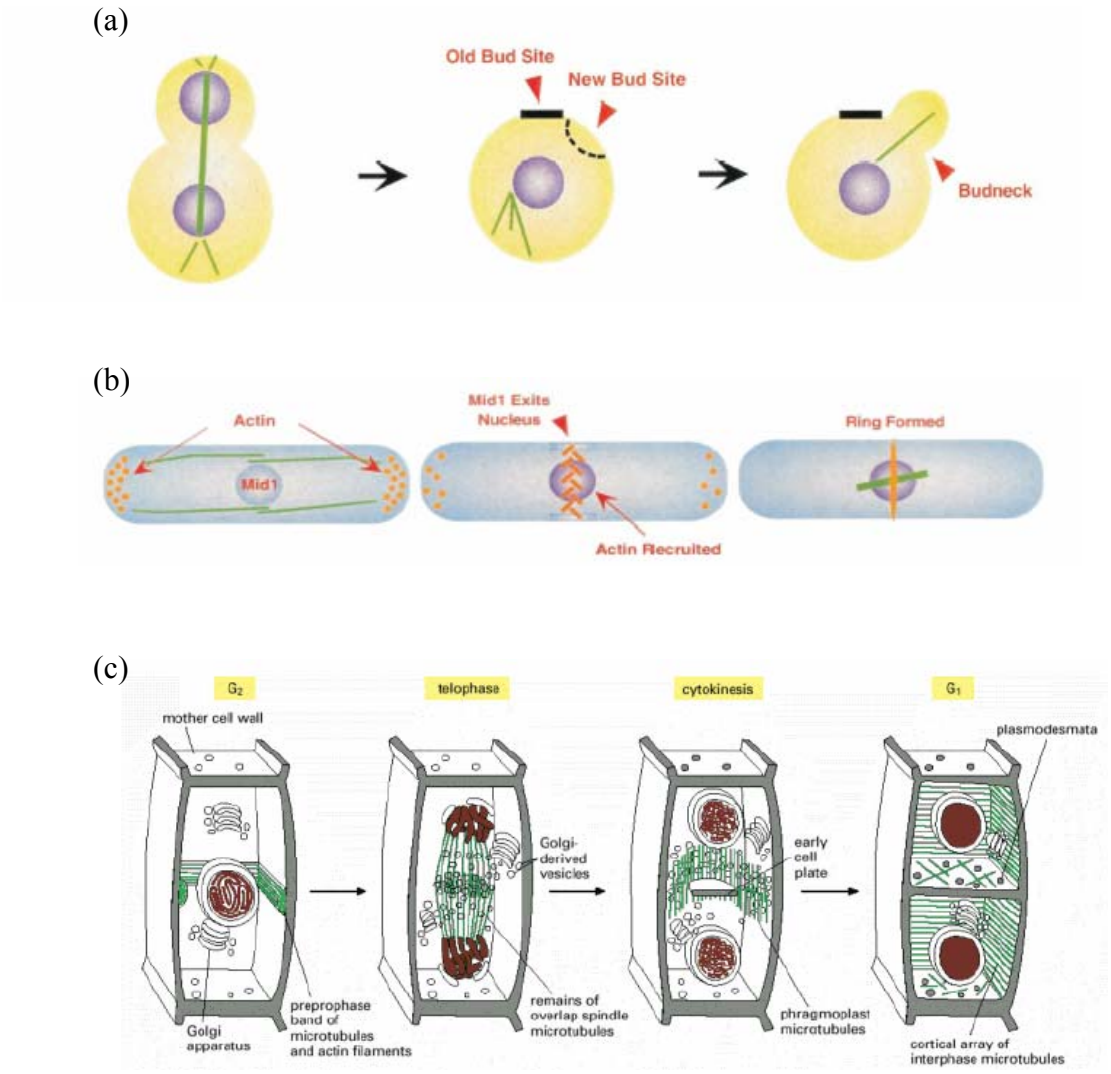

Figure 4. Cytokinesis in yeast and plants.

(a) In budding yeast, the previous bud site is marked on the mother cell cortex by a bud scar. Near the bud scar, a ring containing septins is formed, which marks the site of the new bud. Polarized growth causes the new bud to grow outwards from the mother cell cortex. Image adapted from Guertin et al*, Microbiology and Molecular Biology Reviews, June 2002, p155-178.*

(b) In fission yeast, the position of the nucleus determines the division site. Mid1p is initially in the nucleus in interphase. Before division, it exits the nucleus and marks the division site by associating with the cortex adjacent to the nucleus. Then, actin polymers are recruited to the division site. Image adapted from Guertin et al*, Microbiology and Molecular Biology Reviews, June 2002, p155-178.*

(c) In higher plants, a phragmoplast is formed at the shortest nucleus-cortex distance, which then positions the medial ring like structure called preprophase band (PPB). This marks the division site in plants. Image adapted from Alberts et al*, Molecular Biology of the Cell, fourth edition, 2002.*

Whereas *S. cerevisiae* divides by budding, the fission yeast *Schizosaccharomyces pombe* divides by septum formation (Fig. 4B). In *S. pombe,* the division site is determined in G2 phase and reflects the position of the interphase nucleus. Cells with disrupted MTs have problems in the medial placement of the division plane, however the role of MTs in this process might be indirect as their primary function is to place the nucleus. Moreover, mutants that are defective in spindle assembly have minor defects in contractile ring assembly and its placement (Chang *et al.*, 1996). Recent micromanipulation experiments to physically manipulate the nucleus by cell centrifugation (Daga and Chang, 2005) showed that the nucleus actively induces formation of the contractile ring during metaphase which is much earlier than in animal cells. Although it is not exactly clear how the nucleus positions the contractile ring, one candidate protein that is thought to appear first at the cleavage site is Mid1p (Bahler *et al.*, 1998; Sohrmann *et al.*, 1996). Mid1p is predominantly localized in the nucleus of interphase cells, but upon entry into mitosis it relocates to the cytoplasm in a reaction dependent on *Plo1p* (*S. pombe* polo-like kinase) which is the upstream component of the so called septation initiation network (SIN). In addition to Mid1p regulation, *plo1p* also has additional functions for actomyosin ring placement since Mid1p derivatives lacking a nuclear localization signal are unable to rescue the ring-positioning defect of plo1-1 mutants (Paoletti and Chang, 2000). Cytoplasmic Mid1p forms a ring at the cortex around the equator of the cell division site. Moreover, Anillin, a mammalian orthologue of Mid1p also has properties of a ring organizer, but does not seem to be vital for cleavage furrow formation in animal cells (Oegema *et al.*, 2000). Mid1p physically interacts with type II myosin heavy chain, Myo2p, and promotes the medial accumulation of actomyosin ring components including Myo2p, Rng2p (IQGAP), Cdc15p (PCH) and Cdc12 (formin), independently of actin (Balasubramanian *et al.*, 1998; Kitayama *et al.*, 1997; Motegi *et al.*, 2004; Mulvihill *et al.*, 2000; Rajagopalan *et al.*, 2003). Subsequently, actin, Cdc8p (tropomyosin) and Ain1p (α-actinin) are recruited, leading to the formation of the contractile ring (Wu *et al.*, 2003). Septins do not seem to be important for contractile ring formation in *S. pombe* and only appear later in anaphase (Glotzer, 2001). This contractile ring finally constricts the plasma membrane and at the same time cell wall material is produced to form a septum across the division site.

One major difference between both types of yeast and animal cells is that the nuclear envelope of yeast does not breakdown during mitosis. As a result, the anti-parallel MTs that are present in animal cells in the form of the central spindle (described later) are compartmentalized away from the cortex by the nuclear envelope in yeast. Therefore it might not be surprising that, in contrast to animal cells, these anti-parallel MTs are not important for cytokinesis in yeasts.

Cytokinesis in plants is different from yeast and animal cells. Unlike these organisms which divide the cytoplasm from "outside in", the cytoplasm in plant cells is partitioned from "inside out" by the formation of a new cell wall, called the cell plate, between the daughter cells (Jurgens, 2005; Tabata, 2000) (Fig. 4C). In plant cells, at some point in G2, the cortical MTs and the actin filaments rearrange to form a band, termed preprophase band that encircles the cell, just below the plasma membrane. The preprophase band determines where the new cell plate will join the mother cell wall when the cell divides. During telophase and cytokinesis, the phragmoplast is formed by the overlap of spindle MTs (Lloyd and Hussey, 2001). Golgi-derived vesicles carrying the cell-wall precursors associate with these MTs, accumulate in the equatorial region, and fuse to form the early cell plate (Otegui *et al.*, 2001; Segui-Simarro *et al.*, 2004; Steinborn *et al.*, 2002). Subsequently, new Golgi-derived vesicles are recruited to this region further extending the cell plate outwards and completeing the new cell wall.

1.3 Cytokinesis in mammalian cells

1.3.1 Division site determination in mammalian cells

In animal cells, the cell division site is determined during the transition from metaphase to anaphase. Early studies using either MT inhibitors or cold treatment to depolymerize MTs established that proper positioning of the cleavage furrow requires MTs (Burgess, 1977). Naturally, asymmetrical placement of the mitotic apparatus leads to cell cleavage in the vicinity of the mitotic spindle as observed in *Caenorhabditis elegans*, amphibian zygotes, sea urchin embryos (during formation of micromeres) and oocytes (during formation of polar body and polar lobe) (Burgess, 1977; Conrad and Williams, 1974; Sawai and Yomota, 1990; Schroeder, 1987). Together with a large number of other experiments, it is now well established that the position of the cytokinesis furrow is specified by the position of the mitotic spindle in animal cells. This determnation of the cell division site by the mitotic spindle provides an elegant way to spatially and temporally coordinate cell division with chromosome segregation.

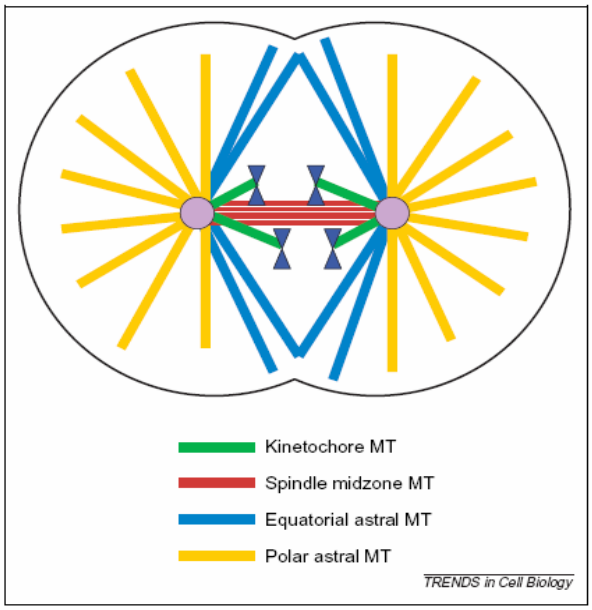

Figure 5. MTs of the mitotic apparatus. MTs here are named after their geometrical relationships rather than their biochemical properties. Image adapted from Burgess et al*, Trends in Cell Biology, vol.15, No.5, March 2005.*

The anaphase mitotic spindle is comprised of different MTs, but which MTs determine the place of cell division still remains unclear. Based on their geometrical placement, rather than their biochemical properties, the following nomenclature has been proposed for these MTs (Burgess and Chang, 2005) (see Fig. 5); kinetochore MTs emanate from centrosomes and attach to the kinetochores at the chromosomes, spindle midzone MTs are anti-parallel MTs that are not associated with kinetochores and are situated between the segregating chromosomes. Furthermore, there are two types of astral MTs, depending on their proximity to the cleavage furrow. Equatorial astral MTs emanate from the centrosomes towards the future cleavage furrow whereas polar astral MTs emanate from centrosomes towards the polar cell surface and away from the equatorial cortex (Fig. 5).

1.3.2 Models for the roles of MTs in cleavage furrow formation

A large number of studies have been conducted to reveal which MTs are important for cleavage furrow formation. Based on these studies, at least three (partly contradicting) models have been suggested (Fig. 6). According to the equatorial stimulation model, equatorial astral MTs determine the site of cleavage furrow formation (Fig. 6). This model was first proposed by Rappaport and co-workers and is based on easily manipulatable echinoderm eggs. For example, blocks (glass beads or oil droplets) were introduced to prevent putative MT signals from reaching the cortex. Only the blocks between asters and the equatorial region prevented cleavage furrow formation, but the blocks between asters and poles had little effect (Rappaport, 1968; Rappaport, 1982). Furrows were formed at sites that lack chromosomes, spindle midzone MTs and at regions where astral MTs of different poles overlapped. Based on these results it was suggested that determination of the cleavage furrow site is dependent on overlapping astral MTs and independent of central spindle MTs and chromosomes (Fig. 7a-7d).

An alternative view is that MTs themselves are sufficient for cleavage furrow formation. This is based on micromanipulation experiments in grasshopper spermatocytes in which centrosomes and chromosomes were removed (Alsop and Zhang, 2003). In

these cells some MTs formed bundles and some partial furrow ingression was observed, even though no real cleavage furrowing occurs. This rather artificial situation suggested that MTs are important, but did not provide evidence as to which MTs induce cleavage furrowing in an unperturbed situation (Fig. 7e-7h).

More recently, monastrol, an inhibitor of the Eg5 kinesin motor, was used to generate monopolar spindles (Canman *et al.*, 2003) (Fig. 7i-7l). Inhibition of the spindle checkpoint in these cells resulted in the induction of a cleavage furrow distal to the chromosomes where equatorial astral MTs interact with the cell cortex. This experiment suggested that the equatorial astral MTs themselves can provide the signal and that it is not necessary to have astral MTs coming from opposite poles as suggested by Rappaport and co-workers. In addition, the authors showed that the plus ends of these MTs were slightly more stable at the future cleavage site, which indicates that factors at these microtubule plus ends might contribute to the furrowing process (Canman *et al.*, 2003). The exact mechanism, however, remains elusive.

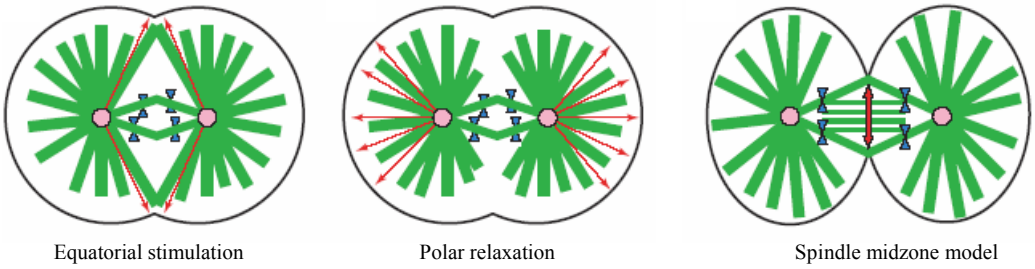

Figure 6. Different models for the roles of MTs in cleavage furrow induction.
Equatorial stimulation model: Here, the overlapping equatorial MTs from opposite poles impart a positive signal (red arrows) for cleavage furrow induction at the equatorial cortex.
Polar relaxation model: The cortical tension of the polar cortical region is relieved by the polar astral MTs (red arrows), resulting in increased tension and cleavage furrow induction at the equatorial cortical region, only.
Spindle midzone model: Proteins associated with the spindle midzone MTs move towards the cell cortex or send signals that induce cleavage furrow formation.
Image adapted and modified from Burgess et al*, Trends in Cell Biology, Vol.15, No.3, March, 2005*

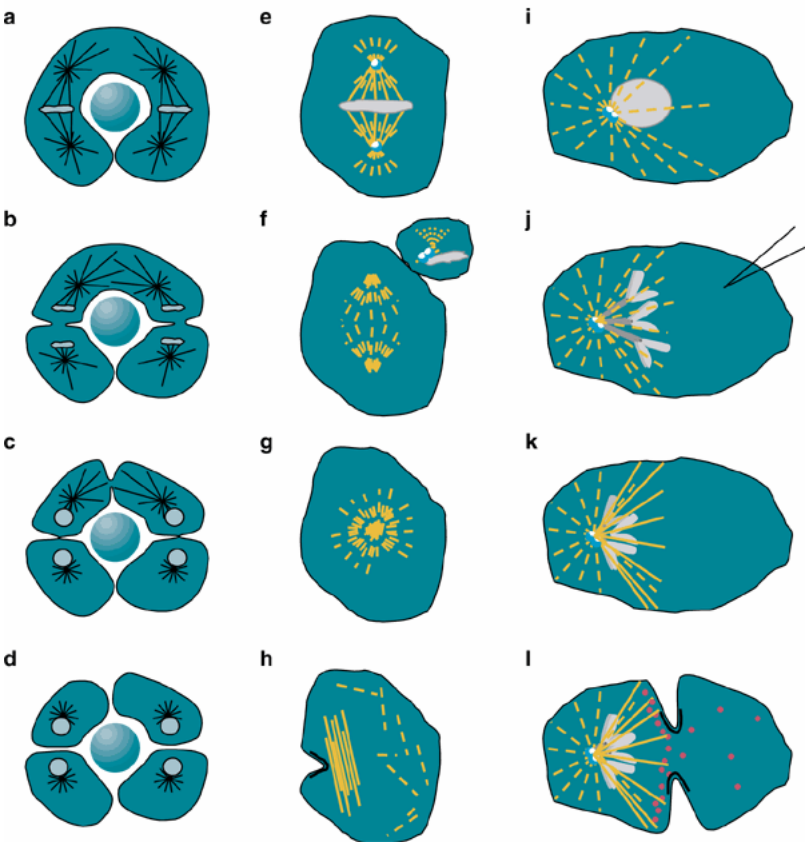

Figure 7. Micromanipulation experiments performed to uncover the structures important for cleavage furrow induction.

Panels a–d show the experiment performed by Rappaport in sand dollar eggs.

A glass bead is pressed through the centre of a sand dollar egg to generate a doughnut-shaped cell. (a) The first cell cleavage generates a horseshoe-shaped cell. Two spindles are present during the second cell division, one in each arm of the horseshoe. (b) During the second cell division, cleavage furrows that bisect each spindle are formed. (c, d) In addition to the cleavage furrows bisecting the two spindles, a third furrow appears between the two aster poles. Image adapted from Maddox et al*, Nature Cell Biology, vol. 5, No.9, September 2003.*

Panels e–h summarize the experiments of Alsop and Zhang in grasshopper spermatocytes.

(e, f) The centrosomes (blue) and chromatin (grey) are removed from a metaphase grasshopper spermatocyte using a micromanipulation needle. (g) The spindle collapses, leaving only dynamic MTs in a disorganized array. (h) After a delay variable duration, some MTs have self-assembled into a bundle. An F-actin-enriched furrow (thickened black line) ingresses in proximity to the centre of this bundle. Image adapted from Maddox et al*, Nature Cell Biology, vol. 5, No.9, September 2003.*

Panels i–l summarize the experiments of Canman and co-workers in Ptk1 cells.
(i) Centrosome separation in a Ptk1 cell is inhibited with monastrol, resulting in a monopolar spindle. (j) The spindle checkpoint is overridden by injection of reagents that inhibit checkpoint components. The cell then enters into anaphase. (k) In anaphase, a sub-population of stable MTs (solid yellow lines) that originate in the vicinity of chromosomes and terminate at the cortex are observed. (l) In telophase, the cell furrows (thickened black lines) where the stable MTs make contact with the cortex. Chromosomal passenger proteins (red dots) are observed in the region of the furrow. Stable MTs are shown as solid lines, whereas more dynamic MTs are indicated with dashed lines. Image adapted from Maddox et al*, Nature Cell Biology, vol. 5, No.9, September 2003.*

Another model, the polar relaxation model, suggests an alternative mechanism, namely that MTs interacting with the cortex inhibit cleavage furrow formation (Fig. 6). This model is based on the observation that equatorial astral MTs in eggs are less dense at the cortex of the future cell division site than polar astral MTs at polar regions (Asnes and Schroeder, 1979; Dechant and Glotzer, 2003; White and Borisy, 1983; Yoshigaki, 2003). This lower MT density at the cell equator is thought to induce a relaxing effect for the invagination of the cleavage furrow.

Currently, one of the most attractive models is the spindle midzone model, which is supported by an increasing amount of genetic evidence, as discussed below (Glotzer, 2001). According to this model, the anti-parallel central spindle MTs are required for cleavage furrow formation (Cao and Wang, 1996; Wheatley and Wang, 1996) (Fig. 6). Disruption of the central spindle by either micromanipulation or genetic approaches cause varying degrees of cytokinesis defects (Bonaccorsi *et al.*, 1998; Cao and Wang, 1996; Dechant and Glotzer, 2003). Moreover, as discussed below, a number of central spindle localized proteins are required for proper cytokinesis. Nevertheless, there is also some evidence that cleavage furrow formation is not entirely dependent on the central spindle. It has been shown that in cells depleted of the central spindle protein PRC1, central spindle formation is severely affected, but cleavage furrowing still occurs (Mollinari *et al.*, 2005). However, it cannot be excluded that some central spindle like MTs are sufficient to induce cleavage furrowing in these cells.

A recent report by Bringmann *et al* (Nature 2005) suggested that the cytokinesis furrow is positioned by two consecutive signals. They examined the relative contributions

of astral and spindle midzone MTs to position the cytokinetic furrow in the *C.elegans* zygote. By using an ultraviolet laser, they ablated one aster and could show that the cytokinesis furrow is first positioned by a signal determined by microtubule asters, and later a second signal is derived from the spindle midzone (Bringmann and Hyman, 2005). Thus, the equatorial stimulation and spindle midzone model seems to co-operate in this system to form a proper cleavage furrow. In eggs unlike mammalian somatic cells, the central spindle is relatively small compared to the whole cell volume and only occupies a small region within the egg. Therefore, in an egg, initial cleavage furrow formation might depend on astral MTs that contact the cell cortex. Once the initial cleavage furrow approaches the neighbourhood of the central spindle, the central spindle dominates further cleavage furrow ingression. Whether this also holds true for mammalian somatic cells is not yet clear. In mammalian somatic cells, as the central spindle is in close proximity of the cell cortex, the initial contribution of astral MTs may not be as dominant as in eggs. All together, these results show that different experiments in diverse cell types, using various techniques, have revealed alternative answers as which MTs are important for cleavage furrow ingression. This is partly owing to the diversity in biology, differences in experimental approaches and multiple or redundant mechanisms.

1.4 Central spindle and contractile ring formation

1.4.1 The central spindle and its components

Cytokinesis is a complex process and involves numerous proteins (Table.1). One of the structures important for cytokinesis is the central spindle which is formed upon the metaphase to anaphase transition. At this point, the chromosomes start to seperate on shrinking kinetochore MTs, and anti-parallel microtubule bundles are formed between the segregating chromosomes. As mentioned above, the central spindle complex is composed of anti-parallel MTs to which a variety of proteins associate that regulate its structure and function. Among these proteins are the kinesin motor proteins, MKlp1 (Kuriyama *et al.*, 2002), MKlp2 (Neef *et al.*, 2003) and Kif4 (Lee and Kim, 2004), the mitotic protein kinases Plk1 and Aurora-B (Barr *et al.*, 2004; Giet *et al.*, 2005), structural proteins like PRC1 (Jiang *et al.*, 1998), a GTPase activating protein termed MgcRacGAP (Hirose *et al.*, 2001) and the guanine nucleotide exchange factor (GEF), Ect2 (Tatsumoto *et al.*, 1999).

PRC1 has been shown to form a complex with Kif4, CENP-E and MKlp1 (Kurasawa *et al.*, 2004). MKlp1 also forms a complex with MgcRacGAP (a complex also termed central spindlin) (Mishima *et al.*, 2002) whereas MKlp2 associates with Plk1 and Aurora-B (Gruneberg *et al.*, 2004; Neef *et al.*, 2003). Depletion of PRC1 by small interfering RNA (siRNA) almost completely abolishes central spindle formation and the depletion of the other subcomplex components also strongly affect central spindle formation resulting in cytokinesis failure (Mollinari *et al.*, 2005). Only mammalian Plk1 was not fully investigated in this regard, since depletion or inactivation of this kinase by antibody microinjection results in a prometaphase like arrest (Lane and Nigg, 1996; van Vugt *et al.*, 2004) and therefore its exact role in later mitotic stages has been difficult to study in mammalian cells. However, over expression studies indicate a role for Plk1 in cytokinesis (Meraldi *et al.*, 2002; Mundt *et al.*, 1997). Moreover, investigations of Plk1 homologues in yeast (Ohkura *et al.*, 1995; Song and Lee, 2001)and *Drosophila* (Carmena *et al.*, 1998) have shown that Plk1 indeed plays an important role in cytokinesis. How these complexes contribute to central spindle formation remains unclear, but at least *in*

vitro these complexes have strong MT bundling activity, suggesting that these complexes can bundle anti-parallel MTs *in vivo*. Interestingly, the formation and microtubule bundling activity of complexes comprising MKlp1 and PRC1 are regulated by reversible phosphorylation (Mishima *et al.*, 2004; Mollinari *et al.*, 2002). Mutations of Cdk1 phosphorylation sites in PRC1 result in premature bundling of spindle MT before the onset of anaphase (Mollinari *et al.*, 2002). Similarly, MKlp1 phosphorylation by Cdk1 prevents the association of MKlp1 with the metaphase spindle and thus inhibits the bundling of MTs nucleated at this stage of the cell cycle (Mishima *et al.*, 2004). Only upon transition from metaphase to anaphase, when Cdk1 activity drops, these proteins are dephosphorylated and therefore able to localize to the central spindle and to function in bundling the anti-parallel MTs of the central spindle. Thus, the formation of the central spindle is intimately linked to Cdk1 inactivation. How MKlp1 and PRC1 central spindle complexes contribute to cytokinesis is not yet clear. On the one hand, the cytokinesis defect may simply be a reflection of their essential role in proper central spindle formation, on the other hand it is also tempting to assume that these proteins could signal to the cell cortex. The latter hypothesis is especially attractive because these central spindle complexes contain signal transduction proteins like the kinases Plk1 and Aurora-B, the GTPase activating protein, MgcRacGAP and the guanine nucleotide exchange factor, Ect2.

1.4.2 Cleavage furrow determination

At the cortex, the small GTPase RhoA seems to be one of the most upstream components required for cleavage furrow positioning, contractile ring formation and contraction (Glotzer, 2001). RhoA exists in two different forms; the GDP bound form of RhoA in an inactive state and the GTP bound form of RhoA in its active form. Binding of GTP to RhoA results in a conformational change of the protein, exposing structural domains required for the interaction with downstream target proteins. RhoA-GTP positively regulates the actin network and appears to carry out three different functions, namely actin polymerization, actomyosin bundle formation and generation of contractility at the

cleavage furrow (Glotzer, 2001). Kishi *et al*, 1993 and Mabuchi *et al*, 1993 provided the first evidence that RhoA is involved in cytokinesis in *Xenopu*s embryos and sand dollar eggs, respectively (Kishi *et al.*, 1993; Mabuchi *et al.*, 1993). Moreover, when cells were either treated with the RhoA specific inhibitor C3 exoenzyme or subjected to RhoA specific siRNA mediated depletion, they became multinucleated (Aktories and Hall, 1989).

More recently, Bement *et al*, used four-dimensional microscopy and a probe recognizing active RhoA, consisting of an EGFP-rhotekin fusion protein (Bement *et al.*, 2005). Rhotekin is a RhoA-GTP target and specifically binds only the active, i.e. GTP-bound form of RhoA (Kimura *et al.*, 2000). Fertilized sea urchin eggs were microinjected with the mRNA encoding this fusion protein and the localization of active RhoA during cell cleavage was indirectly visualized by monitoring the EGFP signal. This revealed that active RhoA concentrated in a precisely defined zone at the cleavage furrow before cytokinesis. To confirm if EGFP-rhotekin labelled specifically active RhoA, fertilized sea urchin eggs were also microinjected with C3 exoenzyme, a specific inhibitor of RhoA in vertebrates and echinoderms. These cells failed to divide and did not show zones of active RhoA. Treatment of sea urchin eggs with cytochalasin dramatically reduced F-actin and furrows failed to develop, nevertheless the active RhoA zone formed at the equator. Thus, RhoA can localize to the site of future cleavage furrow in the absence of actin. However, treatment of sea urchin eggs with nocodazole to depolymerize MTs before furrow formation prevented both RhoA zone formation and furrowing (Bement *et al.*, 2005). Thus, MTs are essential for localizing RhoA and hence for determining the site of cleavage furrow formation. In another experiment, embryos were first treated with cytochalasin to permit anaphase onset and RhoA zone formation followed by treatment with nocodazole. In contrast to embryos treated with cytochalasin alone, which showed zones of active RhoA, in eggs treated subsequently with cytochalasin and nocodazole, RhoA active zones disappeared 5-10 min after nocodazole exposure. Together, these results confirmed the presence of a microtubule-dependent signal for cytokinesis and revealed the important sequence of events for cytokinesis. Firstly, furrowing occurs in the region that coincides with the zone of active RhoA. Secondly, RhoA zone formation precedes furrowing by up to several minutes. Thirdly, active RhoA zone formation occurs

not only during cytokinesis in blastomeres, but also in much smaller epithelial cells of Echinoderm and *Xenopus* blastulae and gastrulae. Fourthly, active RhoA zone forms despite the disruption of actin cytoskeleton. Finally, RhoA zone formation is controlled by MTs (Bement *et al.*, 2005).

1.4.3 The contractile ring and formation of the cleavage furrow

The cleavage furrow is often described as an actin rich "purse string" that draws tight to complete cytokinesis and to separate daughter cells. Early work established that the contractile ring consists of filaments (Schroeder, 1968), which were later identified as being composed of actin (Perry *et al.*, 1971; Schroeder, 1978) and myosin II (Fujiwara and Pollard, 1976). Treatment of cells with actin depolymerizing drugs delays cells in cytokinesis (Bluemink, 1971; Schroeder, 1978) and sliding of the actin filaments was found to be critical for cytokinesis since perturbations of myosin II prevented furrow ingression (Guo and Kemphues, 1996; Mabuchi and Okuno, 1977; Young *et al.*, 1993). Therefore, it has been suggested that the mechanical force required for cleavage furrow ingression is provided by the mechanochemical enzyme myosin II. The force producing ability of myosin II is regulated by phosphorylation, particularly by the phosphorylation of myosin regulatory light chains (MRLC) (Trotter and Adelstein, 1979). It was reported that the activating phosphorylation sites serine 18 and 19 in MRLC are hypophosphorylated during metaphase but becomes rapidly phosphorylated upon mitotic exit (Yamakita *et al.*, 1994). Not surprisingly, therefore, overexpression of non-phosphorylatable mutants of MRLC also causes cytokinesis defects (Komatsu *et al.*, 2000). The above data indicate that assembly and function of the contractile ring requires phosphorylation of MRLC.

The contractile ring protein Anillin has been shown to bind and bundle actin filaments. Anillin is a PH (Plekstrin Homology) domain containing protein that localizes to the cleavage furrow during cytokinesis. Anillin has been shown to be required for cytokinesis as microinjection of anti-Anillin antibodies into cells result in cytokinesis defects (Oegema *et al.*, 2000). Localization of Anillin is dependent on the actin ring as

cells treated with actin depolymerizing drugs, such as latrunculin-A, were devoid of Anillin at the cleavage furrow (Coue *et al.*, 1987). Anillin binds to nonmuscle myosin II and this interaction is regulated by myosin light chain phosphorylation (Straight *et al.*, 2005). Human cells depleted of Anillin fail to properly regulate contraction of myosin II late in cytokinesis and also fail cell abscission (Straight *et al.*, 2005).

The GTPase RhoA is the key regulator of the contractile ring, and active RhoA targets many downstream components during cytokinesis, including Rho kinase (ROCK), Citron kinase, formin homology proteins and a regulatory subunit of the myosin phosphatase. In fibroblasts, activation of RhoA induces the formation of stress fibres which are composed of large actin bundles. The structural similarities between the stress fibres and the cleavage furrow raise the possibility that similar proteins might be involved to induce the formation of these structures (Glotzer, 2001).

Formins are RhoA targets in budding yeast (Evangelista *et al.*, 1997), fission yeast (Chang *et al.*, 1997), *Aspergillus* (Harris *et al.*, 1997) and animal cells (Castrillon and Wasserman, 1994; Swan *et al.*, 1998; Watanabe *et al.*, 1997). These are multidomain proteins that govern dynamic remodelling of the cytoskeleton and can also function as actin nucleators in the formation of new filaments. Formins exert their effects on the actin and microtubule networks during meiosis, mitosis and trafficking (Watanabe and Higashida, 2004). Mutations in the *Drosophila* formin gene *diaphanous* and the nematode formin gene *cyk-1* lead to cytokinesis defects (Castrillon and Wasserman, 1994). Also mammalian mDia1 and mDia2 are essential for cytokinesis, and, moreover, localize to the cleavage furrow (Tominaga *et al.*, 2000; Wasserman, 1998; Watanabe *et al.*, 1997).

RhoA also regulates actin dynamics via ROCK and Citron kinase, which were reported to associate with RhoA during cytokinesis (Kosako *et al.*, 2000; Madaule *et al.*, 1998). ROCK concentrates at the cleavage furrow and phosphorylates myosin light chain *in vitro* (Amano *et al.*, 1996; Kosako *et al.*, 2000). ROCK inhibits myosin phosphatase thereby inhibiting MRLC dephosphorylation (Amano *et al.*, 1996; Kawano *et al.*, 1999). However, an inhibitor of ROCK, Y-27632, blocks neither the initiation nor the completion of cytokinesis in HeLa cells, although it slows down cleavage contraction (Kosako *et al.*, 2000; Madaule *et al.*, 1998). Also, in *Drosophila*, a ROCK mutation does

not seem to affect cytokinesis, in the examined tissues of wings and eyes (Shandala *et al.*, 2004; Winter *et al.*, 2001). Mammalian cells have two isoforms of ROCK, ROCK-I (also called as Rok β) and ROCK-II (also called Rok α and Rho-kinase). Recent studies in mice indicate that knocking out the ROCK-I and ROCK-II genes individually manifests prenatal problems but those mice that survive develop in an apparently normal manner to adulthood and were not reported to show any cytokinesis defects (Shimizu *et al.*, 2005; Thumkeo *et al.*, 2003).

Citron kinase, another target of active RhoA, also phosphorylates MRLC but does not inhibit myosin phosphatase (Yamashiro *et al.*, 2003). Citron kinase was identified in a screen for proteins specifically binding to GTP bound RhoA (Madaule *et al.*, 1998) and inhibition of RhoA by C3 exoenzyme in HeLa cells abolishes the transfer of Citron kinase from the cytoplasm to the cleavage furrow (Eda *et al.*, 2001; Sarkisian *et al.*, 2002). This suggests that RhoA dependent signalling via Citron kinase is required for cytokinesis. In spite of this, it has been reported that Citron kinase knockout mice are viable and showed cytokinesis defects only in specialized cell types, notably proliferating neuronal and spermatogenic precursors (Cunto *et al.*, 2002; Di Cunto *et al.*, 2000). Recently, however, Paolo D'Avino *et al* showed that the Citron kinase homologue of *Drosophila,* called *Sticky*, is present in all post embryonic proliferating tissues (D'Avino *et al.*, 2004). Moreover, mutations in *Sticky* lead to defective formation of the contractile ring (D'Avino *et al.*, 2004). These apparantly contradicting data sets from mouse knockout studies and *Drosophila* mutants leaves open the question of whether Citron kinase is an essential downstream target of RhoA during cytokinesis.

Table 1. Genes that regulate cytokinesis in diverse organisms.

Role in cytokinesis Generic name	*S. cerevisiae*	*S. pombe*	*C. elegans*	*Drosophila*	Humans	Domain function	Selected binding partners
Contractile ring positioning							
Bud proteins	Axl1p, Axl2p, Bud3p, Bud4p, Bud8p, Bud9p, Rsr1p/Bud1p, Bud2p, Bud5p	na/nr	na	na	na	GTPase module	Cdc24p, Cdc42p
Cdc42 GTPase module	Cdc42p, Cdc24p	Cdc42p (nr; cell morphology)	CDC-42 (nr)	Cdc42 (nr)	Cdc42 (nr)	GTPase-signaling	Formin, IQGAP, Rsr1p
Septin	Cdc3p,Cdc10p, Cdc11p,Cdc12p, Shs1p/Sep7p, Spr3p, Spr28p	Spn1-7 (nr; involved in cell separation)	UNC-59, UNC-61	Peanut, Sep1,2,4,5		SEPT1-10	GTPase
Anillin and anillin-related	na	Mid1p, Mid2p	Y49E10.19	Scraps	hAnillin	PH domain	Actin
Contractile ring assembly							
Myosin II heavy chain	Myo1p	Myo2p, Myp2p	NMY-2	Zipper	Myosin II	Myosin ATPase motor protein	Actin, light chains
Myosin essential light chain	Mlc1p	Cdc4p		Mlc-c	Myosin ELC	EF hand	myosin II, IQGAP, myosin V
Myosin regulatory light chain	Mlc2p	Rlc1p	MLC-4	Spaghetti Squash	Myosin RLC	EF hand	myosin II
Actin	Act1p	Act1p	ACT-5 (ACT-1,3)	Actin (multiple genes)	cytoplasmic actin (beta, gamma)	Actin - microfilaments	Actin binding proteins, myosin
Profilin	Pfy1p	Cdc3p	PFN-1	Chickadee	profilin	Actin binding protein	Actin, formin
Formin	Bni1p, Bnr1p	Cdc12p	CYK-1	Diaphanous	Dia1	Formin (FH1, FH2, FH3) - actin nucleation	Rho GTPases, Profilin
ADF/Cofilin	Cof1p (nr)	Cof1p (nr)	UNC-60A	Twinstar	ADF/Cofilin	Actin binding protein	Actin
IQGAP	Iqg1p/Cyk1p	Rng2p					Actin, myosin essential light chain
PCH proteins	Hof1p/Cyk2p	Cdc15p					
RhoA	Rho1p	Rho1p (cell wall assembly)	RhoA	RhoA	RhoA	GTPase-signaling	
Rho GEF	Rom1p, Rom2p	Gef1p, Scd1p	LET-21	Pebble	ECT2	GEF	CYK-4
Rho kinase	na	na	LET-502	DROK	ROCK	Kinase	RhoA
Myosin Phosphatase	na	na	MEL-11	DMYPT	MBS/MYPT	Ankyrin	Myosin, phosphatase PP1 catalytic subunit
Central spindle							
Mitotic kinesin like protein 1	na	na	ZEN-4	Pavarotti	MKLP1	Kinesin	CYK-4, microtubules
CYK-4	na	na	CYK-4	RacGAP50C	CYK-4/ Mgc Kif20a, RacGAP	RhoGAP	ZEN-4/MKLP1
Mitotic kinesin like protein 2	na	na	na	CG12298-PA (nr)	MKLP2, Rab6KifL	Kinesin	Plk1
Mitotic phosphoprotein (MPP1) kinesin	na	nr	na	CG12298-PA (nr)	MPP1		Microtubules
PRC1	Ase1p (nr)	SPAPB1A10.09 (nr)	SPD-1	Fascetto	PRC1	Microtubule binding domain	Microtubules
Membrane insertion							
Syntaxin	Sso1p, Sso2p	psy1 (nr)	SYN-4	Syntaxin1	Syntaxin4, Syntaxin 2, Endobrevin	Syntaxin-vesicle fusion	v-snare
Exocyst complex	Sec3p, Sec5p, Sec6p, Sec8p, Sec10p, Sec15p, Exo70p, Exo80p	Sec6p, Sec8p, Sec10p, Exo70p	nr	nr	nr	Vesicle tethering	Rab GTPases, Rho GTPases
Myosin V	Myo2p, Myo4p	Myo52p	nr	nr	nr	Vesicle and mRNA transport	Actin
Coordination with nuclear division							
MEN/SIN pathway	Tem1p, Lte1p, Bub2p, Bfa1p, Cdc15p, Dbf2p, Dbf20p, Mob1p, Cdc14p, Net1p	Cdc7p, Cdc11p, Cdc14p, Cdc16p, Sid1p, Sid2p, Spg1p, Sid4p, Mob1p, Byr4p, Clp1p/Flp1p	CDC-14	CG7134-PA	Cdc14	GTPase cascade-signaling, kinases, phosphatase	
Regulatory molecules							
Polo kinase	Cdc5p	Plo1p	PLK-1	Polo	Plk1	Kinase	
Aurora B kinase complex	Ipl1p, Sli15p, Bir1p	Ark1p, Cut17p, Pic1p (nr)	AIR-2, ICP-1, BIR-1, CSC-1	Aurora B, Incenp, Deterin	Aurora B, Incenp, Survivin	Kinase	
Cdk1/Cyclin B	Cdc28p/Clb1p, Clb2p, Clb3p, Clb4p	Cdc2p/Cdc13p	CDK-1/CYB-1, CYB-2, CYB-3	Cdk1/CycB1, CycB2, CycB3	Cdk1/ Cyclin B	Kinase	

na: apparently absent in genome; nr: related molecules known, but no known function in cytokinesis.

Table 1. Different genes required for cytokinesis and their homologues in different species. Table adapted from Balasubramanian et al, *Current Biology, Vol.14, September, 2001.*

1.5 Ect2

1.5.1 Ect2, a Rho family GEF required for cytokinesis

As described above, activation of RhoA in a MT dependent manner at the cell cortex is one of the first events that determine cleavage furrow formation and positioning. Activation of Rho proteins is mediated by guanine nucleotide exchange factors (GEFs) and one GEF that has been discovered to be essential for cytokinesis is Ect2. This GEF, which localizes to the central spindle, could therefore be an excellent candidate for signalling from the central spindle to the cell cortex.

The *Drosophila pebble (pbl)* gene product is the founding member of the Ect2 protein family (Lehner, 1992; Prokopenko *et al.*, 1999). In *Drosophila* embryos, the first 13 mitotic cycles occur in a syncytial cytoplasm without cytokinesis. At the onset of anaphase-B in cycle 14, cytokinesis is initiated. *Pbl* mutant embryos proceed through the first 13 syncytial mitoses and cellularize normally during the G2 phase of cell cycle 14. However, these embryos fail to undergo cytokinesis during subsequent cell division cycles (Lehner, 1992). Analysis of wild type embryos with *anti-pbl* antibodies in *Drosophila* at the mitotic cycle 14 revealed that *pbl* was expressed dynamically during mitosis (Prokopenko *et al.*, 1999). *Pbl* protein was first detected in late anaphase of the mitotic cycle 14, when it colocalized with the separating sister chromatids. No *pbl* protein was detected during late prophase, metaphase and early anaphase of the mitotic cycle 14 in *Drosophila* embryos. The highest level of *pbl* protein was detected in telophase nuclei and this staining persisted during interphase of the following cycle. Moreover, at the end of the mitotic cycle 14, *pbl* accumulated at the equator between dividing cells and in the nuclei of the daughter cells. In subsequent divisions, initiation of cytokinesis was marked by the appearance of the cleavage furrow and coincided with the accumulation of *pbl* at the cleavage furrow. Therefore, *pbl* might be required for the initiation of cytokinesis. Most interestingly, *pbl* interacted genetically with *Rho1* (a *Drosophila* orthologue of mammalian RhoA), but not with *Rac1* and *Cdc42*. Furthermore, *pbl* and *Rho1* interaction was observed in a yeast two hybrid assay. Similar to mutations in *pbl*, loss of *Rho1* or expression of a dominant negative form of Rho1 blocked cytokinesis. These results

identify *pebble* as a RhoGEF specifically required for cytokinesis, linked by *Rho1* activity to the reorganization of the actin cytoskeleton at the cleavage furrow (Prokopenko *et al.*, 1999).

Mammalian Ect2, the *Drosophila pebble* homologue, was originally identified as a transforming protein in an expression cloning assay (Miki *et al.*, 1993). The carboxyl-terminal fragment of Ect2 was able to transform mouse fibroblasts. By the use of antibody microinjection experiments and overexpression of an amino-terminal fragment, also a role for mammalian Ect2 in cytokinesis has been established (Tatsumoto *et al.*, 1999). Human Ect2 was shown to catalyze the guanine nucleotide exchange on small GTPases like RhoA, Rac1 and Cdc42, at least *in vitro* (Tatsumoto *et al.*, 1999). Moreover, Ect2 expressed from recombinant baculovirus was able to bind with high specificity to Rho and Rac proteins, but surprisingly not to Cdc42 (Miki *et al.*, 1993). Ect2 is phosphorylated during G2/M phases of the cell cycle and this phosphorylation has been suggested to be required for Ect2's guanine nucleotide exchange activity (Tatsumoto *et al.*, 1999).

1.5.2 Other functions of Ect2

In addition to the established role in cytokinesis, other functions for Ect2 have also been proposed. This includes a role in the regulation of cell polarity. Cell polarity is an important biological phenomenon that governs diverse cell functions, including the localization of embryonic determinants and the establishment of tissue and organ architecture. Although the detailed signalling events are not known, the polarity complex Par-6/Par-3 (partition-defective)/atypical protein kinase C and the Rho family GTPases play a key role in this signalling pathway (Cox *et al.*, 2001; Drubin and Nelson, 1996). It has been shown that Ect2 plays a role in the activation of this polarity complex (Liu *et al.*, 2004). Ect2 interacts with Par-6/Par-3 and PKC-ζ. Co-expression of Ect2 and Par-6 efficiently activates Cdc42 *in vivo*. Moreover, overexpression of Ect2 stimulates PKC-ζ activity, whereas the dominant-negative form of Ect2 inhibits the Par-6 mediated stimulation of PKC-ζ activity. Furthermore, Ect2 can be detected at cell-cell contacts as

well as in the nucleus in MDCK cells and both the expression and localization of Ect2 are regulated by calcium, a critical regulator of cell-cell adhesion. This indicates that Ect2 regulates the activity of the polarity complex Par-6/Par-3/PKC-ζ (Liu *et al.*, 2004).

Also, a role for Ect2 in kinetochore microtubule attachment has been suggested. In the absence of Ect2, cells are delayed in prometaphase and, moreover, show abnormal chromosome segregation and low levels of active GTP bound Cdc42. Furthermore, inhibition or depletion of Cdc42 affects microtubule-kinetochore attachments (Oceguera-Yanez *et al.*, 2005). Cdc42 seems to regulate the formin homology domain protein mDia3, which localizes to kinetochores only in the presence of active GTP bound Cdc42 via interaction with CENP-A (Yasuda *et al.*, 2004). Depletion of mDia3 results in an increase in prometaphase cells, in which many chromosomes fail to attach to kinetochore MTs. Thus, Ect2 has been proposed to regulate mDia3, via Cdc42, which could be important for proper microtubule-kinetochore interactions (Oceguera-Yanez *et al.*, 2005).

Tatsumoto *et al*, 2003 identified XEct2 *(Xenopus* Ect2) and showed that it is required for cytokinesis. Like human Ect2*,* XEct2 is also phosphorylated during mitosis. In *Xenopus* extracts, Ect2 seems to be required for the formation of the metaphase bipolar spindle. When compared to control extracts, which showed bipolar spindles, addition of anti-XEct2 antibodies resulted in the appearance of abnormal spindles including monopolar and multipolar spindles as well as bipolar spindles with misaligned chromosomes. Furthermore, a dominant negative form of Cdc42, but not of RhoA and Rac1 strongly inhibited spindle assembly *in vitro* (Tatsumoto *et al.*, 2003). This indicates that Ect2 and Cdc42 contribute to the formation of spindles atleast in *Xenopus* egg extracts.

1.5.3 Ect2 structure: different domains of Ect2

The carboxyl-terminal domain of Ect2 that results in cellular transformation upon overexpression harbours the GEF (Guanine nucleotide Exchange Factor) domain (Fig.8). This GEF domain is also termed DH domain, which stands for Dbl homology domain (Zheng, 2001). Dbl was the first Rho GEF that was identified as a transforming gene

from diffuse B-cell-lymphomas (hence its name) (Srivastava *et al.*, 1986). Most GEFs have a DH catalytic domain (69 members in humans), but there are also a few bonafide GEFs (e.g. Dock1, Dock2) that have a catalytic domain that is, at least at the primary sequence level, unrelated to DH domains (Cote and Vuori, 2002). The DH domain consists of about 200 residues and family members comprising this domain show catalytic activity to one or more Rho family members. The DH domain is composed of 11 α-helices that are folded into a flattened, elongated α-helix bundle in which two of the three conserved regions, conserved region 1 (CR1) and conserved region 3 (CR3), are exposed near the centre of one surface. CR1 and CR3, together with a part of α-6 and the DH/PH junction site (Plekstrin homology), constitute the Rho GTPase interacting pocket (Liu *et al.*, 1998; Worthylake *et al.*, 2000). In *Drosophila*, mutations within the catalytic DH domain in the most highly conserved region (CR3) inactivate *pbl* function (e.g. the pbl^5 allele that carries the V531D mutation) and abolish *pbl* interaction with Rho1 (Prokopenko *et al.*, 1999). Mutation of this conserved residue also dramatically reduces the catalytic activity in other GEF's (Liu *et al.*, 1998).

In most GEFs, the DH domain is associated with a carboxyl-terminally located Plekstrin homology (PH) domain, and this is also true for Ect2 (Fig. 8). The PH domain which consists of a stretch of 100-120 amino acids was originally identified in Plekstrin from platelets and neutrophils (Tyers *et al.*, 1988). It has now been found in many proteins and constitutes the 11^{th} most common domain in the human genome. PH domains are known for their ability to bind to phosphoinositides, but also functions in protein-protein interactions have been reported (Lemmon, 2004). The PH domain is found in a multitude of intracellullar proteins with widespread functions. Many of the PH domain containing proteins participate in signalling cascades, but there are also other classes of proteins such as cytoskeletal proteins (Spectrin), which carry a PH domain (Hyvonen *et al.*, 1995). The PH domain family is very divergent at the sequence level; the average pair wise identity is below 20%. Although the PH domain is almost invariably present carboxyl-terminal to DH domains, its exact function in these GEFs is still not resolved. Different functions have been proposed, including membrane targeting, protein-protein interactions and allosteric regulation all of which are likely to be GEF specific (Blomberg *et al.*, 1999).

Figure 8. Schematic representation of the primary structure of human Ect2.
Human Ect2 comprises two BRCT (BRCA1 Carboxy-Terminal) repeats (in orange) spanning residues 143-313, a bipartite nuclear localization signal (NLS) between residues 346-374, a Rho GEF domain (in blue) spanning residues 425-605 and a PH (Plekstrin Homology) domain (in brown) spanning residues 636-763.

Whereas the Ect2 catalytic centre is located in the carboxyl-terminus, a supposed regulatory domain is present in its amino-terminus. This domain comprises two tandem BRCT (BRCA carboxyl-terminal) repeats and is, therefore, termed the BRCT domain (Fig. 8) (Callebaut and Mornon, 1997; Koonin *et al.*, 1996). This domain was originally identified in BRCA1 (Breast Cancer gene1), a tumour suppressor gene involved in breast and ovarian tumour formation. BRCA1 is inactivated in more than 50% of the hereditary breast cancers (Easton *et al.*, 1994). The carboxyl-terminal (BRCT domain containing) half of BRCA1 is important for tumour suppression and this region has been proposed to have evolved through an internal duplication. Sequence analysis using hydrophobic cluster analysis revealed the presence of 50 copies of the BRCT domain in 23 different proteins including BRCA1, 53BP1 (p53 Binding Protein), RAD9, XRCC1 (X Ray Repair Cross Complementing), RAD4, Ect2, RAP1 (Repressor Activator Protein), terminal deoxynucleotidyl transferases (TdT) and three eukaryotic ligases. Most of these proteins have been implicated in DNA repair and are associated with cell cycle checkpoint functions (Bork *et al.*, 1997). Although the BRCT domain is located in the carboxyl-terminus of BRCA1, it is not limited to the carboxyl-termini. It can also be found in multiple copies or as a single copy, as in RAP1 and TdT, respectively, suggesting that it could constitute an autonomous folding unit of approximately 90-100 amino acids (Callebaut and Mornon, 1997). In human Ect2, a tandem BRCT repeat is present in the amino-terminal half of the protein.

Signalling through phosphorylation is a central theme in biology. Like the PBD domain (Polo Box binding Domain of Plk1), 14-3-3 proteins and R-Smads (Wu *et al.*, 2001; Yaffe and Elia, 2001; Yaffe and Smerdon, 2001), the BRCT domains have recently been implicated in phosphopeptide binding (Clapperton *et al.*, 2004; Manke *et al.*, 2003; Williams *et al.*, 2004; Yu *et al.*, 2003). The identification of BRCT repeats as general phosphopeptide binding modules nicely complements the need of DNA damage-induced signalling, which relies on specific phosphorylation and recruitment of multiple DNA damage-responsive proteins (Caldecott, 2003). It has been shown that the BRCA1 BRCT repeats recognize proteins that have pSer-X-X-Phe residues where X indicates any residue (Manke *et al.*, 2003). The signalling specificity of the binding of BRCT domain to phosphopeptides is guaranteed by the distinct preferences for amino acids flanking the phosphoserine residue. Different BRCT motif-containing proteins were found to prefer different phosphopeptides with the strongest selection at the +3 position of the phosphopeptide (Manke *et al.*, 2003; Rodriguez *et al.*, 2003).

1.5.4 Regulation of Ect2 during mitosis

In eukaryotes, reduction of Cdk1/cyclin B activity is a prerequisite for completion of cytokinesis, and this allows the timely coordination of chromosome alignment and segregation with cytokinesis (Echard and O'Farrell, 2003). This is nicely exemplified by *Drosophila* cyclin B and B3 mutant embryos in which the cytokinesis furrow appears at an earlier stage during mitosis. Moreover, stable cyclin B prevents cytokinesis in these cells, and expression of stable cyclin B3 delays cytokinesis. Reduction of *pebble (pbl)* function also delays cytokinesis and incomplete furrows are finally aborted in these cells. Genetic interaction studies with *pbl* and cyclin B3 mutant flies showed that there is a synergetic inhibition of cytokinesis by stable cyclin B3 expression and *pbl* mutations. Moreover, cyclin B and cyclin B3 inhibit the contribution of the *pebble* pathway to cytokinesis. From these data it is tempting to suggest that phosphorylation by Cdk1/cyclin B or B3 might negatively regulate *pebble* function (Echard and O'Farrell, 2003).

In mammalian cells, mitotic Ect2 has a retarded electrophoretic mobility on SDS-PAGE gels, which is a result of hyperphosphorylation. This hyperphosphorylated Ect2 form, isolated from mitotically (prometaphase) arrested cells showed activity towards Cdc42, RhoA and Rac in *in vitro* GTP loading assays. Dephosphorylation of mitotic Ect2 resulted in a strong reduction in its GEF activity. Thus, according to these results, Ect2 seems to be highly active already during prometaphase and phosphorylation positively influences its activity (Tatsumoto *et al.*, 1999). This is somewhat surprising, considering that Cdk1/cyclin B inhibits cytokinesis, which in *Drosophila* is at least partly mediated via *pebble*. Moreover, bulk measurements of an active GTP bound RhoA, using a GST tagged GTP-RhoA binding domain of rhotekin, showed that maximal levels of GTP bound RhoA were present 90 min after release from a nocodazole block (Kimura *et al.*, 2000). This most likely reflects the time when cells undergo cytokinesis. Therefore, the *in vivo* regulation of Ect2 might be more complex and probably also requires timely targeting to its sites of action.

The targeting of Ect2 to the central spindle is mediated via its amino-terminal BRCT-containing domain. In *Drosophila*, a two hybrid interaction between *pebble* and *RacGAP50C* (the *Drosophila* orthologue of human MgcRacGAP) was observed (Somers and Saint, 2003). This interaction was mapped to the first BRCT repeat of *pebble* and the amino-terminal coiled coil domain of *RacGAP50C*. Like in *C. elegans, Drosophila RacGAP50C* interacts with the kinesin *Pavarotti* (the *Drosophila* orthologue of MKlp1) forming the central spindlin complex (Mishima *et al.*, 2002; Somers and Saint, 2003). Also, in *Drosophila,* it was proposed that the MT bound *RacGAP50C-Pavarotti* complex travel on cortical MTs to the cell equator and associates with *pebble* thereby activating its GEF activity to position the contractile ring (Somers and Saint, 2003).

The amino-terminal domain of Ect2 is not only important for its proper localization, but has also been suggested to regulate the function of Ect2. It was shown that Ect2 normally exists in an inactive conformation, whereby the amino-terminus of Ect2 interacts in an intramolecular fashion with the carboxyl-terminus of Ect2 (Saito *et al.*, 2004). Overexpression of amino-terminal Ect2 containing the BRCT domains apparently resulted in reduced RhoA-GTP levels during the time of cytokinesis,

suggesting that the amino-terminus of Ect2 might negatively regulate GEF activity (Kim *et al.*, 2004; Kimura *et al.*, 2000).

1.6 Goal of my research

Previous studies of Ect2 have revealed that Ect2 localizes to the central spindle and is required for cytokinesis (Tatsumoto *et al.*, 1999). However, the exact mechanisms that regulate central spindle targeting of Ect2 and its role during cytokinesis have remained elusive. Furthermore, the role of the different Ect2 domains (BRCT, GEF and PH domains) is still unknown. Although Ect2 is phosphorylated in mitosis (Tatsumoto *et al.*, 1999), the role of phosphorylation of Ect2 and its function during cytokinesis still remained unknown. Therefore, I set out to explore the mechanism for targeting of Ect2 to the central spindle and to identify the molecular interactions with other central spindle components in this process. I also aimed at identifying the residues phosphorylated on Ect2 in mitosis and discovering the upstream kinase(s) responsible for the various phosphorylations.

2.0 Results

2.1 Mitotic phosphorylation of human Ect2

2.1.1 Production of polyclonal Ect2 antibodies

In order to explore the function of human Ect2, polyclonal antibodies were raised in rabbits against an amino-terminal fragment of Ect2 (residues 1-388) (Fig. 9A). This fragment was expressed as a polyhistidine-tagged fusion protein in *E.coli* and purified using Ni-NTA agarose beads. This resulted in a relatively pure Ect2 protein fragment as revealed by Coomassie Blue staining of a SDS-PAGE gel (Fig. 9B). After preparative gel isolation of this protein fragment it was used for immunization of rabbits. Two rabbits were boosted several times and the immune sera were tested by Western blot analysis performed on cell extracts from exponentially growing U2OS cells. Whereas with serum of rabbit 762 a band could be detected migrating at around 100 kDa, the expected size of Ect2, no specific signal was observed with serum of rabbit 763 (Fig. 9C). Nevertheless, after immunopurification, using the Ect2 fusion protein immobilized on nitrocellulose, purified antibodies from sera of both rabbits 762 and 763 detected a similar band at around 100 kDa on Western blots (Fig. 9C). The absence of reactivity with the serum of rabbit 763 is therefore most likely a result of a low titre in this serum, which is in agreement with the observation that only low amounts of specific Ect2 antibodies could be isolated from this serum. No specific signals were observed with the pre-immune sera, attesting to the specificity of these antibodies. Moreover, the specificity of the antibody 762 (763 not tested) was further confirmed by immunoprecipitations and by siRNA depletion of Ect2, as described later. Therefore, for all subsequent experiments affinity purified specific Ect2 antibodies from serum of rabbit 762 were used.

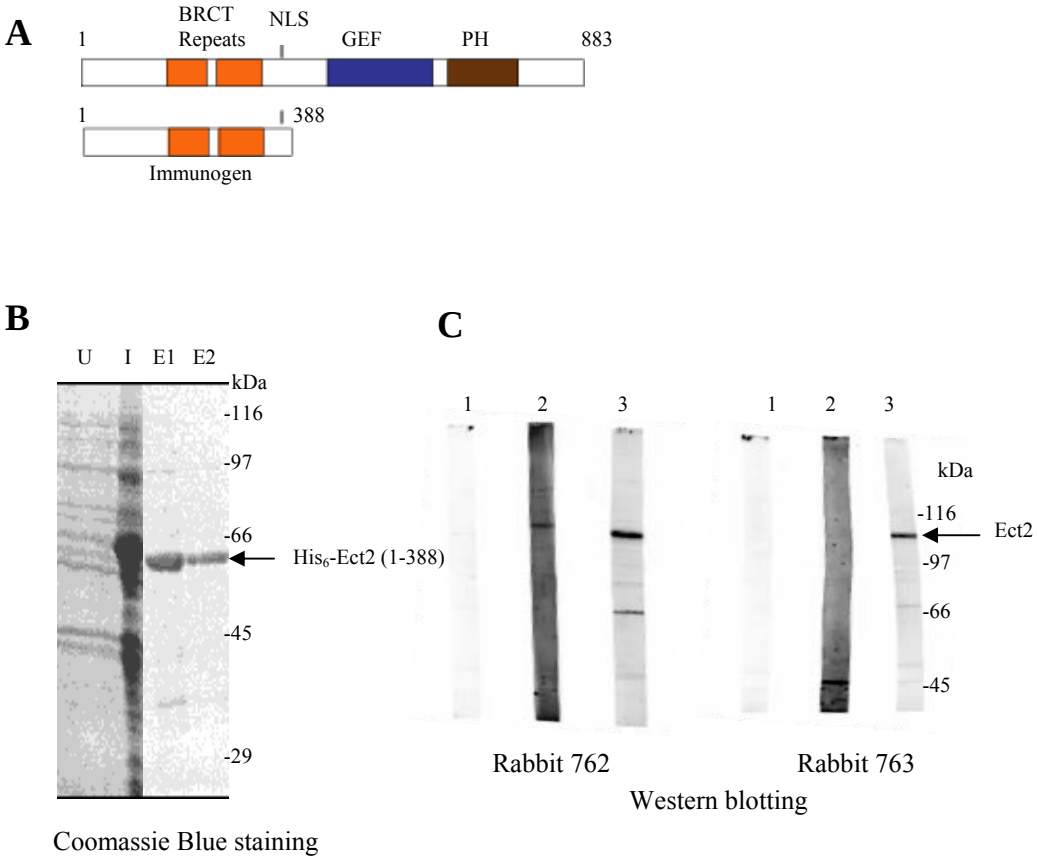

Figure 9. Production of rabbit polyclonal anti-Ect2 antibodies.

(A) Schematic representation of the amino-terminal Ect2 1-388 protein fragment used for raising polyclonal antibodies in rabbits.

(B) Coomassie Blue stained gel containing samples from different purification steps of His_6-Ect2 1-388 protein expressed in E.coli *strain JM109. The lanes represent: U, uninduced bacteria; I, bacteria induced with IPTG; E1 and E2, Ni-NTA eluted His_6-Ect2 1-388 fusion protein.*

(C) About 20 µg of U2OS whole cell lysates were separated by SDS-PAGE and transferred onto nitrocellulose membranes. These membranes were probed with: lane1, pre-immune serum (1:2000 dilution); lane2, immune serum (1:2000 dilution); lane3, affinity purified Ect2 antibodies (1 µg/ml) from the serum of rabbit 762 (left) and rabbit 763 (right), respectively.

2.1.2 Ect2 is phosphorylated during early mitosis

To analyze cell cycle dependent changes in Ect2, HeLa S3 cells were synchronized using a drug arrest-release protocol. HeLa S3 cells were first synchronized at the G1/S phase boundary using aphidicolin, a drug that inhibits DNA-polymerases (Heintz *et al.*, 1983). After 14 hours incubation, cells were released from the aphidicolin block by washing out the drug and were subsequently blocked in M-phase using low doses of nocodazole, a drug that depolymerizess MTs, resulting in the activation of the spindle checkpoint (De Brabander *et al.*, 1986). Mitotic cells were collected by shake off and subsequently released into nocodazole free medium. Cell samples for immunofluorescence microscopy inspection, FACS and Western blot analysis were collected every 20 min. FACS analysis of the propidium iodide stained cell samples confirmed proper synchronization of the cells and showed that cells entered interphase about 100 min after release from the nocodazole block (Fig. 10A). This was further confirmed by counting of DAPI stained cells, using immunofluorescence microscopy (Fig. 10B). Moreover, the latter analysis revealed that cells entered anaphase between 60 and 80 min after the nocodazole release (Fig. 10B). Western blot analysis showed that Ect2 protein levels were relatively constant throughout the cell cycle. Ect2 showed, however, a retarded electrophoretic mobility during early stages of mitosis (0-60 min), as compared to Ect2 from asynchronously growing cells. This change in electrophoretic mobility of Ect2 has been described before and has been attributed to mitotic phosphorylation (Tatsumoto *et al.*, 1999). This retarded electrophoretic mobility paralleled the presence of cyclin B during this stage of mitosis and moreover shows that Ect2 became dephosphorylated upon meta- to anaphase transition. This indicates that Cdk1 could be responsible for the observed Ect2 phosphorylation. The mitotic kinase Plk1 has also been shown to be cell cycle regulated, but its levels clearly fluctuated less strongly than cyclin B levels and no direct correlation between Plk1 protein levels and Ect2 phosphorylation could be observed.

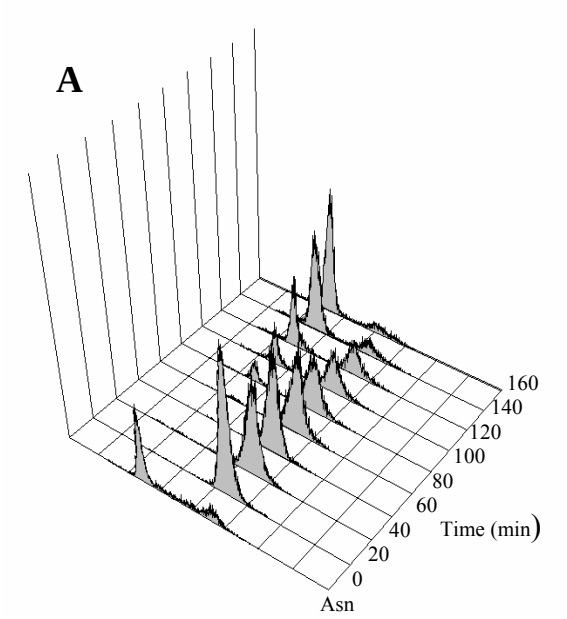

B

Time after nocodazole release in min

	Asn	0	20	40	60	80	100	120	140	160
I	94	2	2	1	1	2	15	48	86	95
PM	1	98	93	76	51	23	5	1	2	1
M	1	0	5	23	33	14	6	5	0	0
A	2	0	0	0	15	30	6	3	1	1
T	2	0	0	0	0	31	68	42	11	3

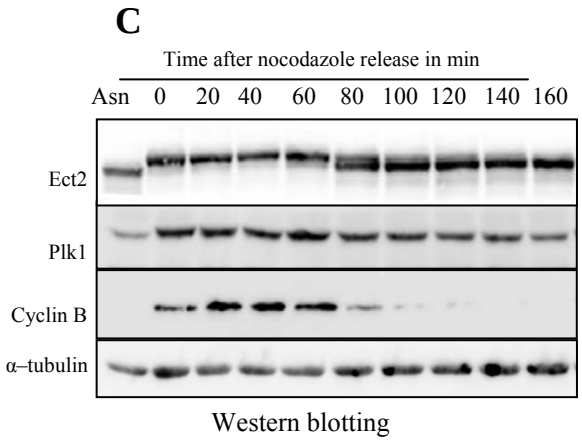

Figure 10. Changes in Ect2 electrophoretic mobility during mitotic progression.

Mitotic HeLa S3 cells were released from a nocodazole block and samples were taken at the indicated time intervals (min). As a control, cells from asynchronously growing cultures (Asn) were used. (A) Ethanol fixed cell samples were stained with propidium iodide and analyzed by FACS. (B) Cells were simultaneously fixed and permeabilized with PTEMF and stained with DAPI. Based on DNA morphology, these cells were counted and classified as I (interphase), PM (prometaphase), M (metaphase), A (anaphase) and T (telophase). Numbers indicate percentages (%) and at least 200 cells were counted for each time point. (C) Cell extracts were separated by SDS-PAGE and proteins were transferred onto nitrocellulose membranes. Western blots were probed with anti-Ect2 (upper panel), anti-Plk1 (2nd panel), anti-Cyclin B (3rd panel) and anti-α-tubulin antibodies (bottom panel).

2.1.3 Identification of multiple phosphorylation sites in mitotic Ect2

Our cell cycle analysis confirmed mitosis dependent changes in the Ect2 phosphorylation state. Since many mitotic proteins are regulated by post-translational modifications, notably reversible phosphorylation, it is tempting to believe that Ect2 functions could be regulated by phosphorylation. In fact, it has been suggested that Ect2 GEF activity might be regulated by reversible phosphorylation (Tatsumoto *et al.*, 1999). To identify putative regulatory phosphorylation sites, Ect2 was immunoprecipitated from HeLa S3 cells using our purified rabbit polyclonal Ect2 antibody (762). HeLa S3 cells were grown in spinner culture flasks and synchronized using a sequential aphidicolin/nocodazole block release protocol, as described above. Cells were released for about 60 min from the nocodazole block before harvesting. Since spinner culture cells need a longer recovery time than attached cells, most cells were still in a prometaphase state at this time point (as checked by microscopy). In parallel, cells were arrested with aphidicolin and released for 60 min into S phase. Highly concentrated cell extracts were prepared from these mitotic and S phase HeLa S3 cells for immunoprecipitation using purified polyclonal anti-Ect2 antibodies bound to affiprep protein A beads (Biorad) and as a control, pre-immune IgG antibody beads were used. The immunoprecipitates were separated on a 4-12% NuPAGE gradient gel (Invitrogen) and upon Coomassie Blue staining revealed a specific protein in the Ect2 immunoprecipitates, migrating at approximately 100 kDa (Fig. 11A). This protein showed a retarded electrophoretic mobility in immunoprecipitates from mitotic cells as compared to immunoprecipitates from interphase cells (Fig. 11A). The gel bands were excised in a dust free environment and tryptic digestion was performed. Using matrix-assisted laser desorption/ionization time of flight (MALDI-TOF) mass spectrometry (MS) the protein in these bands was identified to be Ect2. No Ect2 was detected in corresponding gel slices from control pre-immune IgG immunoprecipitates.

For identification of phosphorylation sites within these tryptic digests (Shevchenko *et al.*, 1996), phosphorylated peptides were first identified by MALDI-TOF mass spectrometry (Brucker Daltonik, Bremen, Germany) and subsequently confirmed by post source decay (PSD) (Hoffmann *et al.*, 1999).

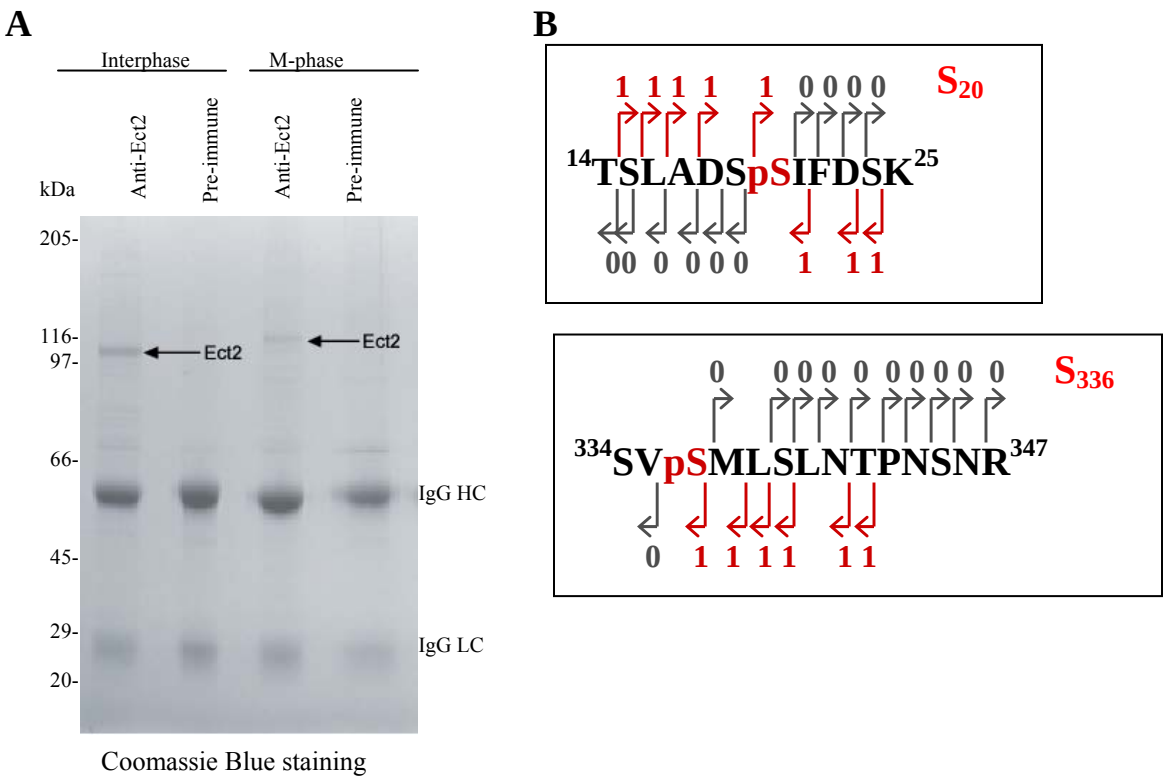

Figure 11. Mass-spectrometry identification of mitotic Ect2 phosphorylation sites.

(A) Anti-Ect2 and pre-immune immunoprecipitates from S- and M-phase HeLa S3 cell extracts were separated by SDS-PAGE gel and stained with Coomassie Blue. Ect2, as identified by MS analysis is indicated. IgG HC and IgG LC, indicate antibody heavy chains and light chains, respectively.

(B) Fragmentation of the phosphorylated peptides ^{14}TSLADSSIFDSK^{25} and ^{334}SVSMLSLNTPNSNR^{347} by nanospray ionization Q-TOF (quadrupole-time of flight) mass spectrometry in positive ion mode. Arrows marked in red indicate phosphorylated fragments and arrows in black indicate unphosphorylated fragments.

(C) Schematic representation of the identified mitosis specific phosphorylation sites in Ect2 and their respective localization within Ect2.

With the latter method, peptides showing losses of 98 mass units (phosphoric acid) and 80 mass units (phosphate group) were considered as phosphopeptides. The exact localization of the phosphorylated residues within the peptides was determined by MS-MS based sequencing using a quadrupole time-of-flight (QTOF) mass spectrometer. The phosporylation pattern of tryptic peptides of Ect2 protein from mitosis specific samples was compared to that of interphase specific samples. In this way we could map six phosphorylation sites in six different Ect2 peptides that were specifically present in mitotic Ect2 (Fig. 11C, Table 2). All the phosphorylation sites mentioned here were from mitosis specific samples. As an example, the fragments of two phosphorylated peptides, ^{14}TSLADSpSIFDSK^{25} and ^{334}SVpSMLSLNTPNSNR^{347}, are schematically depicted in Fig. 11B. Bioinformatic analysis of the evolutionary conservation of these sites showed that five out of these sites were conserved among human *(Homo sapiens),* mouse *(Mus musculus),* frog (*Xenopus leavis*), fish (*Takifugu rubripes*) and fruitfly (*Drosophila melanogaster)* (Table 2, Fig. 12A). This suggests that these five phosphorylation sites could constitute important regulatory sites. Three of the identified conserved sites matched Cdk1 and MAPK consensus phosphorylation sites (pS/pT P), suggesting that Cdk1 or MAPK might be responsible for creating these phosphosites.

Table 2. Summary of the phosphorylation sites identified in mitotic endogenous Ect2, in recombinant Ect2 phosphorylated by Plk1 in vitro *and in recombinant Ect2 purified from okadaic acid (OA) treated Sf9 insect cells. Two other Ect2 phosphorylation sites, S411 and S417, have been reported to be phosphorylated in interphase cells (Beausoleil et al, 2004). T815 was mentioned to be phosphorylated* in vitro *by Cdk2/Cyclin A kinase (Stefan Geley, personal communication). The phosphorylated residues are indicated in red.*

S.No	Residue	Peptide	*In vivo*	Plk1 *in vitro*	OA in Sf9 cells	Others
1	S20	TSLADS**pS**IFDSK	√	√	√	
2	S40	ENLLIGST**pS**YVEEEMPQIETR	√	√		
3	T328	AN**pT**PELK	√			
4	S336	SV**pS**MLSLNTPNSNR		√		
5	S366	ETDV**pS**PFPPR	√		√	
6	S685	**pS**PHGQTRPPASLK	√		√	
7	S811	AF**pS**FSK	√	√	√	
8	S411, S417	**pS**TPVP**pS**K				**Nuclear**
9	T815	AFSFSK**pT**PK				**Cdk2/cyclin A**

A

Figure 12. Multiple sequence alignment of Ect2 and its homologues in other species.
*(A) Clustal-W sequence alignment of Ect2 and its homologues in different species. Only parts of the sequences representing the phosphorylation sites are shown. The phosphorylated peptides identified by MALDI-TOF mass spectrometry are depicted in green colour and the phosphorylated residues are depicted in red colour. The abbreviations indicate: Hs (*Homo sapiens*), Mm (*Mus musculus*), Xl (*Xenopus laevis*), Tr (*Takifugu rubripes*) and Dm (*Drosophila melanogaster*).*

2.1.4 Plk1 can phosphorylate Ect2 in vitro

To investigate which kinase(s) could be responsible for the phosphorylation of Ect2 during mitosis, *in vitro* kinase assays were performed. For this, a GST-tagged recombinant Ect2 protein was produced in Sf9 insect cells using a recombinant baculovirus expression system (Pharmingen). As shown in Fig. 13A, a considerable amount of soluble GST-Ect2 could be produced in Sf9 insect cells and isolated with glutathione sepharose beads (Fig. 13A). Since a PreScission protease site was engineered

between the GST-tag and the Ect2 protein, we could remove the GST-tag by incubation of GST-Ect2 protein with PreScission protease (Amersham), resulting in the isolation of GST-tag free recombinant Ect2 protein (Fig. 13A).

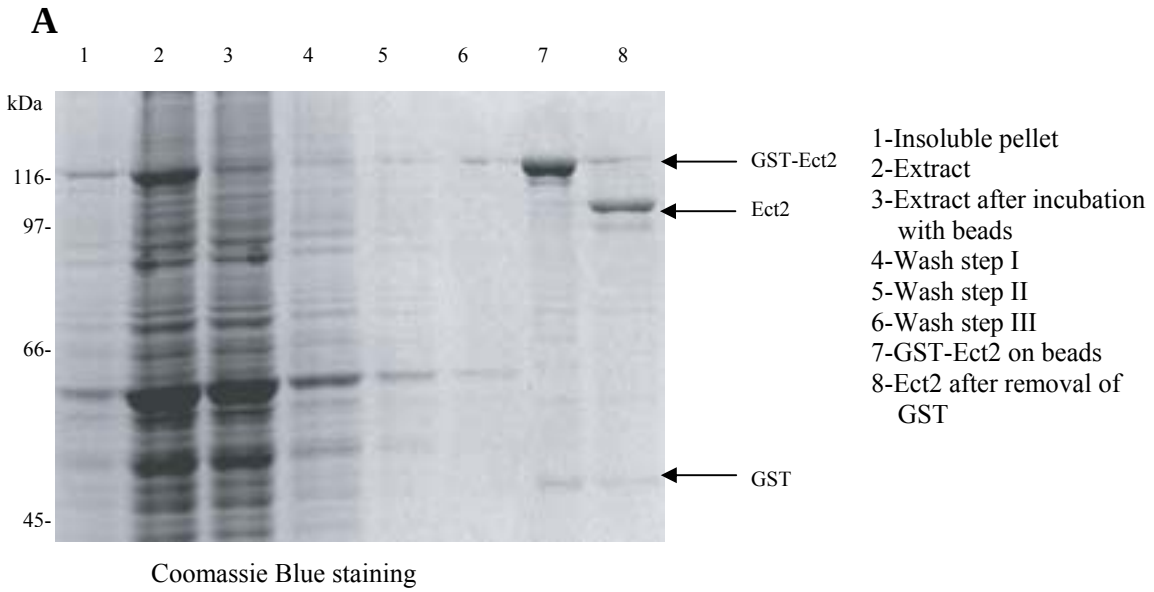

Figure 13. Purification of recombinant human Ect2 from Sf9 insect cells.
(A) Different cell fractions and GST-Ect2 isolation steps of Sf9 insect cells infected with a GST-Ect2 recombinant baculovirus were separated on a SDS-PAGE gel and stained with Coomassie Blue.

For *in vitro* kinase assays recombinant human GST tagged Plk1 WT (wild type) and Plk1 KD (catalytically impaired, K82R) were produced in Sf9 insect cells, according to standard isolation procedures present in the laboratory (Casenghi *et al.*, 2003). A GST-Aurora-B WT/INCENP complex and Aurora-B KD (K106R)/INCENP complex produced in Sf9 insect cells were a kind gift from Dr. Reiko Honda (Honda *et al.*, 2003) and recombinant Cdk1/cyclin B, also purified from Sf9 insect cells, was kindly provided by Dr. Rüdiger Neef. *In vitro* kinase assays with radioactive [γ^{32}-P]-ATP were performed for 20 min at 30^{o}C with recombinant Ect2 as a substrate in the presence of the different kinases mentioned above. As a negative control, Ect2 was also incubated in the kinase buffer without the addition of exogenous kinase. Proteins in the different samples were then separated by SDS-PAGE and phosphorylation of Ect2 was determined by

autoradiography of the Coomassie Blue stained gels. As shown in Fig. 14A and 14B, a substantial amount of radioactive phosphate was already incorporated into Ect2 in the absence of exogenously added kinases. This suggests that although the isolated Ect2 protein looked relatively pure (Fig. 13A), contaminating kinase(s) were present in the Ect2 isolate resulting in a significant background phosphorylation. Additional wash steps (with higher salt concentrations) during the purification of recombinant Ect2 did not significantly improve this background problem. Nevertheless, incubation of Ect2 with Plk1 resulted in a strong increase in Ect2 phosphorylation, and, moreover, this resulted in a retarded mobility of Ect2 on a SDS-PAGE gel.

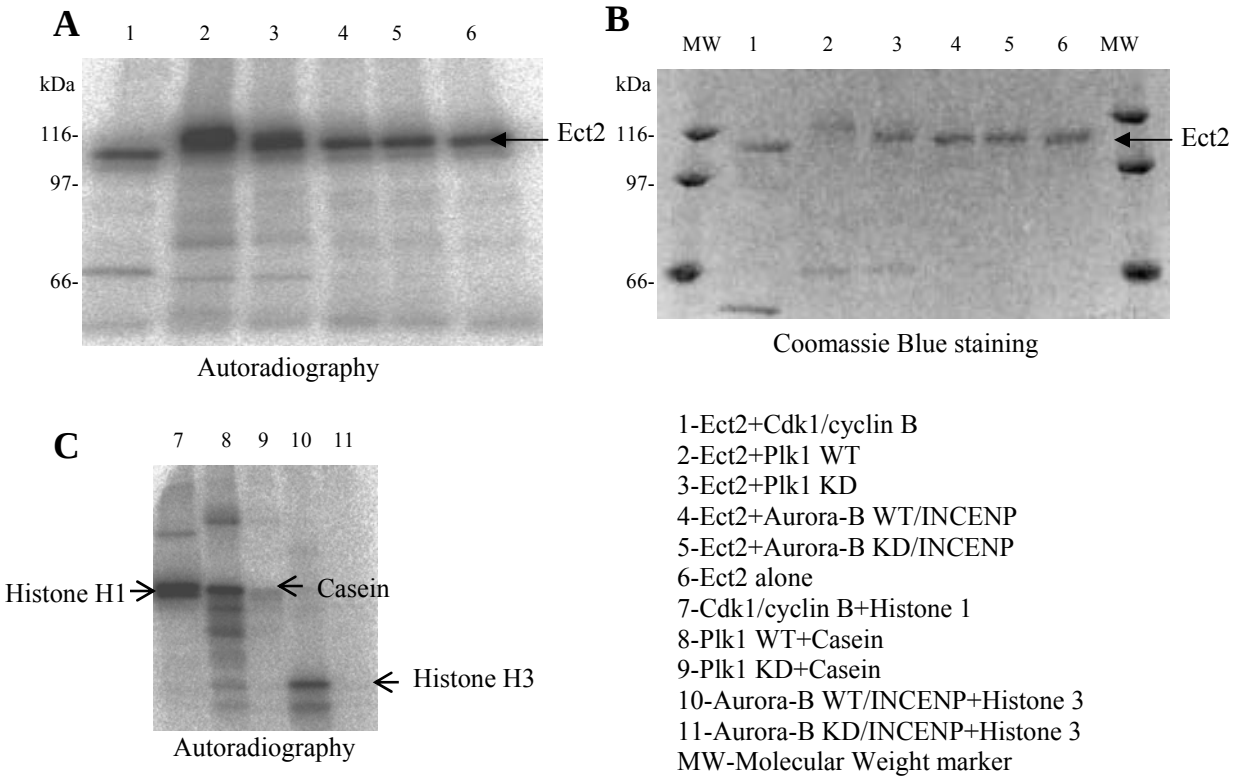

Figure 14. In vitro *phosphorylation of Ect2 by mitotic kinases.*

(A) Recombinant Ect2 protein was incubated with the different, indicated, mitotic kinases in the presence of [γ^{32}-P]-ATP for 20 min. Proteins were subsequently separated by SDS-PAGE and the Coomassie Blue stained gel was then subjected to autoradiography.

(B) The Coomassie Blue stained gel corresponding to the autoradiography in A is shown. Note the retarded mobility of Ect2 phosphorylated by Plk1 (lane 2).

(C) Different exogenous substrates were incubated with the indicated mitotic kinases in the presence of [γ^{32}-P]-ATP. Phosphorylation of these proteins was determined by autoradiography as in (B).

Some increase in Ect2 phosphorylation was also observed in the presence of the catalytically impaired Plk1 (K82R) mutant, which is probably a result of low residual kinase activity of this mutant kinase. Surprisingly, no obvious increase in Ect2 phosphorylation was observed upon incubation with Cdk1/cylin B or Aurora-B/INCENP. This was not a result of the absence of kinase activity, because these kinases readily phosphorylated other exogenous substrates (Fig. 14C). Because of the high background activity with Ect2, it cannot be ruled out that low amounts of phosphate are incorporated into Ect2 by these kinases *in vitro*. In particular, as some of the consensus Cdk1/cyclin B sites on Ect2 were phosphorylated *in vivo*, we assume that Ect2 might be phosphorylated by Cdk1/cyclin B at least *in vivo*. An alternate possibility to be tested for reducing the background activity of Ect2 is to treat the recombinant Ect2 with protein phosphatases prior to performing *in vitro* kinase assays.

Since Ect2 was phosphorylated by Plk1 *in vitro*, resulting in a retarded electrophoretic mobility of Ect2, we wondered if Plk1 could be responsible for the phosphorylation of some of the identified endogenous Ect2 phosphorylation sites. To investigate this, non-radioactive kinase assays were performed with recombinant Ect2 in the presence or absence of exogenous Plk1. After separation on a SDS-PAGE gel, the Ect2 protein bands were excised and processed for mass spectrometry analysis as described in the previous section. In total, four Plk1 specific phosphorylation sites were identified in recombinant Ect2 (Table 2, Fig. 12). Of these, three did correspond to endogenous Ect2 phosphorylation sites, strongly arguing that Plk1 might be responsible for the phosphorylation of these sites *in vivo.* Interestingly, one of the identified sites S20 is a putative PBD (Polo-Box Domain) docking site. The PBD is located in the carboxyl-terminal half of Plk1 and has recently been shown to bind to phosphorylated peptides containing the consensus sequence X-S-pS/pT-P/X. To investigate if phosphorylation of these sites was responsible for the marked upshift of Ect2 in mitosis, we depleted Plk1 from HeLa S3 cells by siRNA. Depleted cells were then arrested in interphase (aphidicolin) and in mitosis (nocodazole), respectively. As a control, cells were treated with siRNA duplex against the luciferase gene (GL2) (Elbashir *et al.*, 2001). Cell lysates were subsequently separated by SDS-PAGE and transferred onto nitrocellulose membranes. As shown in Fig. 15A, Western blot analysis revealed that Ect2 was clearly

upshifted in mitotic control (GL2) cells, but also in Plk1 siRNA treated cells. The effective depletion of Plk1 in these cells was confirmed by Western blot analysis (Fig. 15A). Therefore, Plk1 seems not to be the only kinase that is responsible for the upshift of Ect2 *in vivo*. Alternatively, it cannot be excluded that low residual levels of Plk1 might be sufficient for effective Ect2 phosphorylation.

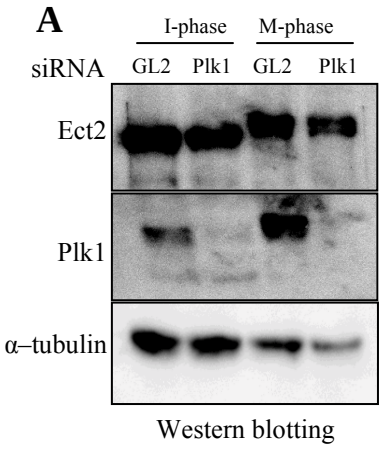

Figure 15. Retarded Ect2 electrophoretic mobility is also observed in mitotic Plk1 depleted cells. GL2 and Plk1 siRNA oligo duplexes were transfected into HeLa S3 cells. These cells were subsequently arrested in interphase (I-phase) with aphidicolin and in mitosis (M-phase) with nocodazole. Protein extracts of these cells were separated by SDS-PAGE and transferred onto nitrocellulose membranes. The Western blots were probed with the indicated antibodies.

2.1.5 No obvious interaction between Ect2 and Plk1 kinase

As described above, the PBD of Plk1 has recently been shown to bind to phosphorylated peptides containing the consensus site X-S-pS/pT-P/X (Barr *et al.*, 2004; Elia *et al.*, 2003). One of the identified Ect2 sites (S20) matches this consensus site and hence Plk1 might bind directly to Ect2. Indeed Anja Hanisch in our laboratory could show that endogenous Ect2 from human cells binds to the wild type PBD of Plk1 but not to a phosphopeptide binding mutant of the PBD. We therefore tested if Ect2 could co-precipitate endogenous Plk1 from mitotic cell lysates. As shown in Fig. 16A, we could readily precipitate Ect2 from mitotic cells, but Plk1 was not present in these cell lysates. Moreover, the over expressed flag-tagged amino-terminal domain of Ect2 (1-333) could not be identified in immunoprecipitates of the myc-Plk1 precipitated using anti-myc 9E10 antibodies from mitotic HeLa S3 cells (Fig. 16B). Thus, although we cannot

exclude the possibility that our antibodies interfere with the Plk1-Ect2 interaction, so far there is no clear evidence that this S20 site is a functional Plk1 docking site. Furthermore, as shown below, no obvious phenotype could be detected with the S20 mutants.

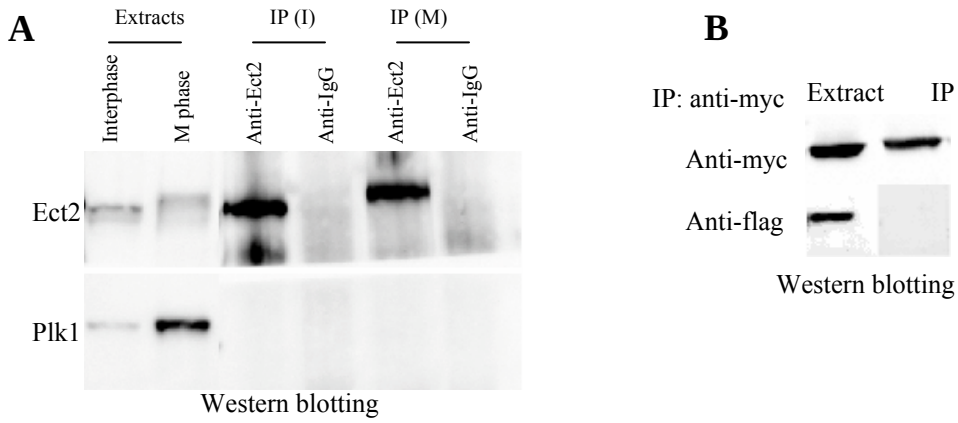

Figure 16. No in vivo *interaction was observed between Ect2 and Plk1 kinase.*
(A) HeLa S3 cells were synchronized either with thymidine-aphidicolin or with aphidicolin-nocodazole block release protocols to enrich cells in interphase (I) and mitosis (M), respectively. Endogenous Ect2 was immunoprecipitated from these cell extracts. These immunoprecipitates (IP) were separated by SDS-PAGE and transferred onto nitrocellulose membranes. The blots were probed with anti-Ect2 and anti-Plk1 antibodies.
(B) HeLa S3 cells were transfected with myc-Plk1 and flag-Ect2 (1-333) constructs for 36 hours and myc-Plk1 was immunoprecipitated using anti-myc beads. The immunoprecipitates (IP) were separated by SDS-PAGE and transferred onto nitrocellulose membranes and probed with anti-myc and anti-flag antibodies.

2.1.6 Analysis of Ect2 phosphorylation site mutants

To explore the physiological significance of the identified Ect2 phosphorylation sites, site directed mutagenesis was performed. The identified phosphorylated serine and threonine residues were singly mutated to alanine residues, thus mimicking an unphosphorylated state, and into aspartic acid residues, which can sometimes mimic a phosphorylated state.

In addition, all alanine mutations (except the non-conserved S40A) were also combined into one construct and the same was done with the aspartic acid mutations.

We first analyzed the overexpression phenotype of wild type and mutant myc-tagged Ect2 constructs. Again these constructs were transiently expressed in HeLa S3 cells and 48 hours after transfection, cells were analyzed by immunofluorescence microscopy. Since Ect2 is required for cytokinesis we particularly investigated the presence of binucleated cells, an indication of cytokinesis failure. Expression of wild type Ect2 resulted in a clear increase in the number of binucleated cells, as compared to control myc-Tlk1 (Tousled Like Kinase) transfected or untransfected cells (Fig. 17) (Sillje *et al.*, 1999). Thus, high levels of Ect2 interfered with proper cytokinesis. We next analyzed the percentages of binucleated cells expressing mutant Ect2 proteins. As shown in Fig. 17A, expression of some of the alanine mutants (especially S20) resulted in a higher percentage of binucleated cells, as compared to the wild type. However, expression of the Ect2 mutant form with all six residues mutated into alanine residues showed an almost similar increase in binucleated cells as wild type Ect2.

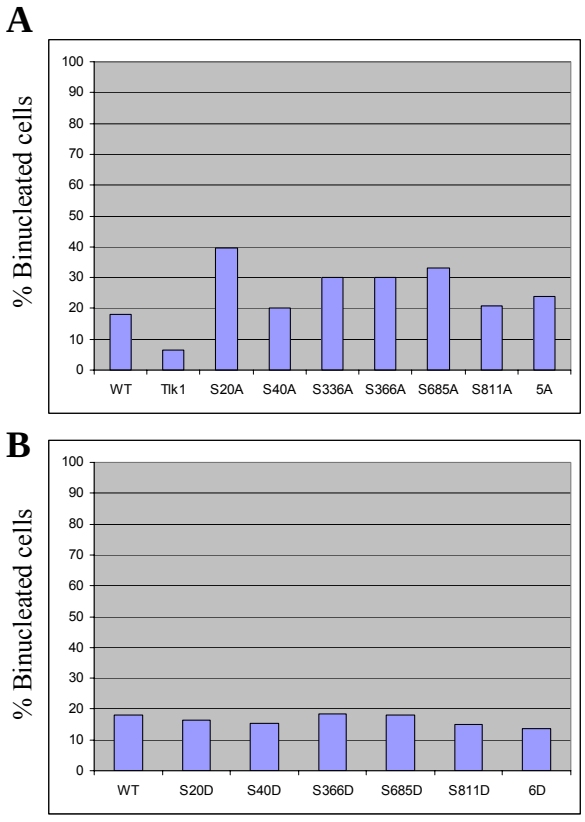

Figure 17. Increase in the number of binucleated cells with overexpressed myc-tagged wild type and mutant Ect2 proteins. The indicated myc-tagged proteins were overexpressed in HeLa S3 cells for 48 hours. Cells were then fixed and stained with anti-myc (9E10) antibody to identify the transfected cells. Cells were counterstained with DAPI for the determination of the percentage of binucleated cells. This experiment was done in duplicates and always the difference of values between the two experiments was not more than 10%.
(A) Analysis of cells expressing the alanine mutant Ect2 proteins. As a control, myc-Tlk1 was used.
(B) Analysis of cells expressing the aspartic acid mutantEct2 proteins.

The low numbers of Ect2 transfected cells could possibly be the reason for the strong variation in the number of binucleated cells which we obtained with the different mutants, and these numbers must hence be interpreted with caution. Cells expressing the mutant Ect2 forms in which the phosphorylated residues were mutated to aspartates, all showed percentages of binucleated cells as was observed with wild type Ect2 (Fig. 17B). Under the conditions tested here, we could not obtain a clear indication whether the mutant Ect2 proteins showed an effect on cytokinesis, which was different from that of the overexpressed wild type Ect2 protein.

To analyze if the localization of these mutant Ect2 proteins to the central spindle was altered, the myc-tagged wild type and mutated full length constructs were transfected into HeLa S3 cells and their localization was analyzed by indirect immunofluorescence, using anti-myc (9E10) antibodies. As shown in Fig. 18A, wild type myc-tagged Ect2 localized to the central spindle in anaphase and to the midbody in telophase cells, in agreement with previous reports (Tatsumoto *et al.*, 1999) and data shown below (see chapter 2.2). Similarly, all mutant Ect2 proteins tested localized to these spindle structures, suggesting that central spindle and midbody localization of Ect2 is not regulated by reversible phosphorylation of these specific residues. An example of one Ect2 mutant (S20A) localizing to the central spindle is shown in Fig. 18A.

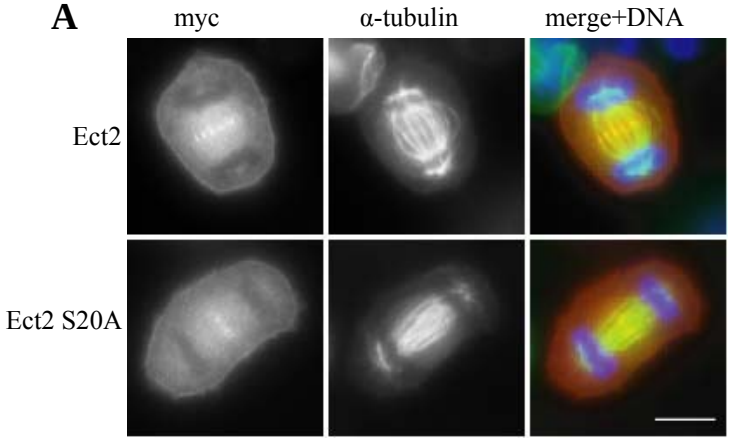

Figure 18. Localization of myc-tagged Ect2 wild type and myc-Ect2^{S20A} to the central spindle.
(A) The indicated myc-Ect2 proteins were transiently overexpressed in HeLa S3 cells for 36 hours and fixed and permeabilized with paraformaldehyde/Triton X-100. These cells were stained with anti-myc (9E10) antibodies (red), anti-α-tubulin antibodies (green) and DNA was labelled with DAPI (blue). Scale bar 10 µm.

Ect2 is a GTP exchange factor and hence we next tested Ect2 GEF activity. Except for one publication (Tatsumoto *et al.*, 1999), showing Ect2 GEF activity towards RhoA, Rac1 and Cdc42 small GTPases, no other studies on Ect2 GEF activity have been reported. As this is not an assay commonly used in our laboratory, we asked Dr. Anja Schmidt from Prof. Allan Hall's laboratory to help us with these assays. Since immunoprecipitations from cells only resulted in the purification of low amounts of Ect2 we decided to use recombinant Ect2 purified from Sf9 insect cells. To obtain phosphorylated Ect2 from Sf9 insect cells we treated these cells with Okadaic acid (OA), a PP1A and PP2 (Protein Phosphatase) phosphatase inhibitor (Cohen *et al.*, 1990), which has been shown to result in a mitosis-like phosphorylation of many proteins. For example, OA is generally used to produce phosphorylated active recombinant Plk1 kinase (Jackman *et al.*, 2003). Using the recombinant GST-Ect2 encoding baculoviruses described above we generated recombinant Ect2 from untreated and OA treated Sf9 insect cells and removed the GST- tag using PreScission protease. As shown in Fig. 19A, OA treatment resulted in an upshift of recombinant Ect2 on a SDS-PAGE gel, similar to what has been observed in mitotic cell extracts. Moreover, MS/MS analysis of this protein revealed that at least four of the five identified conserved endogenous Ect2 phosphorylation sites (S20, S366, S685 and S811) were specifically phosphorylated in this recombinant protein isolated from OA treated Sf9 insect cells. Thus, the phosphorylation pattern of this recombinant Ect2 is similar to the phosphorylation pattern of endogenous mitotic Ect2. Since only RhoA has been implicated to be essential for cytokinesis, we tested the GEF activity of these recombinant Ect2 proteins with RhoA as the substrate (performed by Dr. Anja Schmidt). Equal amounts of recombinant Ect2 protein treated with and without OA were used for GEF assays. For measuring the exchange activity, Ect2 together with [γ^{32}-S]-GTP was added to the pre-loaded GDP-RhoA. Samples were then collected every five min and the reactions were terminated by addition of ice-cold termination buffer, followed by filtration through nitrocellulose filters. Filters were washed once with the termination buffer and radioactivity was measured using a liquid scintillation counter. Initial experiments with 50 pmol Ect2 in the reaction assays did hardly show any GEF activity. Only when the amount of Ect2 was increased to 150 pmol some GEF activity could be measured, but this was clearly much

less as compared to a positive SopE GEF control (Fig. 19B). SopE is a GEF from *Salmonella typhimurium* that is often used as a positive control in GEF assays (Rudolph *et al.*, 1999). Unfortunately, no significant differences in activity between hypophosphorylated recombinant Ect2 [no OA treatment] and phosphorylated-Ect2 (OA treated) were observed in this assay. Since this assay required high amounts of Ect2, it was not possible to analyze the mutant proteins isolated from transiently transfected cells. This would require additional efforts, including the generation of recombinant baculoviruses. Since the obtained results were not very promising we have not further followed up this line of investigation.

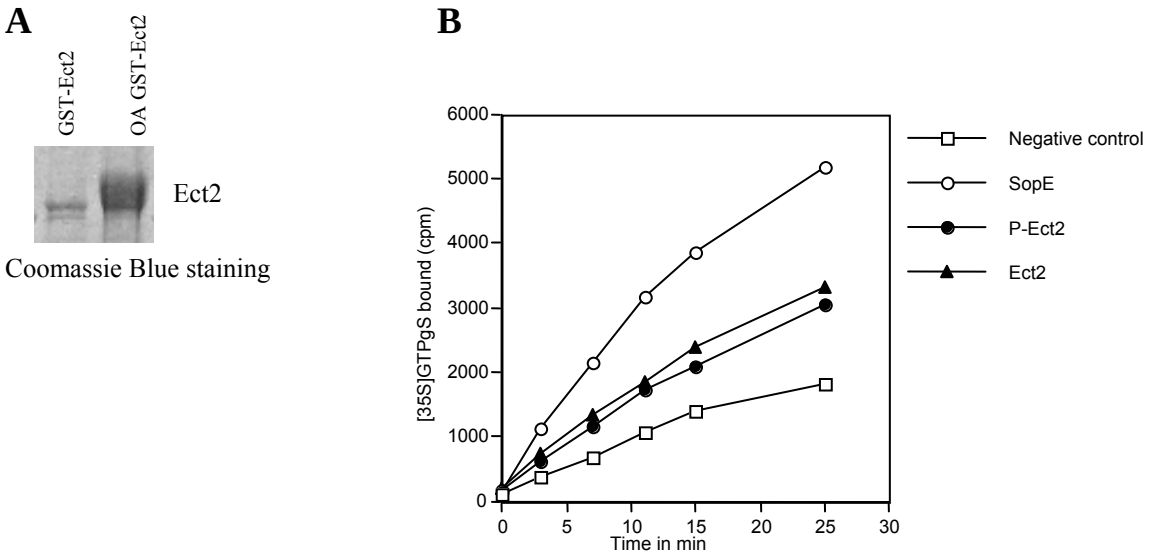

Figure 19. In vitro *GEF assay of recombinant Ect2 proteins on RhoA.*

(A) GST-Ect2 protein bound to glutathione sepharose beads was purified from Sf9 insect cells, which were either treated with OA or left untreated. Note the retarded mobility shift of phosphorylated GST-Ect2 purified from OA (okadaic acid) treated Sf9 insect cells compared to GST-Ect2 purified from untreated cells.

(B) Based on the gel shown in A, the concentrations of GST cleaved recombinant Ect2 proteins isolated from non-treated (Ect2) and OA treated (P-Ect2) Sf9 insect cells were normalized and equal amounts were used for in vitro *GEF assays with RhoA in the presence of [^{35}S]-GTPγS. As a positive control, recombinant SopE GEF was used. Samples were taken every five min, filtered and measured by liquid scintillation. Results are plotted in a graph.*

2.1.7 Conclusion:

In this part of the study, we demonstrated that Ect2 becomes hyperphosphorylated during early mitosis and is dephosphorylated upon metaphase to anaphase transition. Using mass spectrometry we could identify conserved mitosis specific phosphorylation sites in endogenous Ect2 as well as in recombinant Ect2 phosphorylated by Plk1 kinase in *in vitro* kinase assays. Upon site directed mutagenesis of these phosphorylation sites, no clear functions could be attributed to individual sites. In particular, we could not determine any significant difference in activity between hypophosphorylated and phosphorylated Ect2 in *in vitro* GEF assays. This result is contradictory to the report made by Tatsumoto *et al* (Tatsumoto *et al.*, 1999) who claimed that Ect2 becomes active only upon phosphorylation. Future studies will be required to resolve the function of these phosphorylation sites and will probably require improved protocols to analyze the GEF activity of these mutant proteins.

2.2 Regulation of Ect2 localization

2.2.1 Ect2 localizes predominantly to the central spindle and cell cortex

To examine the exact localization of Ect2 in HeLa S3 cells, indirect immunofluorescence microscopy was performed with anti-Ect2 antibodies. These antibodies predominantly stained the central spindle and midbody in mitotic cells (Fig. 20A, upper two rows) in accordance with a previous report (Tatsumoto *et al.*, 1999). In addition, however, we could observe cortical staining of Ect2 throughout mitosis. In interphase cells Ect2 localized predominantly to the nucleus, but also a weak cortical staining could be observed especially at cell-cell contacts (data not shown). No such staining was observed with pre-immune IgG attesting to the specificity of the used anti Ect2-antibodies (data not shown).

To further confirm that this staining was specific for Ect2 protein, we depleted Ect2 in HeLa S3 cells by siRNA duplex specifically targeting Ect2 and indirect immunofluorescence microscopy was performed. In Ect2 siRNA transfected cells (48 hours), the central spindle, midbody and cell cortex staining was strongly reduced and also nuclear staining was clearly diminished in interphase cells (Fig. 20A bottom two rows). To confirm efficient depletion of Ect2, cell extracts were prepared from control (GL2) and Ect2 siRNA treated HeLa S3 cells after 24 and 48 hours of transfection. These cell extracts were separated by SDS-PAGE and after Western blotting, the membranes were probed with anti-Ect2 antibodies. As compared to the control (GL2), Ect2 levels were clearly diminished in Ect2 siRNA treated cells (Fig. 20B upper panel). As a loading control, α-tubulin was detected with anti-α-tubulin antibodies (Fig. 20B lower panel).

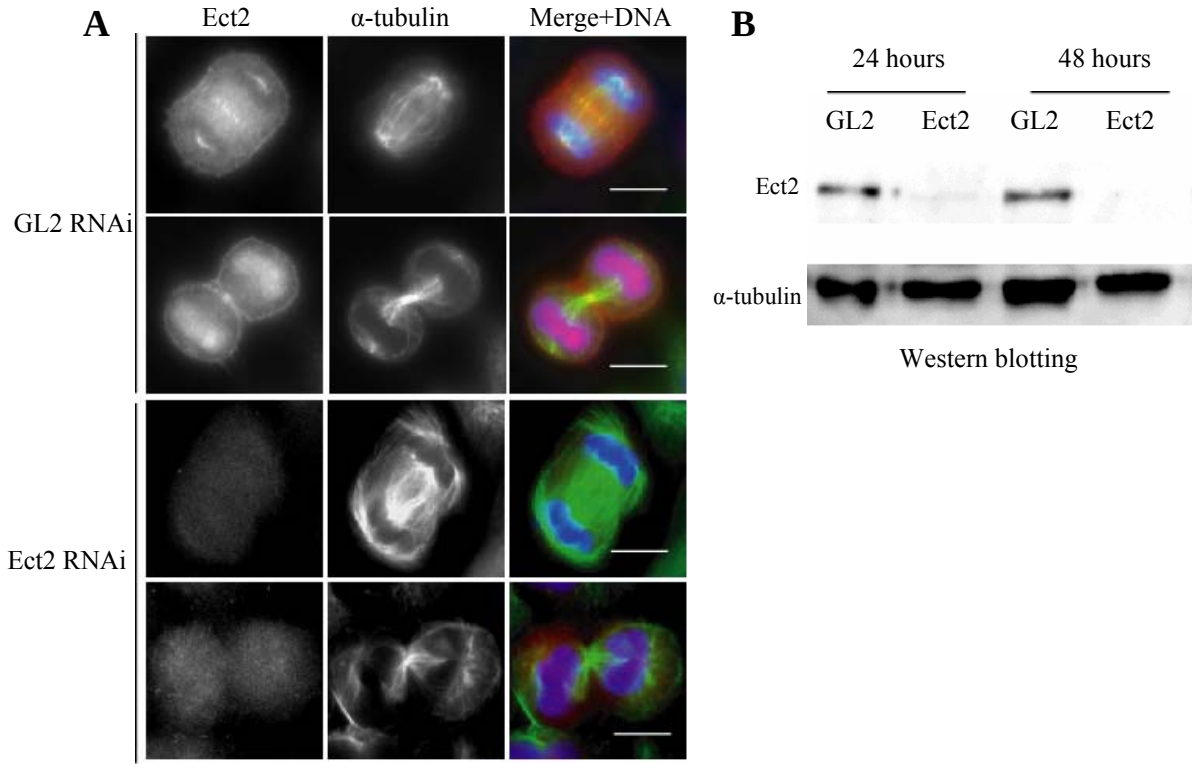

Figure 20. Ect2 localizes to the central spindle, midbody and cell cortex during mitosis.
(A) HeLa S3 cells were treated with GL2 or Ect2 siRNA duplexes for 48 hours and were subsequently fixed and permeabilized with paraformaldehyde/Triton X-100. These cells were stained with anti-Ect2 antibodies in red (left),anti-α-tubulin antibodies in green (middle) and DNA was labelled with DAPI in blue. Merged images are shown at the right. Scale bar 10 µm.
(B) HeLa S3 cells were transfected with GL2 or Ect2 siRNA duplexes and after 24 hours and 48 hours of transfection, Hepes lysis buffer extracts were made. Proteins were separated by SDS-PAGE and transferred onto nitrocellulose membranes. These membranes were probed with anti-Ect2 antibodies (upper panel) and, as a loading control, with anti-α-tubulin antibodies (lower panel).

2.2.2 The amino-terminal BRCT domain is required for central spindle targeting, whereas the carboxyl-terminal PH domain targets Ect2 to the cell cortex

To analyze which domains target Ect2 to the central spindle and the cell cortex, different myc-tagged Ect2 fragments (Fig. 21A) were transiently expressed in HeLa S3 cells. As shown in Fig. 21B, full length myc-tagged Ect2 localized to both the central spindle and

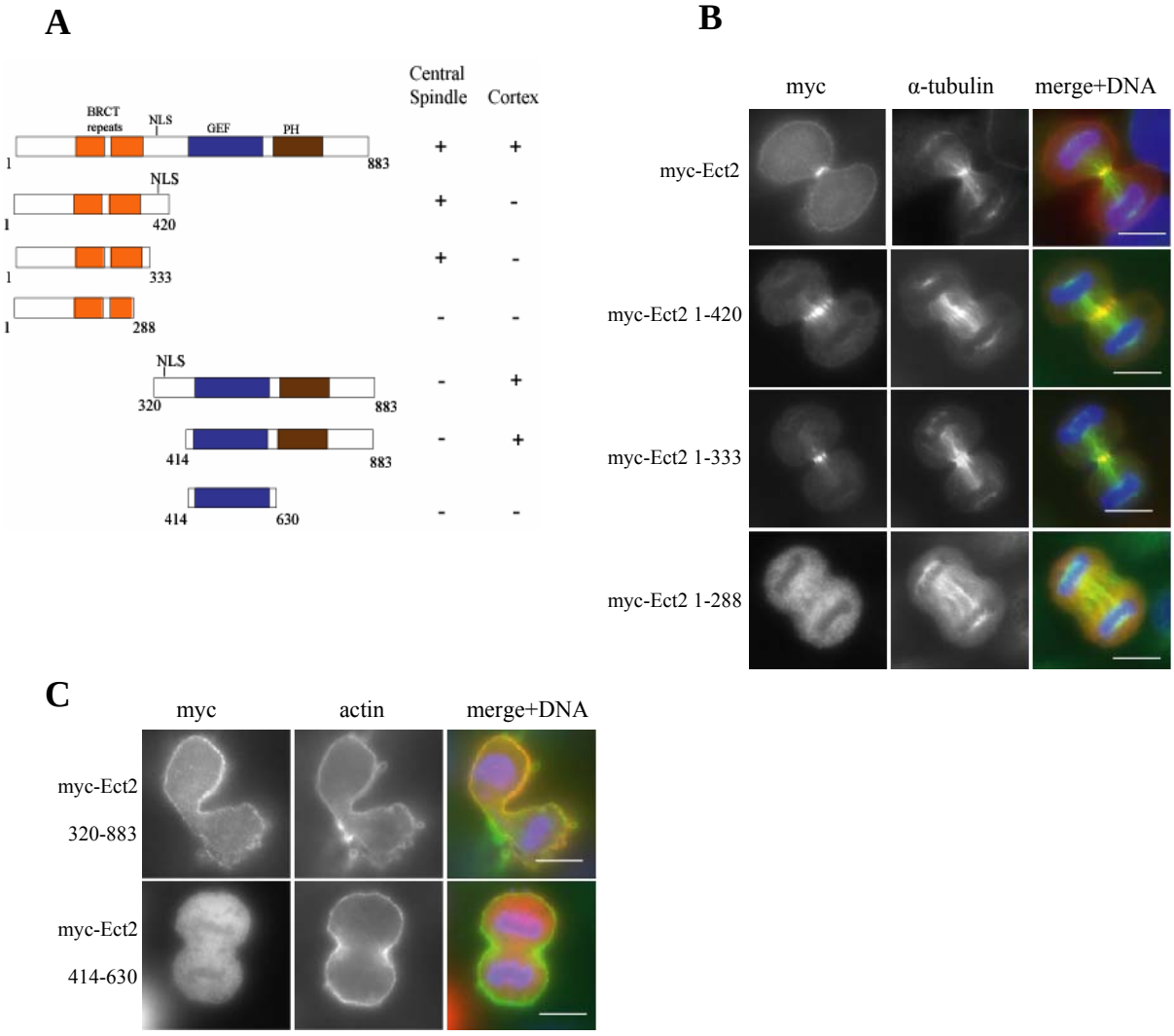

Figure 21. The intact BRCT domain targets Ect2 to the central spindle, whereas the PH domain is required for cell cortex localization.

(A) Schematic representation of different amino-terminal and carboxyl-terminal fragments of Ect2 and their presence at the central spindle and cell cortex is indicated with '+', whereas the absence is indicated with '-'.

(B) HeLa S3 cells were transfected with 3x-myc tagged constructs of Ect2 for 36 hours and were subsequently fixed and permeabilized with paraformaldehyde/Triton X-100. These cells were stained with anti-myc antibodies in red (left), anti-α-tubulin antibodies in green (middle) and DNA was labelled with DAPI in blue. Merged images are shown at the right. Scale bar 10 µm.

(C) HeLa S3 cells were transfected with myc-tagged constructs for 36 hours and were simultaneously fixed and permeabilized with formaldehyde/Triton X-100. These cells were stained with anti-myc antibodies in red (left) and with FITC-phalloidin for staining of actin in green (middle). DNA was labelled with DAPI in blue. Merged images are shown at the right. Scale bar 10 µm.

cell cortex. Amino-terminal Ect2 fragments containing the full BRCT domain (two BRCT repeats, residues 1-420 and 1-333) also localized to the central spindle, but were absent from the cell cortex (Fig. 21B). However, another amino-terminal construct encoding myc-Ect2 1-288, which has a truncated second BRCT repeat, did not localize to the central spindle in anaphase cells (Fig. 21B, lower panel). This strongly suggests that an intact BRCT domain, consisting of two BRCT repeats, is required for targeting Ect2 to the central spindle.

Whereas the amino-terminal half of Ect2 was sufficient for central spindle targeting, the carboxyl-terminal half of Ect2 strongly associated with the cell cortex, but was absent from the central spindle (Fig. 21C). The carboxyl-terminus of Ect2 consists of a DH domain (Dbl Homology) which is a Rho GEF domain, followed by a PH domain (Plekstrin Homology). Further truncation analysis revealed that the PH domain was essential for targeting Ect2 to the cell cortex (Fig. 21C). Considering that PH domains constitute lipid-binding motifs (Blomberg *et al.*, 1999), it is attractive to postulate that the cortex association of Ect2 reflects a direct interaction with the plasma membrane. The PH domain has been shown to be essential for the cell transforming activity of Ect2 in NIH/3T3 cells by an yet unknown mechanism (Miki *et al.*, 1993; Solski *et al.*, 2004), suggesting that the cortex-associated pool of Ect2 is critical for its oncogenic potential.

2.2.3 Ect2 is targeted to the central spindle via the MKlp1/MgcRacGAP and Aurora-B/MKlp2 complexes

The central spindle is composed of non-kinetochore, anti-parallel MTs and many proteins required for cytokinesis are localized to this structure. Therefore we next asked which central spindle proteins were required for targeting Ect2 to the central spindle. Specifically, we depleted the kinesins MKlp1 and MKlp2, the mitotic kinase Aurora-B and the GTPase activating protein MgcRacGAP from HeLa S3 cells, using previously validated siRNA duplexes. In agreement with previous reports (Kitamura *et al.*, 2001; Matuliene and Kuriyama, 2002; Neef *et al.*, 2003; Terada *et al.*, 1998), depletion of all

these proteins resulted in a significant increase in binucleated cells, indicative of cytokinesis defects (data not shown).

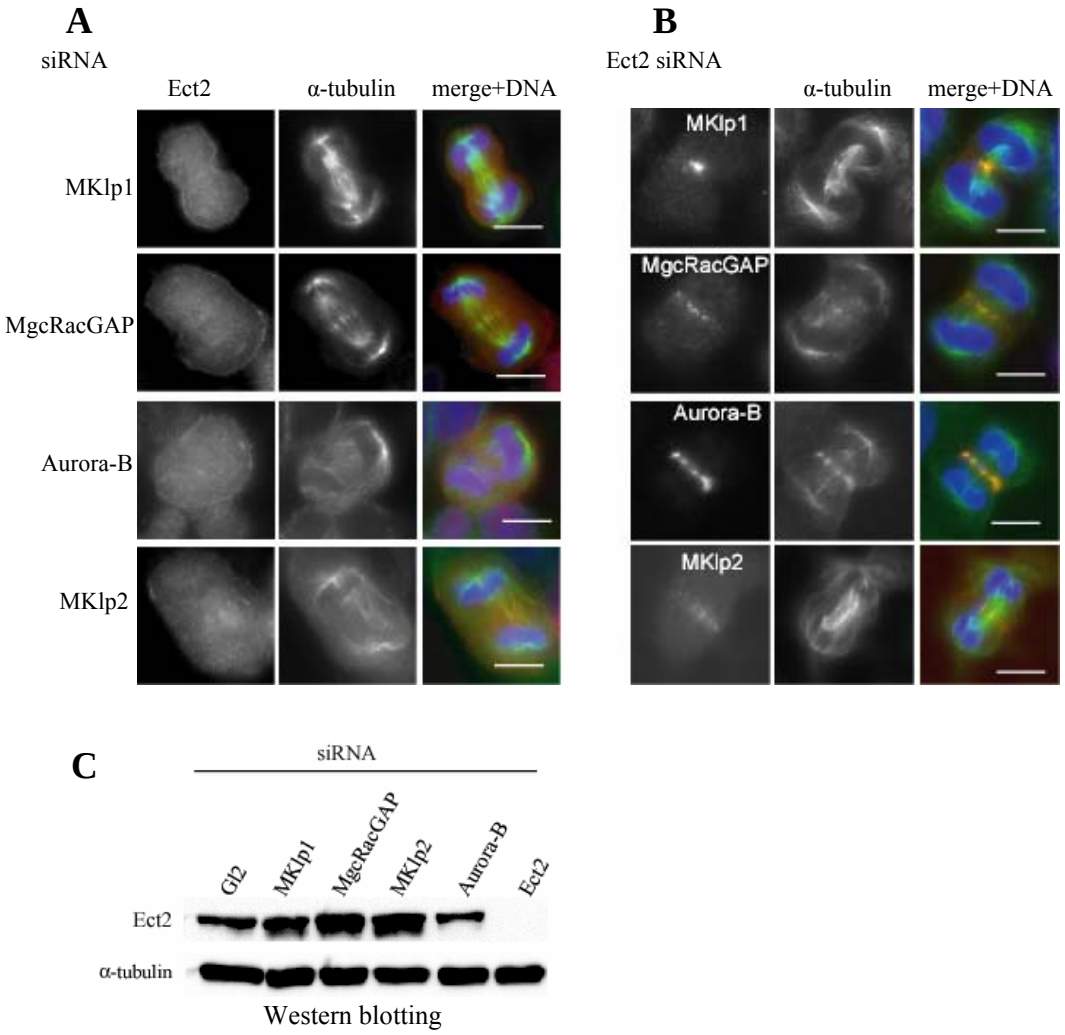

Figure 22. Ect2 requires the MKlp1/MgcRacGAP and Aurora-B/MKlp2 complexes to localize to the central spindle.

(A) HeLa S3 cells were transfected with siRNA duplexes against MKlp1, MgcRacGAP, Aurora-B and MKlp2 genes for 36 hours and were subsequently fixed and permeabilized with paraformaldehyde/Triton X-100. These cells were stained with anti-Ect2 antibodies in red (left), anti-α-tubulin antibodies in green (middle) and DNA was labelled with DAPI in blue. Merged images are shown at the right. Scale bar 10 µm.

(B) HeLa S3 cells were transfected with an Ect2 siRNA duplex for 36 hours and were subsequently fixed and permeabilized with paraformaldehyde/Triton X-100. These cells were stained with anti-MKlp1, anti-MgcRacGAP (Cyk4), anti-Aurora-B and anti-MKlp2 antibodies in red (left), anti-α-tubulin antibodies in green (middle) and DNA was labelled with DAPI in blue. Merged images are shown at the right. Scale bar 10 µm.

(C) HeLa S3 cells were transfected with siRNA duplexes against GL2, MKlp1, MgcRacGAP, MKlp2, Aurora-B and Ect2 genes for 36 hours. Cell extracts were made in Hepes lysis buffer and after SDS-PAGE, the separated proteins were blotted onto nitrocellulose membranes and probed with anti-Ect2 antibodies (upper panel) and anti-α-tubulin antibodies (lower panel) as loading control.

In MKlp2 and Aurora-B depleted cells, the central spindle was often strongly deformed, missing many of the anti-parallel MTs in this region. Also in MKlp1 and MgcRacGAP depleted cells central spindle formation was affected, but to a lesser extent than in Aurora-B and MKlp2 depleted cells. At present it is not clear if this reflects a stronger dependency of central spindle formation on MKlp2 and Aurora-B or if this reflects the efficiency of the depletion. These data are consistent with the view that all the above proteins contribute to central spindle formation (Fig. 22A). Importantly, depletion of each of these four proteins abolished the interaction of Ect2 with residual central spindle and midbody structures, but did not affect its localization to the cell cortex (Fig. 22A and data not shown). Since the absence of Ect2 from central spindle and midbody could not be explained by diminished Ect2 levels (Fig. 22B), we conclude that MKlp1, MKlp2, Aurora-B and MgcRacGAP were all required for proper localization of Ect2 to these structures. In Ect2 depleted cells, on the other hand, MKlp1, MKlp2, Aurora-B and MgcRacGAP localization to the central spindle was not affected. These results strongly suggest that Ect2 acts downstream of MKlp1, MKlp2, Aurora-B and MgcRacGAP and merely uses the central spindle to position itself.

We could not directly compare the respective localization of these endogenous proteins at the central spindle as most antibodies were generated in rabbits. Hence, we could only determine co-localization at the central spindle of all these proteins with Plk1 which was detected with a mouse monoclonal antibody. Although MKlp1, MKlp2, Aurora-B, MgcRacGAP, Plk1 and Ect2 all co-localize at the central spindle during early anaphase (Fig. 23A), close examination of late stage dividing cells revealed distinct localization patterns for some of these proteins. In late anaphase and telophase cells, MKlp2 co-localized with Aurora-B and Plk1 in two bands adjacent to the midbody structure (Fig. 23B), consistent with the notion that MKlp2 interacts with these two kinases (Gruneberg *et al.*, 2004; Neef *et al.*, 2003). In contrast, both MKlp1 and MgcRacGAP localized more closely to the midbody structure (Fig. 23B), in line with

their ability to form a stable complex, called central spindlin (Mishima *et al.*, 2002; Mishima *et al.*, 2004). When Ect2 localization was analyzed carefully, it clearly matched the localization of the MKlp1/MgcRacGAP complex near the midbody (Fig. 23B), suggesting that this complex could be involved in targeting Ect2 to the central spindle and midbody.

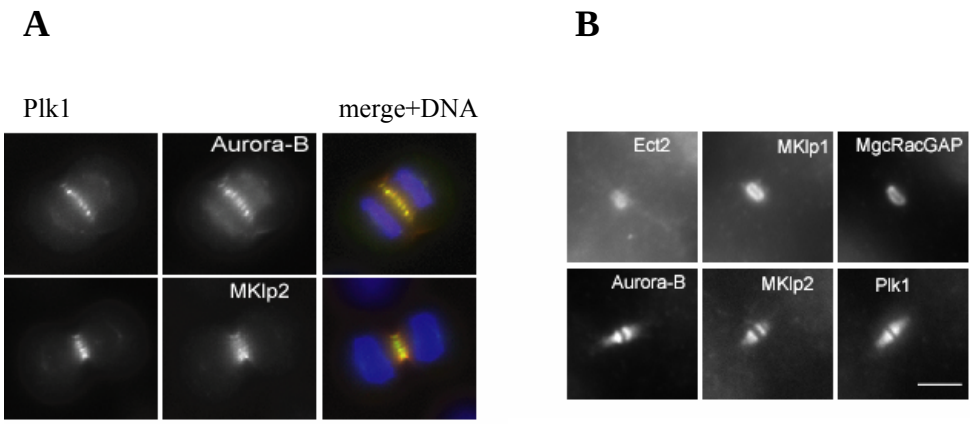

Figure 23. Ect2 co-localizes with MKlp1 and MgcRacGAP in telophase.

(A) HeLa S3 cells were fixed and permeabilized with paraformaldehyde/Triton X-100 and stained with anti-Plk1 antibodies in red (left) and anti-Aurora-B, anti-MKlp2, anti-Ect2, anti-MKlp1 and anti-MgcRacGAP antibodies in green (middle). DNA was labelled with DAPI in blue. Merged images are shown at the right. Scale bar 10 µm.

(B) HeLa S3 cells were fixed and processed as in A and stained with the above mentioned antibodies. Midbody structure localization at telophase is shown. Scale bar 3.3 µm.

2.2.4 Ect2 interacts with the MKlp1/MgcRacGAP complex via the amino-terminal BRCT domain

Since Ect2 localization to the central spindle is dependent on the MKlp1 and MgcRacGAP proteins and Ect2 co-localizes with these proteins at the midbody, we next asked whether these proteins exist in a complex. To determine whether Ect2 interacts with the MKlp1/MgcRacGAP complex, co-immunoprecipitation experiments were performed. HeLa S3 cells were synchronized by an aphidicolin/nocodazole block release protocol and harvested when most cells were present in anaphase or telophase. Endogenous Ect2 was then immunoprecipitated using anti-Ect2 antibodies or pre-immune antibodies for control (Fig. 24A). The resulting immune complexes were probed after Western blotting for the presence of various central spindle components. The mitotic kinesin MKlp1 (Kuriyama *et al.*, 2002; Matuliene and Kuriyama, 2002) and the GTPase activating protein MgcRacGAP (Hirose *et al.*, 2001) could readily be detected in Ect2 immunoprecipitates, whereas the mitotic kinase Aurora-B (Terada *et al.*, 1998) and the mitotic kinesin MKlp2 (Hill *et al.*, 2000; Neef *et al.*, 2003) were absent, and none of these proteins were observed in control immunoprecipitates (Fig. 24A). These data indicate that Ect2 interacts specifically with the MKlp1/MgcRacGAP complex. These results are in agreement with the dependency of Ect2 on MKlp1 and MgcRacGAP proteins for its central spindle and midbody localization (Fig. 22A). In addition, these results suggest that MKlp2 and Aurora-B might have an indirect regulatory function in targeting Ect2 to the central spindle.

Since Ect2 localization is mediated via the amino-terminal BRCT domain (Fig. 21B), we next investigated whether this domain could directly interact with the MKlp1/MgcRacGAP complex. To investigate this possibility, different amino-terminal myc-tagged fragments were transiently expressed in HeLa S3 cells and immunoprecipitated using anti-myc (9E10) antibodies after synchronization, as described above. As shown (Fig. 24B), the amino-terminal fragments comprising residues 1-420 and 1-333 were able to co-precipitate MKlp1 and MgcRacGAP. A smaller fragment with a truncated BRCT domain (residues 1-288) on the other hand was unable to co-precipitate MKlp1 and MgcRacGAP and the same was true for an unrelated control

protein, hWW45 (Fig. 24B and 25C) (Chan *et al.*, 2005; Valverde, 2000). In agreement with Ect2's requirement to localize to the central spindle (Fig. 21A and 21B), the minimal domain identified here that could still bind to the MKlp1/MgcRacGAP complex comprised again the complete BRCT domain. These results show that targeting of Ect2 to the central spindle is mediated via the interaction of its BRCT domain with the MKlp1/MgcRacGAP complex.

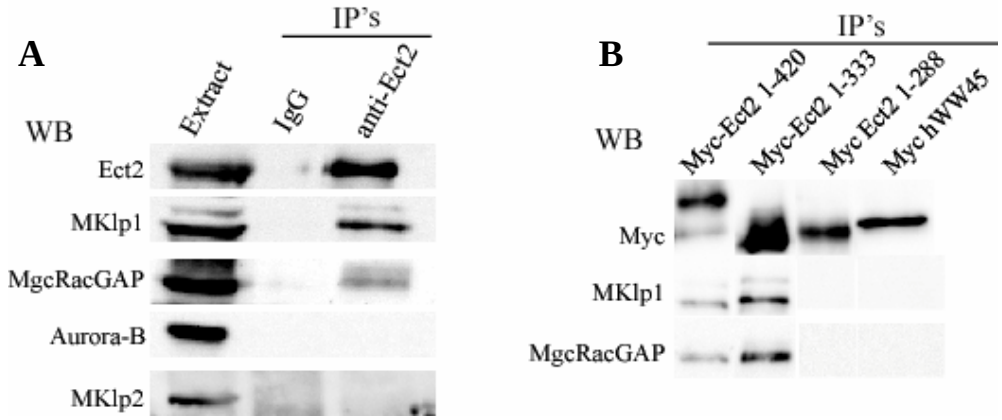

Figure 24. The MKlp1/MgcRacGAP complex co-immunoprecipitates with Ect2.

(A) Hepes lysis buffer extracts were made of HeLa S3 cells synchronized in anaphase and telophase stages by an aphidicolin-nocodazole block and release protocol. Immunoprecipitation experiments were performed on these extracts using anti-Ect2 antibodies and IgG pre-immune antibodies as a control. These immunoprecipitates were separated on SDS-PAGE, transferred onto nitrocellulose membranes and probed with anti-Ect2, anti-MKlp1, anti-MgcRacGAP, anti-Aurora-B and anti-MKlp2 antibodies.

(B) HeLa S3 cells were simultaneously synchronized and transfected with myc-Ect2 1-420, myc-Ect2 1-333, myc-Ect2 1-288 and myc-hWW45 as a control. Immunoprecipitation experiments were done as described above with anti-myc antibodies. Blots were then probed with anti-myc, anti-MKlp1 and anti-MgcRacGAP antibodies.

2.2.5 The interaction between the BRCT domain of Ect2 and the MKlp1/MgcRacGAP might be phosphorylation dependent

Recently, it was shown that the BRCT domain of BRCA1 constitutes a phosphopeptide-binding domain (Clapperton *et al.*, 2004; Manke *et al.*, 2003; Williams *et al.*, 2004; Yu *et al.*, 2003). The crystal structure of the BRCA1 BRCT domain in complex with the BACH1 (BTB and CNC homology 1) phosphopeptide has been determined (Fig. 25A). This structure revealed that two amino acid side chains of S1655 and K1702 in the BRCT domain directly interact with the phosphate group of the phosphopeptide and another direct interaction was made with an amide bond of glycine residue G1656. Given that the two side-chain interactions critical for phosphoprotein binding in BRCA1 are present and highly conserved in Ect2 (T153, K195), we considered the possibility that the interaction of Ect2 with the MKlp1/MgcRacGAP complex could require a phosphorylated docking site. Also, the Clustal-W sequence alignment of the first Ect2 BRCT repeat with BRCT repeats of BRCA1, BARD1, XRCC1, RFC1 and PTIP revealed that although the primary sequence of BRCT repeats is not well conserved, the critical residues that have been implicated in phosphopeptide binding are conserved in all the BRCT repeats analyzed (Fig. 25B). Therefore, we mutated the two highly conserved residues (T153, K195) in the Ect2 1-333 BRCT domain to alanine residues (Fig. 25B) (Clapperton *et al.*, 2004; Williams *et al.*, 2004). This myc-tagged mutant fragment (1-333, T153A/K195A) was transiently overexpressed in HeLa S3 cells and immunoprecipitated after synchronization in ana- and telophase of the cell cycle. As shown in Fig. 25C, the wild type 1-333 fragment readily co-precipitated MKlp1 and MgcRacGAP, but only low levels were bound to the mutant BRCT (T153A/K195A) domain. Immunofluorescence microscopy analysis revealed that the BRCT T153A/K195A mutant fragment was only present at low levels at the central spindle, in accordance with its weak interaction with the MKlp1/MgcRacGAP complex (Fig. 25D). Together, these data strongly suggest that the localization of Ect2 to the central spindle could be mediated via the BRCT dependent binding to the MKlp1/MgcRacGAP complex and probably involves a phosphorylation-site specific docking mechanism.

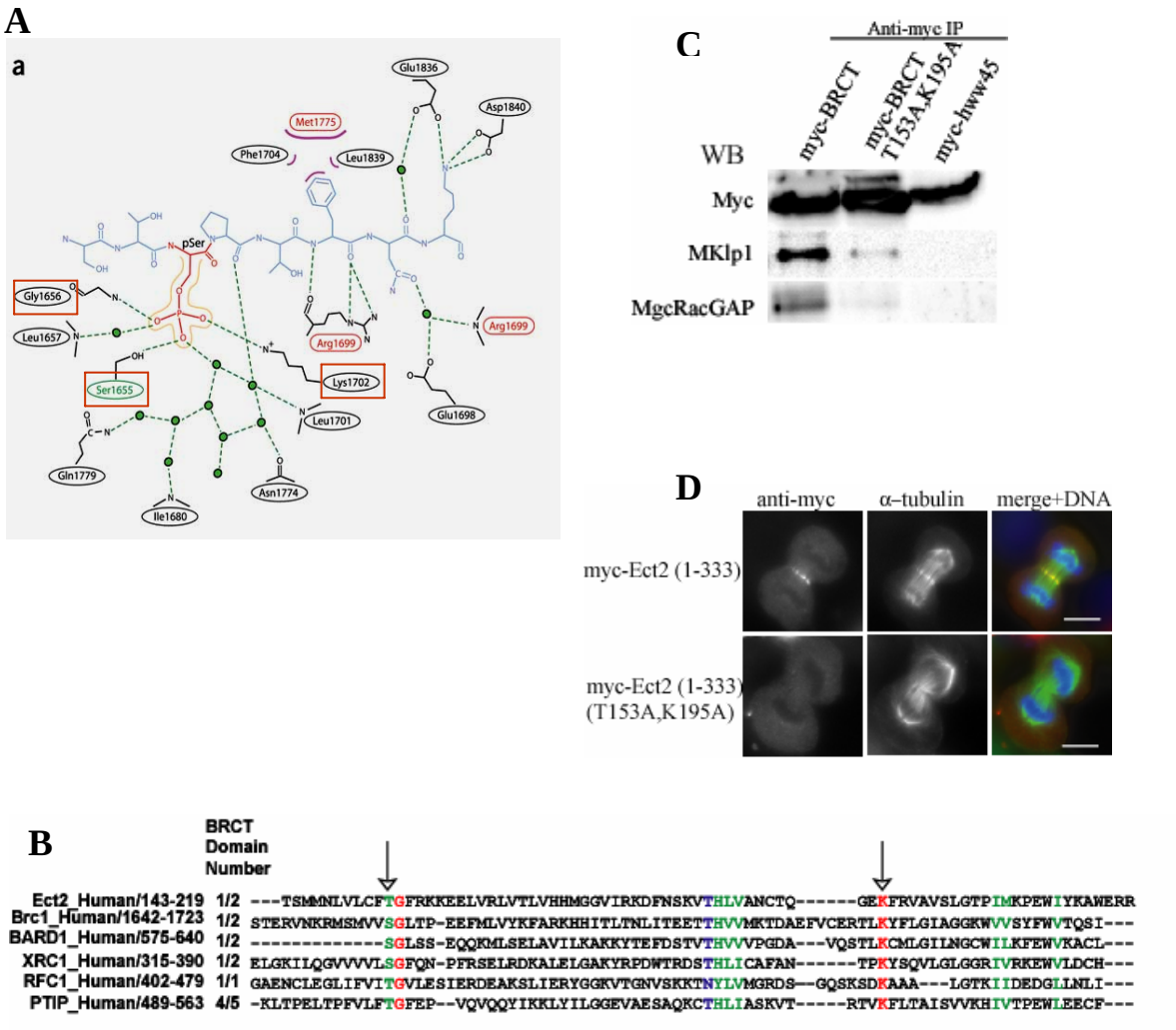

Figure 25. The MKlp1/MgcRacGAP complex interacts with the BRCT domain of Ect2 possibly in a phosphorylation dependent manner.

(A) Schematic representation of BACH1 phosphopeptide (blue) contacts with the tandem BRCT domains of BRCA1. The residues marked in red coloured boxes within the BRCT domain are highly conserved throughout the whole family of BRCT domains (see arrows in Fig. 25B). Dashed lines, hydrogen bonds; pink crescent, van der waals interactions; green circles, water molecules.Image adapted and modified from Clapperton et al*, Nature Structural and Molecular Biology 11, 512-518 (2004).*

(B) Clustal-W sequence alignment of the first Ect2 BRCT repeat with BRCA1 (Breast Cancer Carboxyl terminal), BARD1 (BRCA1 associated ring domain1), XRCC1 (X-ray repair complementing defective repair in chinese hamster cells 1), RFC1 (replication factor C1) and PTIP (pax transactivation domain-interacting protein). The BRCT domain number indicates the BRCT repeat used for alignment out of the total number of BRCT repeats present in each protein. Arrows indicate the highly conserved residues in this alignment.

(C) HeLa S3 cells were simultaneously synchronized and transfected with myc-Ect2 1-333, myc-Ect2 1-333 T153A/K195A and myc-hWW45 (as a control), respectively. Anti-myc antibodies coupled to protein G sepharose beads were used to immunoprecipitate these proteins from cell extracts of cells synchronized in anaphase and telophase of the cell cycle. The immunoprecipitates were separated by SDS-PAGE, blotted and probed with anti-myc, anti-MKlp1 and anti-MgcRacGAP antibodies.
(D) U2OS cells were transfected with myc-Ect2 1-333 and myc-Ect2 1-333 T153A/ K195A plasmids for 36 hours and were subsequently fixed and permeabilized with paraformaldehyde/Triton X-100. These cells were stained with anti-myc in red (left) and anti-α-tubulin antibodies in green (middle). DNA was labelled with DAPI in blue. Merged images are shown at the right. Scale bar 10 µm.

2.2.6 Ect2 central spindle localization is not essential for cytokinesis

As shown above, the intact BRCT domain is necessary and sufficient for central spindle localization of Ect2. We next wondered if overexpression of this domain could displace endogenous Ect2 from the central spindle. To examine this, an antibody that detects a carboxyl-terminal epitope in Ect2 recognizing only endogenous Ect2 protein was used. Examination of cells overexpressing the amino-terminal fragments (1-333 and 1-420) showed that endogenous Ect2 was indeed displaced from the central spindle by these fragments (Fig. 26A). Expression of a shorter amino-terminal fragment (1-288) with a truncated BRCT domain (1-288) that does not localize to the central spindle did not interfere with endogenous Ect2 localization. This indicates that the BRCT domain is able to displace endogenous Ect2 from the central spindle, most likely as a result of competition with endogenous Ect2 for binding to the MKlp1/MgcRacGAP complex.

Despite displacement of endogenous Ect2 from the central spindle by the large amino-terminal Ect2 fragment (1-420), these cells did not show obvious cytokinesis defects (Fig. 26, right panel) as revealed by their mononuclear appearance (data not shown). This suggests that Ect2 central spindle localization is not absolutely required for cytokinesis and that the cortical pool of Ect2 might be sufficient to carry out cytokinesis in these cells. Surprisingly, though, cells expressing the smaller BRCT containing Ect2 fragment (1-333) became binucleated after 48 hours of expression, indicative of a cytokinesis failure in these cells (Fig. 26, right panel). Since both BRCT domain-

containing fragments displaced endogenous Ect2 equally well (Fig. 26), the cytokinesis defect upon overexpression of the 1-333 fragment is unlikely to be a result of Ect2 central spindle displacement.

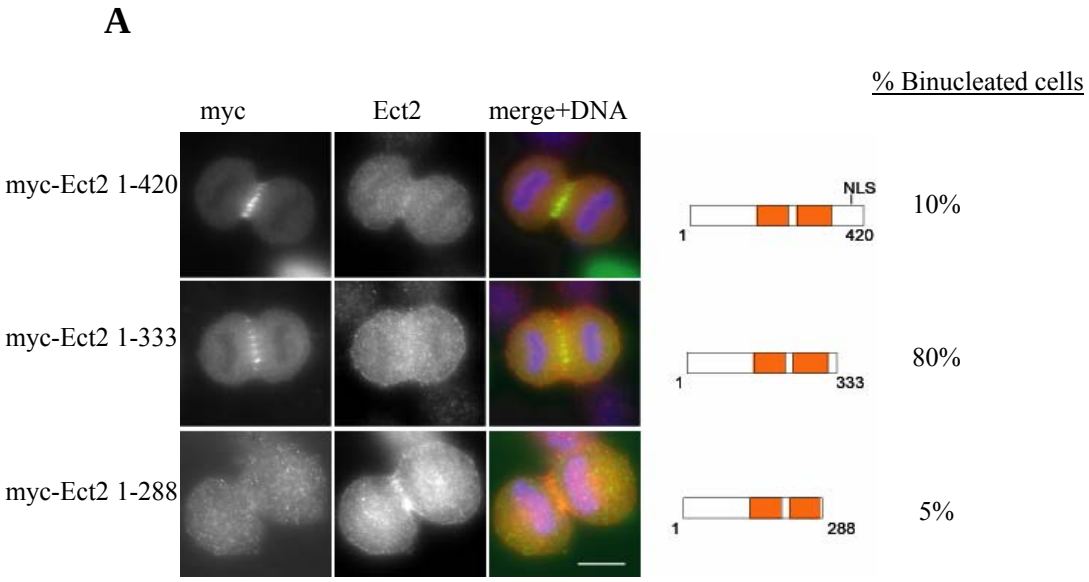

Figure 26. Exogenously expressed myc tagged Ect2 fragments at the central spindle displaces endogenous Ect2.

(A) HeLa S3 cells were grown on cover slips and transiently transfected with myc-Ect2 1-420, myc-Ect2 1-333 and myc-Ect2 1-288 constructs for 36 hours and were simultaneously fixed and permeabilized with formaldehyde/Triton X-100. These cells were stained with anti-Ect2 antibodies recognizing a carboxyl-terminally located Ect2 epitope in red (left) and anti-myc 9E10 antibodies in green (middle). DNA was labelled with DAPI in blue. Merged images are shown at the right. Scale bar 10 µm.

2.2.7 Conclusion:

In this part of the study, we examined the localization of endogenous Ect2 in human cells and, moreover, identified the domains and interacting proteins that control the subcellular localization of Ect2. We show that Ect2 localizes both to the central spindle and the cell cortex during mitosis. The central spindle localization is dependent on the amino-terminally located BRCT domain, whereas the cell cortex localization is mediated by the carboxyl-terminal PH domain. Although the central spindle targeting of Ect2 requires both the MKlp1/MgcRacGAP and MKlp2/Aurora-B complexes, only the former complex directly interacts with Ect2. We also show that targeting of Ect2 to the central spindle requires the interaction of its BRCT domain to the MKlp1/MgcRacGAP complex and is probably mediated by a phosphorylation dependent docking mechanism. Finally, we show that Ect2 central spindle localization is not absolutely essential for cytokinesis, indicating that localized GEF activity is not critical for cytokinesis. Taken together, these data show that although the targeting of Ect2 to the central spindle is mediated by protein complexes through phosphorylation dependent docking mechanism, other unknown mechanisms operate in the cell to faithfully complete cytokinesis in the absence of localized Ect2 at the central spindle.

2.3 Requirement of Ect2 in cytokinesis

2.3.1 Ect2 controls both early and late cytokinesis events

Cytokinesis involves several steps including cleavage furrow specification, contractile ring formation, cleavage furrow ingression and abscission. To explore the role of human Ect2 in this process we investigated the cytokinesis defects in Ect2 depleted cells, as well as in cells expressing the BRCT domain containing amino-terminal Ect2 fragment (1-333) in more detail. For the latter, a stable tetracycline inducible HeLa S3 cell line was generated. Addition of tetracycline to this cell line for 24 hours resulted in a strong induction of this myc-tagged Ect2 fragment as determined by Western blotting (Fig. 27A). About 50 % of the cells became binucleated within this 24 hours induction period, confirming that this fragment strongly interfered with cytokinesis.

To analyze and compare the cytokinesis defects in Ect2 depleted and amino-terminal Ect2 (1-333) overexpressing cells, spindle formation in these cells was analyzed. In cells expressing the amino-terminal Ect2 fragment (1-333), normal central spindle formation, midbody formation and cleavage furrow ingression were observed (Fig. 27B, upper panel). Despite this, these cells finally failed cytokinesis at a late stage during cytokinesis and became binucleated. In Ect2 depleted cells, bipolar spindle formation and initial central spindle formation looked apparently normal (Fig. 27B, middle panel). This is in clear contrast to what was observed after depletion of other central spindle proteins and suggests that Ect2 is not required for central spindle formation *per se*. Nevertheless, in most late anaphase cells, spindles were aberrant in that they were very voluminous and MTs were present all over the equatorial cortical region. The cause of this is most likely the absence of cleavage furrow ingression. As a result of this ingression defect, midbodies were practically absent in Ect2 depleted telophase cells and instead an abnormal spindle-like structure was present between the two reforming nuclei. Finally, the interphase microtubule structure was reformed in these cells without having undergone any form of cytokinesis. Thus, in contrast to cells expressing the BRCT-

containing fragment, cells depleted of Ect2 were not even able to form a proper cleavage furrow to start ingression.

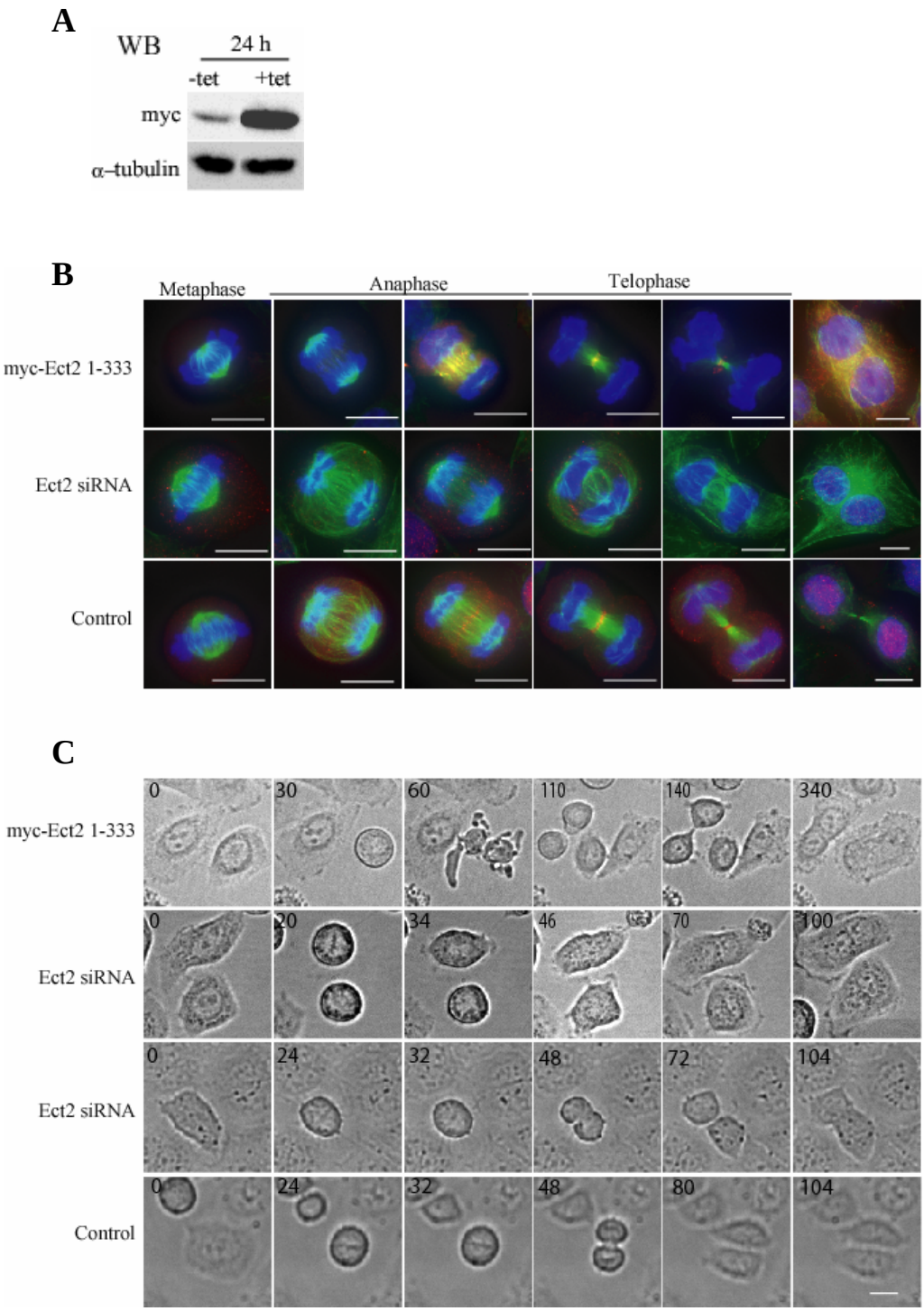

To confirm the distinct phenotypes of cells overexpressing the amino-terminal Ect2 fragment and cells depleted of Ect2, live-cell imaging was performed. In cells expressing the amino-terminal fragment, cleavage furrow formation and ingression was observed (Fig. 27C, upper panel). However, this was accompanied by extensive membrane blebbing during metaphase to anaphase transition in more than 50% of the cells. The cause of this blebbing is not clear, but we like to note that blebs are caused by rupture of the plasma membrane from the cytoskeleton, suggesting that these cells have problems with cytoskeleton rearrangements during this phase of mitosis (Charras *et al.*, 2005). The time spent in mitosis was highly variable and it seemed that cells often had difficulties to position the cleavage furrow properly. Only at a very late stage during cytokinesis the cleavage furrow regressed, finally resulting in one cell with two nuclei. We often observed that one cell had already flattened on the culture dish surface, whereas the other cell was still rounded up, suggesting that the cytoplasmic contents of these cells were practically separated. However, these cells finally regressed and fused to form one cell, suggesting that these cells exhibited a late cytokinesis defect and that abscission failed.

Figure 27. Requirement of Ect2 during cytokinesis.

(A) Western blots analysis of lysates from myc-Ect2 1-333 expressing stable cell line before and after induction with tetracycline for 24 hours are shown. Blots were probed with anti-myc and anti-α-tubulin antibodies (as a loading control).

(B) HeLa S3 cells were treated for 24 hours with GL2 (control) and Ect2 siRNA duplexes and the inducible myc-Ect2 1-333 stable cell line was induced for 24 hours with tetracycline. After fixation and permeabilization with paraformaldehyde/Triton X-100, the myc-Ect2 1-333 expressing cells were stained with anti-myc 9E10 antibodies (red), α-tubulin antibodies (green) and with DAPI (blue) and the siRNA treated cells were stained with anti-Ect2 antibodies (red), anti-α-tubulin antibodies (green) and DNA was labelled with DAPI (blue). Images are projection of deconvolved images of a series of Z stacks. Scale bar 10 µm.

(C) Live-cell imaging of myc-Ect2 1-333 expressing cells (upper panel), Ect2 depleted HeLa S3 cells (middle 2 panels) and cells treated with GL2 control oligos (lower panel). Images were made every two min and only representative frames are shown. In the myc-Ect2 1-333 expressing cell line time '0' is the last time frame for the cell on the right side, in which the cell still showed an interphase appearance. In Ect2 depleted cells and control cells (cells treated with GL2 oligos), time '0' is the last time frame for both cells that still showed an interphase appearance. Scale bar 10 µm.

In contrast, in most of the Ect2 depleted cells no obvious cleavage furrow formation or ingression could be observed and cells exited mitosis without showing any signs of cytokinesis (Fig. 27C, 2nd panel). These cells spent about 100 min in mitosis, which is similar to control cells (Fig. 27C, lower panel). Only a small number of Ect2 depleted cells showed signs of furrow formation and ingression, but then failed cytokinesis at later stages of cytokinesis. This late stage cytokinesis defect was more prominent, when cells were treated with less efficient siRNA duplex (Fig. 27C, 3rd panel).

Together, these results show that Ect2 is required for cleavage furrowing, but that overexpression of the amino-terminal Ect2 fragment affected predominantly cell-abscission.

2.3.2 RhoA and Citron kinase are not targeted to the cleavage furrow in Ect2 depleted cells

One of the early critical steps during cytokinesis is the activation of RhoA (Bement *et al*., 2005). This GTPase then controls several proteins that regulate the dynamics of the actin cytoskeleton, leading to contractile ring formation and contraction (Glotzer, 2001). A recent study in Drosophila showed that both Rho1 (RhoA) and one of the downstream targets, Sticky (Citron kinase), required *pebble* (Ect2) for proper localization to the contractile ring (Shandala *et al.*, 2004). In *Drosophila*, both Rho1 and Sticky are required for cytokinesis, but in mammalian cells the role of Citron kinase in cytokinesis has remained controversial (Cunto *et al.*, 2002; Di Cunto *et al.*, 2000). To examine this issue, we used siRNA to deplete Citron kinase and monitored HeLa S3 cells for the formation of binucleated cells, implying cytokinesis defects. As shown in Fig. 28A, in cells depleted of Citron kinase a strong increase in binucleated cells was observed and the effective depletion of Citron kinase was confirmed by Western blot analysis (Fig. 28B). Thus, Citron kinase is clearly essential for cytokinesis in HeLa S3 cells.

We next analyzed the localization of RhoA and Citron kinase during cytokinesis in human cells. In undisturbed cells, both proteins localized to the contractile ring during cytokinesis (Fig. 28C, 28D, upper panels), confirming previous results (Eda *et al.*, 2001;

Mabuchi *et al.*, 1993; Madaule *et al.*, 1998). The localization was more difficult to analyze in Ect2 depleted cells, as most of these cells do not form a cleavage furrow at all. However, in those Ect2 depleted cells that showed some cleavage furrow formation both RhoA and Citron kinase was strongly diminished at this site (Fig. 28C and 28D, middle panels), confirming and extending recent observations (Yuce *et al.*, 2005). Therefore, these data indicate that Ect2 regulates RhoA, as well as its target Citron kinase, also in human cells.

In contrast to the situation in Ect2 depleted cells, RhoA and Citron kinase could readily be detected at the cleavage furrow in cells expressing the amino-terminal Ect2 fragment (Fig. 28C and 28D, bottom panels). This result falls in line with the observation that these cells showed cleavage furrow formation and ingression (Fig. 27C). Taken together, our data indicate that the inability to target RhoA and Citron kinase to the cleavage furrow may constitute the main reason for the cytokinesis defects observed in Ect2 depleted cells. On the other hand, since RhoA and Citron kinase were properly targeted to the cleavage furrow in cells expressing the amino-terminal Ect2 fragment, it follows that cytokinesis failure in these latter cells must result through another mechanism.

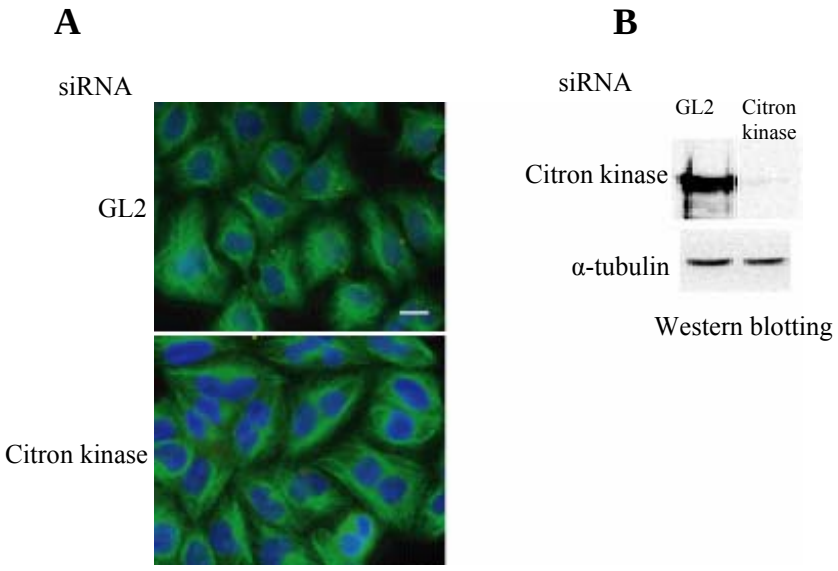

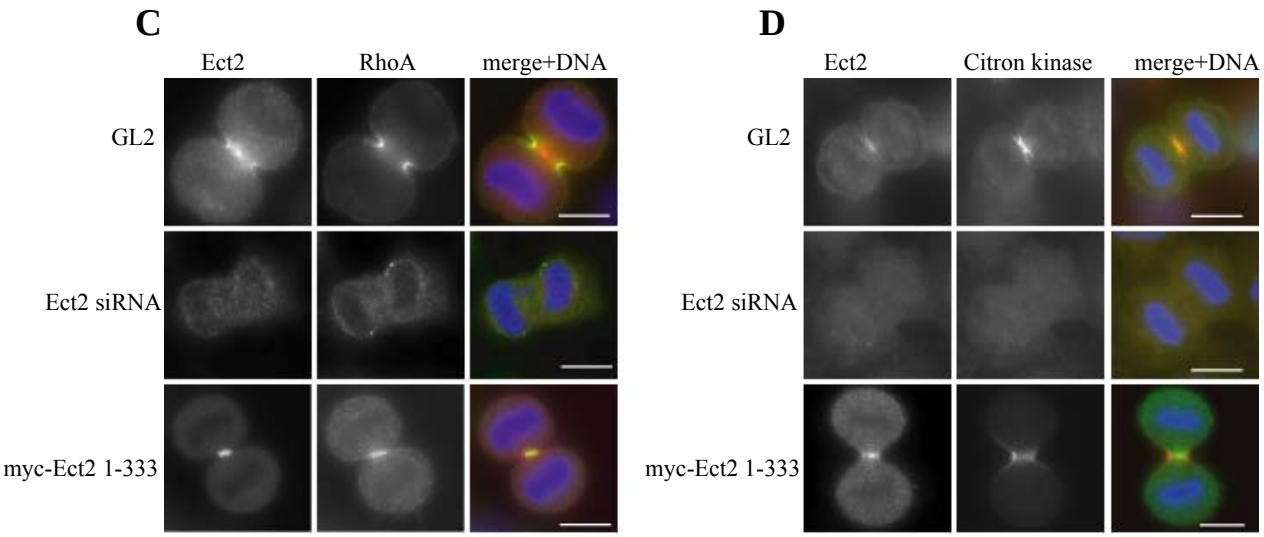

Figure 28. Ect2 targets RhoA and Citron kinase to the cleavage furrow.

(A) HeLa S3 cells were treated with siRNA duplexes against GL2 and Citron kinase for 48 hours and subsequently fixed and permeabilized with paraformaldehyde/Triton X-100. These cells were stained with anti-α-tubulin antibodies (green). DNA was labelled with DAPI (blue). Scale bar 10 µm.

B) Same as in A, but now Hepes lysis buffer extracts were made and the proteins were separated by SDS-PAGE, blotted and probed with anti-Citron kinase antibodies and anti-α-tubulin antibodies (as loading control).

C) HeLa S3 cells were treated for 36 hours with control (GL2) and Ect2 siRNA duplexes and the myc-Ect2 1-333 expressing stable cell line was induced for 36 hours with tetracycline. After fixation and permeabilization with 10% TCA/Triton X-100, siRNA treated cells (upper and middle panels) were stained with anti-Ect2 (left) in red, anti-RhoA (middle) antibodies in green and DNA was labelled with DAPI in blue. Merged images are shown on the right. The stable cell line (lower panel) was stained with anti-myc 9E10 (left) in green, anti-RhoA (middle) antibodies in red and DNA was labelled with DAPI in blue. Merged images are shown on the right. Scale bar 10 µm.

D) HeLa S3 cells were treated for 36 hours with control (GL2) and Ect2 siRNA duplexes and the myc-Ect2 1-333 expressing stable cell line was induced for 36 hours with tetracycline. After simultaneous fixation and permeabilization with paraformaldehyde/Triton X-100, siRNA treated cells (upper and middle panels) were stained with anti-Ect2 (left) in red, anti-Citron kinase (middle) antibodies in green and DNA was labelled with DAPI in blue. Merged images are shown on the right. The stable cell line (lower panel) was stained with anti-myc 9E10 (left) in green, anti-Citron kinase (middle) antibodies in red and DNA was labelled with DAPI in blue. Merged images are shown on the right. Scale bar 10 µm.

2.3.3 Nuclear targeting of the amino-terminal Ect2 (1-333) fragment can prevent cytokinesis defects

The above results clearly revealed why in Ect2 depleted cells cleavage furrow ingression is impaired, but do not explain why overexpression of the Ect2 1-333 fragment interfered with cell abscission. Whereas overexpression of full length Ect2 and the larger Ect2 amino-terminal fragment (1-420), hardly interfered with cytokinesis and localized to the nucleus during interphase, this smaller fragment localized to the cytoplasm (Fig. 30, data not shown). This is in agreement with the presence of two potential nuclear localization signals (NLS) or alternatively one bipartite NLS between residues 346-374. Based on this observation it is tempting to speculate that nuclear translocation of Ect2 during telophase could be essential for cell abscission.

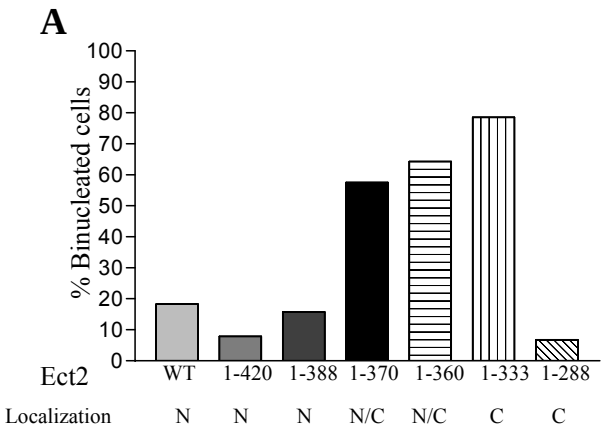

Figure 29. Overexpression of amino-terminal constructs with intact BRCT repeats but lacking an NLS caused multinucleated phenotype.

(A) Myc-tagged wild type Ect2 (WT) and myc-tagged deletion constructs, Ect2 1-420, Ect2 1-388, Ect2 1-370, Ect2 1-360, Ect2 1-333 and Ect21-288 were transfected into HeLa S3 cells for 48 hours and fixed and permeabilized with paraformaldehyde/Triton X-100. These cells were stained with anti-myc antibodies and DAPI. About 300 transfected cells each from two different experiments were independently analyzed for the presence of either a single nucleus or binucleation. The mean value of the percentage binucleated cells from both experiments is represented in the form of a histogram. The localizations of the various constructs in interphase cells are indicated as N (nuclear) or N/C (nuclear and cytoplasmic) or C (cytoplasmic).

We therefore analyzed additional myc-tagged Ect2 truncation fragments and observed that myc-tagged Ect2 fragments 1-360 and 1-370, which localized both to the cytoplasm and the nucleus during interphase, resulted in a clear increase in binucleated cells, whereas the amino-terminal fragment 1-388, which localizes predominantly to the nucleus resulted only in a small increase in the number of binucleated cells (Fig. 29). Thus, only those fragments that do not have an intact NLS and hence localize predominantly to the cytoplasm affect proper cytokinesis. To further examine the requirement of nuclear translocation, we generated a construct that could express the Ect2 1-333 fragment with three SV40 NLS sequences tagged to its amino-terminus. Analysis of cells transiently expressing this NLS-Ect2 (1-333) fragment revealed that this fragment now localized predominantly to the nucleus in interphase cells, although some weak cytoplasmic staining could sometimes be observed (Fig. 30). Interestingly, this fragment was much less potent in generating binucleated cells (30 % as compared to 80 % with the fragment lacking the NLS). These results show that nuclear translocation of this Ect2 fragment during late telophase can prevent cytokinesis failure.

To further investigate the requirement of nuclear translocation, the NLS´s in full length Ect2 and in the 1-388 fragment were removed by mutating lysine residues in the NLS sequences to aspargine residues and arginine residues to glutamine residues (^{348}KRR^{350} to ^{348}NQQ^{350} and ^{371}RKR^{373} to ^{371}QNQ^{373}) (Robbins *et al.*, 1991). Overexpression of these mutated Ect2 proteins in HeLa S3 cells showed that both mutants localized to the cytosol in interphase cells (data not shown). Overexpression of the NLS mutant version of myc-Ect2 did, however, not result in an increase in binucleated cells as compared to cells overexpressing wild type Ect2 (measured values being 12% and 17%, respectively). However, although the NLS mutated 1-388 fragment did localize to the cytoplasm, its overexpression only marginally increased the formation of binucleated cells when compared to its nuclear counterpart (25% to 9%, respectively). Thus, although the NLS motifs contribute to determine the extent of cytokinesis failure produced by various Ect2 fragments, additional sequences flanking the central Ect2 NLS region also appear to be important.

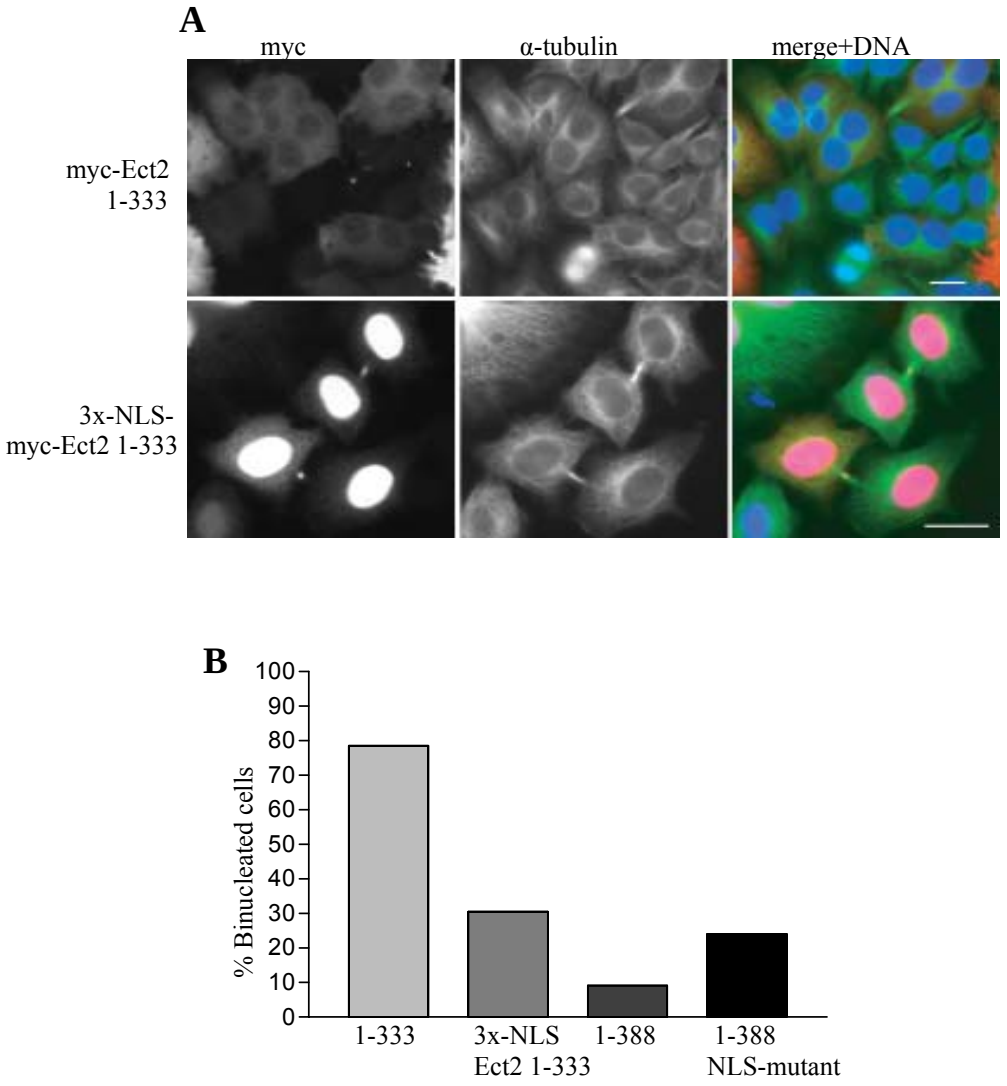

Figure 30. Effects of cytoplasmic and nuclear localization of the Ect2 fragments 1-333 and 1-388 on proper cytokinesis.

(A) HeLa S3 cells were transfected with myc-Ect2 1-333 and 3x-NLS-myc-Ect2 1-333 constructs for 36 hours and subsequently were fixed and permeabilized with paraformaldehyde/Triton X-100. These cells were stained with anti-myc antibodies in red, anti-α-tubulin antibodies in green and DNA was stained with DAPI in blue. Merged images are shown at the right. Scale bar 10 µm.

(B) HeLa S3 cells were transfected with myc-Ect2 1-333 and 3x-NLS-myc-Ect2 1-333 constructs for 48 hours and subsequently were fixed and permeabilized with paraformaldehyde/Triton X-100. These cells were stained as described above and the transfected cells were analyzed for the presence of either a single nucleus or binucleation. The mean value of the percentage binucleated cells from two independent experiments is represented in the form of a histogram.

2.3.4 The amino-terminal BRCT-containing fragment (1-333) is mislocalized as a ring-like structure perpendicular to the midbody during cytokinesis

Careful analysis of the localization of the Ect2 1-333 fragment showed that this fragment mislocalized as a ring-like structure perpendicular to the midbody in most telophase cells around the time of nuclear envelope reformation (Fig. 31A, lower panel). Co-staining with FITC-phalloidin, which stains the actin cytoskeleton, showed that this fragment partly co-localized with the contractile ring during cytokinesis (Fig. 31B). Surprisingly, when we analyzed MKlp1 and MgcRacGAP localization in these cells, we observed that those proteins also co-localized with this Ect2 fragment (Fig. 31C). MKlp1 and MgcRacGAP contain NLS sequences, like Ect2, and upon completion of cytokinesis, these proteins are translocated into the nucleus. In the presence of this amino-terminal Ect2 (1-333) fragment, however, MKlp1 and MgcRacGAP were partly retained at the midbody/contractile ring structure. This mislocalization was not observed when we overexpressed the larger fragments (1-420 and 1-388) and the Ect2 (1-333) fragment that contains the SV40 NLS sequences (Fig. 31A and data not shown). All these latter fragments were translocated to the nucleus during telophase and interfered only slightly with cytokinesis. Surprisingly, the Ect2 1-388 fragment containing the NLS mutations did not show this abnormal accumulation at the midbody/contractile ring (Fig. 31A), although it remained in the cytoplasm during telophase and, as mentioned above, it interfered with cytokinesis only slightly. Thus, a clear correlation exists between the abnormal midbody/central spindle localization of the Ect2 fragments and cytokinesis failure. Both nuclear translocation and sequences located between residue 333 and 388 can prevent this abnormal localization. Although the exact nature of this mislocalization is still unclear, these results indicate important regulatory functions of the region between the BRCT domain and the GEF domain, including the targeting of Ect2 to the nucleus.

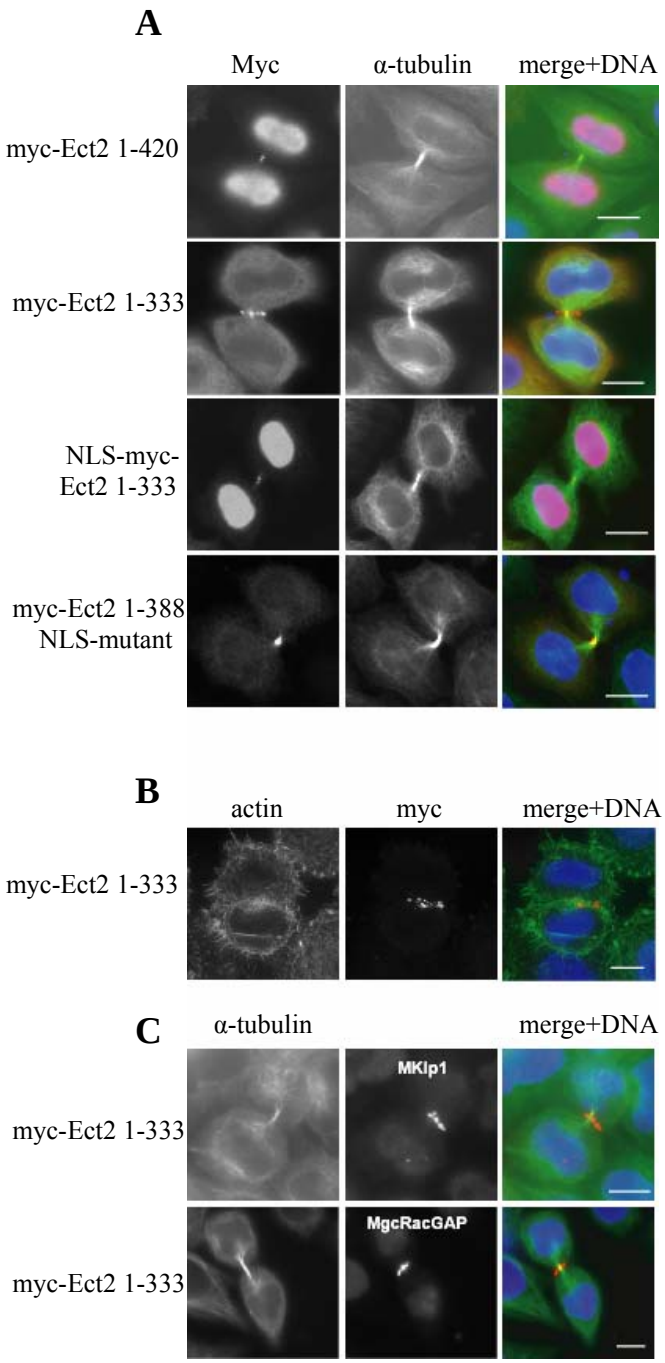

Figure 31. Ect2 1-333 is mislocalized as a ring at the cell cortex near the midbody during cytokinesis.

(A) Myc-Ect2 1-420, myc-Ect2 1-333, and NLS-myc-Ect2 1-333 and myc-Ect2 1-388-NLS-mutant were transiently overexpressed in HeLa S3 cells and grown for 48 hours before fixation and permeabilization with paraformaldehyde/Triton X-100 as described above. Cells were stained with anti-myc in red, anti-α-tubulin in green and DNA was labelled with DAPI in blue. Merged images are shown at the right. Scale bar 10 μm.

(B) Myc-Ect2 1-333 stable cell line was induced for 36 hours and stained with FITC-phalloidin in green, anti-myc antibodies in red and DNA was stained with DAPI in blue. Merged images are shown at the right with scale bar 10 μm.

(C) Myc-Ect2 1-333 stable cell line was induced for 36 hours and stained with anti-MKlp1 and anti-MgcRacGAP antibodies in red, anti-α-tubulin antibodies in green and DNA was labelled with DAPI in blue. Merged images are shown at the right. Scale bar 10 μm.

2.3.5 Conclusion:

Although Ect2 has been shown to be required for cytokinesis, the exact mechanisms by which Ect2 controls cell division were not known. Here we show that depletion of Ect2 impaired cleavage furrow formation and ingression. Concomitantly, two proteins required for cytokinesis, RhoA and Citron kinase, fail to accumulate at the cell cortex. Also, overexpression of appropriate amino-terminal Ect2 fragments blocked cytokinesis, but in these cells, RhoA and Citron kinase localized to the cell cortex concomitant with the ingression of the cleavage furrow. However, cell abscission finally failed in these cells. This abscission failure could be correlated with the persistence of the amino-terminal Ect2 fragments at striking ring-like structures surrounding the midbody, indicating that completion of cell division requires the displacement of Ect2 from the contractile ring and its re-import into the reforming cell nucleus. These data show that interference with Ect2 function blocks cytokinesis by both impairing cleavage furrow formation and cell abscission. They also provide evidence that Ect2 is required throughout cytokinesis accompanied with multiple regulation mechanisms.

3.0 Discussion

Cytokinesis is the process that completes the programme of cell division resulting in two daughter cells. This process is fundamental to life and has recently attracted a lot of attention, primarily because it is essential for genome maintenance, and thus its proper functioning is essential for human health. Despite this, relatively little is know about it, partly due to its complexity. Moreover, because of the low conservation of the regulatory processes that control cytokinesis, extrapolation from genetically tractable organisms, like yeasts, is often not possible. Nevertheless, in the past years a number of proteins have been identified that are required for proper cytokinesis in animal cells. These include components required for central spindle formation, assembly of the contractile ring, cleavage furrow ingression and addition of new membranes during the invagination of plasma membrane (Balasubramanian *et al.*, 2004; Guertin *et al.*, 2002). Here we have investigated the human guanine nucleotide exchange factor (GEF) Ect2, an orthologue of the *Drosophila pebble* gene, which is essential for cytokinesis. In particular, we have explored the potential regulatory role of Ect2 phosphorylation by mitotic kinases, its targeting to the central spindle and its functions during cytokinesis.

3.1 Mitotic phosphorylation of Ect2

Reversible protein phosphorylation by protein kinases is one of the main regulatory posttranslational mechanisms controlling mitotic progression (Nigg, 2001). Phosphorylation not only directs the allosteric regulation of enzyme activity, but is also important for controlling protein-protein interactions and regulating the subcellular localization of proteins. In agreement with a previous report (Tatsumoto *et al.*, 1999), we could show here that Ect2 is hyperphosphorylated during mitosis indicating that Ect2 may possibly be regulated by reversible phosphorylation. Although it has been suggested that phosphorylation of Ect2 is required for its maximal GEF activity (Tatsumoto *et al.*, 1999), this observation seemed to be somewhat controversial. In *Drosophila*, cyclin B and cyclin B3 interfered with cytokinesis in a *pebble* dependent manner suggesting that

pebble's function is inhibited, rather than activated, by Cdk1 activity (Echard and O'Farrell, 2003). We observed that in human cells, Ect2 phosphorylation paralleled the presence of cyclin B and recent results have shown that Ect2 is rapidly dephosphorylated in cells upon addition of the Cdk1 inhibitor BMI-1026 (Niiya *et al.*, 2005), suggesting that human Ect2 is a direct substrate of Cdk1. Since Ect2 activity is required for cleavage furrow formation during anaphase and telophase, a period of low Cdk1 activity, it is more likely that Ect2 dephosphorylation, rather than phosphorylation, could be important for its activation. Our attempts to investigate the effects of Ect2 GTP exchange activity on RhoA *in vitro* did not reveal a difference between phosphorylated and dephosphorylated recombinant Ect2 suggesting that phosphorylation might not directly regulate Ect2 activity. These experiments were performed with recombinant Ect2 purified from Sf9 insect cells. Although Ect2 from OA treated Sf9 insect cells showed a phosphorylation pattern similar to endogenous recombinant Ect2 (as determined by MS), the phosphorylation pattern might not be identical. Therefore, these results do not rigorously exclude a contribution of Ect2 phosphorylation in regulating its GEF activity. Alternatively, (de)phosphorylation might not directly regulate Ect2 GEF activity, but rather its localization or interaction with upstream and downstream binding partners as described below.

To further explore the function of Ect2 phosphorylation during mitosis, we used mass spectrometry to identify mitosis specific phosphorylation sites in endogenous Ect2. In total, we could identify six sites that were specifically phosphorylated during mitosis. Of these, five sites are highly conserved throughout evolution, suggesting that these could have important regulatory functions. Three of the identified phosphorylation sites were followed by a proline residue, indicating that these sites were phosphorylated by proline directed kinases, e.g. Cdks or MAPKs. Although we could not directly demonstrate that Ect2 is a Cdk1 substrate *in vitro*, Niiya and co-workers showed that inhibition of Cdk1 resulted in the dephoshorylation of Ect2, indicating that Ect2 is a Cdk1 substrate *in vivo* (Niiya *et al.*, 2005). Moreover, recently an important Cdk1 phosphorylation site has been identified in Ect2 as described further below (Hara *et al.*, 2005; Yuce *et al.*, 2005). Three of the identified sites that were phosphorylated *in vivo* could also be phosphorylated by Plk1 *in vitro* suggesting that these are Plk1 sites. Indeed, one of them (S20) is located

within the Plk1 consensus phosphorylation sequence (D/E-X-pS/pT). Thus, both Plk1 and Cdk1 might be prime regulators of Ect2. Unfortunately, however, our mutational analysis did not clearly reveal important roles for these phosphorylation sites in regulating Ect2 function. Although some elevated increase in multinucleated cells was observed upon expression of the individual alanine mutants, especially S20A, the mutant form in which all these mutations were combined did not result in any increase in multinucleate cells when overexpressed. This is rather surprising, but might indicate that too many mutations have an adverse effect on the protein (e.g. folding problems). All Ect2 mutants still localized properly, indicating that the observed effect could not be attributed to improper targeting and suggesting that these phosphorylation sites are not required for localizing Ect2 to its sites of action. Since endogenous Ect2 was still present in all these cells, we cannot exclude the possibility that the absence of more severe phenotypes (and proper localization) could be a result of the presence of the endogenous protein. Ideally, these experiments should be performed in an Ect2 depleted cell line. However, despite the fact that siRNA rescue experiments are becoming more common, we were not able to perform such experiments with human Ect2. The main reason for this is the low transfection efficiencies of Ect2 encoding constructs, a problem that has also been reported by others (Hara *et al.*, 2005). Thus, although we have identified a number of potentially interesting Plk1 and Cdk1 phosphorylation sites in Ect2, we have so far not been able to discover the functions of these phosphorylation sites. While one could suggest that these phosphorylation sites might not be important for Ect2 regulation, their strong conservation among different species implies that they fulfill evolutionarily conserved functions. Improvements of siRNA rescue experiments will hopefully reveal the function of these intriguing phosphorylation sites in the near future.

3.2 Ect2 targeting and oncogenic potential

Ect2 has been shown to localize to the central spindle and the midbody during mitosis and we could confirm these observations (Tatsumoto *et al.*, 1999). In addition, however, we observed cortical staining of Ect2 throughout mitosis. This suggests that two different pools of Ect2 exist, one targeted to spindle structures and the other one to the cortex. To further investigate the targeting of Ect2 to these structures, a number of truncation constructs were generated. Analysis of the localization of these truncated proteins in HeLa S3 cells revealed that the central spindle targeting domain was located in the amino-terminal half, whereas the cortical targeting was mediated by the carboxyl-terminal domain. In particular, the central spindle localization required an intact BRCT domain whereas the cortical localization was dependent on the PH (pleckstrin homology) domain. Considering that PH domains constitute lipid-binding motifs (Blomberg *et al.*, 1999), it is likely that the cortex association of Ect2 reflects a direct interaction with the plasma membrane. The PH domain has been shown to be essential for the cell transforming activity of the carboxyl-terminal (GEF containing) Ect2 domain (Miki *et al.*, 1993; Saito *et al.*, 2004; Solski *et al.*, 2004). Recent results in *C. elegans* indicate that the human Ect2 homologue in *C. elegans* positively regulates the Ras signalling pathway during vulval development in a Rho1 dependent manner (Canevascini *et al.*, 2005). This raises the possibility that the transforming activity of the mammalian Ect2 could be due to hyperactivation of the RAS/MAPK pathway. The fact that only the carboxyl-terminal Ect2 fragment containing the PH domain has this potential, and not the full length protein, is most likely due to the reason that this fragment localizes to the cytoplasm (and membranes) and therefore can interact with RhoA during interphase, in contrast to full length Ect2 which is present in the nucleus. Accordingly, it has been shown that full length Ect2 lacking an NLS also has transforming potential, albeit to a lesser extent than the carboxyl-terminal domain (Saito *et al.*, 2004). The requirement of the PH domain for the transforming activity indicates that membrane targeting of Ect2 is important for this activity.

3.3 A model for Ect2 targeting to the central spindle

To explore the mechanism(s) responsible for targeting of Ect2 to the central spindle, we depleted the central spindle components MKlp1, MgcRacGAP, MKlp2 and Aurora-B, respectively. Even though MKlp1, MgcRacGAP, MKlp2 and Aurora-B complexes contribute to the central spindle formation, some central spindle structures were still present in these depleted cells, allowing us to analyze the localization of Ect2. This revealed that both the MKlp1/MgcRacGAP and MKlp2/Aurora-B complexes were required for targeting Ect2 to the central spindle. However, although both complexes were required for Ect2 targeting, only the MKlp1/MgcRacGAP complex showed a direct interaction with Ect2 in biochemical experiments. Moreover, only the MKlp1/MgcRacGAP complex co-localized with Ect2 at the midbody in telophase cells. The MKlp2/Aurora-B complex might therefore have a more indirect role in targeting Ect2 to the central spindle, as discussed below. The interaction of Ect2 with the MKlp1/MgcRacGAP complex was mediated via the Ect2 BRCT domain. The BRCT domains of BRCA1 have recently been shown to bind to their target proteins in a phosphorylation dependent manner (Clapperton *et al.*, 2004; Manke *et al.*, 2003) and the critical residues required for binding the phosphate moiety are highly conserved. The Ect2 BRCT domain has been shown to preferentially bind to phosphopeptides (Yu *et al.*, 2003) and this encouraged us to mutate the two critical phosphopeptide binding residues (T153A, K195A) in the Ect2 BRCT domain. Interestingly, this mutant Ect2 (1-333) fragment was much less efficient in co-precipitating the MKlp1/MgcRacGAP complex from mitotic cell lysates and only showed weak central spindle localization and was predominantly spread throughout the cytoplasm as compared to the wild type fragment. These results strongly suggest that the binding of Ect2 to the MKlp1/MgcRacGAP complex requires a phosphorylated docking motif within this complex. Unfortunately, so far, no consensus docking site for Ect2 BRCT domains has been identified and hence, the exact mechanism of docking of Ect2 to the MKlp1/MgcRacGAP complex is still unknown. However, it is interesting that the Aurora-B kinase has been shown to phosphorylate MgcRacGAP and, moreover, the MKlp2/Aurora-B complex is required for targeting Ect2 to the central spindle. It is therefore tempting to speculate that Aurora-B

might generate a docking site on MgcRacGAP (Fig. 32). Alternatively, Plk1, another mitotic kinase targeted to the central spindle via MKlp2, could be another interesting candidate kinase that could create a potential docking site.

Recently, Yuce *et al* identified a phosphorylation site, T342, in mitotic Ect2 that prevents the interaction of Ect2 with MgcRacGAP in metaphase (Yuce *et al.*, 2005). Hara *et al* independently identified the same site (although they erroneously termed it T341) by analyzing recombinant Ect2 protein, which was simultaneously phosphorylated *in vitro* by Cdk1 and Plk1 (Hara *et al.*, 2005). A proline residue follows this site, indicating that it is a consensus Cdk1 phosphorylation site. We have not been able to identify this interesting site in endogenous mitotic Ect2, which might either reflect a low phosphorylation stochiometry *in vivo*, and/or the use of different MS protocols and possibly poor ionization or flight behaviour of this particular peptide. According to Yuce *et al*, this site becomes dephosphorylated upon metaphase to anaphase transition allowing interaction of Ect2 with MgcRacGAP only during ana- and telophase of the cell cycle. Taken together, we therefore like to propose that both Ect2 dephosphorylation (from metaphase to anaphase transition) and the simultaneous generation of a BRCT docking site on MgcRacGAP by Aurora-B (or Plk1) could be important for targeting Ect2 to the central spindle (Fig. 32). This dual mechanism would provide a tight regulation of the spatial and temporal localization of Ect2 to spindle structures.

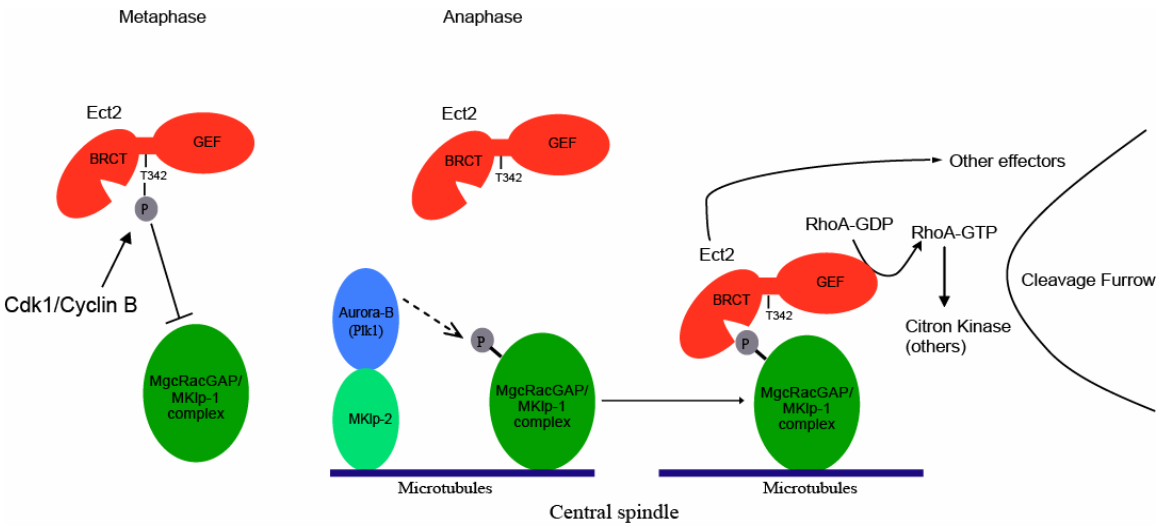

Figure 32. Proposed model for the targeting of Ect2 to the central spindle. For details see text.

3.4 Ect2 targets RhoA to the cleavage furrow independently of its central spindle localization

Several theories have been put forward for signals that determine cleavage plane specification (Burgess and Chang, 2005). In mammalian somatic cells, the central spindle and/or astral MTs are believed to be required for this specification. Spindle MTs are necessary for activation of RhoA and its specific targeting to the plane of future cell division (Bement *et al.*, 2005). In turn, RhoA regulates the actin cytoskeleton and hence is required for the formation and contraction of the actomyosin based contractile ring. How exactly the MTs signal to RhoA has long been a mystery. The identification of Ect2 GEF proteins in different higher eukaryotes and their essential function during cytokinesis provided a possible link between central spindle MTs and RhoA activation.

Here, we could show that Ect2 is essential for RhoA targeting to the cleavage furrow. It has recently been shown that RhoA at the cleavage furrow is in its active state (GTP bound), indicating that Ect2 targets RhoA to the cleavage furrow by exchanging GDP for GTP on RhoA (Bement *et al.*, 2005; Glotzer, 2005). In the absence of Ect2 (using siRNA mediated gene silencing), RhoA was not targeted to the cortex and no cleavage furrow formation and ingression occurred. This resulted in the exit of mitosis, without any form of cytokinesis, resulting in the formation of binucleated cells. Some cells depleted of Ect2 still showed some signs of cleavage furrow ingression and this percentage increased when a siRNA duplex was used that depleted Ect2 less efficiently. This indicates that Ect2 is not only required for cleavage site determination, but also for ingression. This is in agreement with the role of RhoA in both processes.

The striking localization of Ect2 suggested that a precisely localized population of Ect2 would activate RhoA locally, thereby ensuring cleavage furrow formation at a position determined by the central spindle. Surprisingly, however, we found that we could displace endogenous Ect2 from the central spindle without abolishing cytokinesis. This was achieved by overexpression of particular Ect2 amino-terminal fragments, which compete with endogenous Ect2 for binding sites on the MKlp1/MgcRacGAP complex. Similarly, RhoA was still targeted to the site of cleavage furrow formation in cells depleted of MKlp1, which also results in mislocalization of Ect2 (Yuce *et al.*, 2005), and

cleavage furrow ingression still occurred in cells depleted of PRC1, which essentially lack central spindle structures (Mollinari *et al.*, 2005). Although it is difficult to rigorously exclude that very low amounts of Ect2 might have persisted at the central spindle (or remnants thereof) under all these conditions, these results indicate that physiological levels of localized Ect2 activity are not strictly required for cytokinesis. These results suggest that it is not solely the localized Ect2 GEF activity that targets RhoA specifically to the cleavage furrow but that additional landmarks might be present at the cleavage furrow to which RhoA is recruited. If so, this would mean that RhoA is not the most upstream component at the cortex that specifies the place of cleavage furrow formation, but that other "earlier" factors must be involved. The placement of this potential landmark is, however, microtubule dependent (astral microtubules?), since in the absence of MTs, RhoA is not targeted to the cleavage furrow.

Mitotic cells treated with actin depolymerizing drugs cannot undergo cytokinesis, because the actomyosin ring is absent and these cells delay mitotic exit. Remarkably, cells depleted of Ect2 cannot undergo cytokinesis either, but do not show any obvious mitotic delay. However, cells overexpressing the amino-terminal Ect2 (1-333) domain that interfered with cytokinesis did show great variations in the duration of cytokinesis. Although not tested, this could indicate that the presence of Ect2 is involved in delaying cytokinesis under unfavourable conditions. If true, this might suggest a role for Ect2 in some kind of cytokinesis checkpoint.

One of the established downstream targets of RhoA is Citron kinase (Naim *et al.*, 2004; Shandala *et al.*, 2004) and, in agreement, we observed that Citron kinase is targeted to the cleavage furrow in an Ect2 (and hence RhoA-GTP) dependent manner. The role of Citron kinase in cytokinesis in mammalian cells is, however, still controversial (Di Cunto *et al.*, 2000; Eda *et al.*, 2001; Madaule *et al.*, 1998). We therefore analyzed HeLa S3 cells depleted of Citron kinase (using siRNA oligoduplexes) and discovered that this kinase is essential for cytokinesis in these cells. Since mice lacking Citron kinase display relatively mild phenotypes (Di Cunto *et al.*, 2000), this either suggests that mouse cells are less dependent on Citron kinase or that other homologous kinases, including ROCK kinases, could complement this function in mice.

3.5 Interference with Ect2 function blocks cytokinesis by impairing both cleavage furrow formation and abscission

It has been suggested that the cytokinesis defect in cells overexpressing the amino-terminal Ect2 domain (1-333) could be a result of low Rho-GTP levels, because this domain interacts with the carboxyl-terminal half of endogenous Ect2 that harbours the catalytic GEF domain (Kimura *et al.*, 2000). Our detailed analysis of the cytokinesis defects caused by the 1-333 fragment showed, however, that RhoA and Citron kinase were still targeted to the cleavage furrow. Since it is the active form of RhoA that localizes to the cleavage furrow, this shows that still enough active RhoA was formed in these cells and, in agreement, cleavage furrow formation and ingression still occured in these cells. Moreover, we observed extensive membrane blebbing in these cells, suggestive of highly dynamic cortical cytoskeletal rearrangements. Rho regulates various cortical activities through actin remodelling and it has been shown that depletion of RhoA could suppress membrane blebbing. This implies that cells overexpressing the amino-terminal Ect2 domain (1-333) produce sufficient amounts of mislocalized RhoA-GTP. The membrane blebbing in these cells could therefore be caused by mislocalized Rho-GTP resulting from displaced Ect2. These results strongly argue against the hypothesis that the amino-terminal fragment induces cytokinesis failures by its effect on Ect2 GEF activity (Kimura *et al.*, 2000).

Not only the 1-333 fragment interfered with cytokinesis, but also larger fragments (Ect2 1-360, Ect2 1-370) resulted in cytokinesis defects (80%, 65% and 58% multinucleated cells, respectively), albeit to a lesser extent than the Ect2 1-333 fragment (80%). These larger fragments contained the T342 phosphorylation site excluding the possibility that it is the absence of this regulatory site that determines the potential to interfere with cytokinesis. Further investigations showed that all Ect2 amino-terminal fragments that interfered with cytokinesis lacked a proper NLS sequence and remained in the cytosol throughout the cell cycle. Therefore, the sustained presence of these fragments at the central spindle and the contractile ring during telophase could be an explanation why these particular fragments interfered with cell abscission. In agreement, addition of SV40 NLS sequences to the fragment (Ect2 1-333) that interfered maximally

with cytokinesis, strongly reduced the potential of this fragment to interfere with cytokinesis, indicating that nuclear relocalization during telophase can prevent cell abscission failure. However, when we mutated the NLS in full length Ect2 and expressed this cytoplasmic protein, it did not interfere with cytokinesis. One reason for this could be the low expression of full length Ect2 even when expressed from a CMV promoter. However, even expression of an amino-terminal fragment, Ect2 1-388, with a mutated NLS resulted in only a marginal increase in the number of multinucleated cells compared to the wild type Ect2 1-388 fragment (approximately 25% multinucleated cells compared to 9% multinucleate cells). Therefore, it is not only the nuclear targeting that prevents larger Ect2 amino-terminal fragments to interfere with cytokinesis. Instead, sequences around NLS might play an essential role in preventing cytokinesis. The NLS mutant 1-388 fragment showed a normal midbody localization during telophase, in clear contrast to those fragments that interfered with abscission, which all showed a midbody associated speckled ring-like localization at the contractile ring.

In *Drosophila*, *pebbl*e has been shown to localize predominantly at the site of the contractile ring and so far has not been reported to be present at the central spindle. Nevertheless, also *Drosophila pebble* interacts with the *Drosophila* homologues of human MgcRacGAP and MKlp1 (Somers and Saint, 2003). In *Drosophila*, a model has therefore been proposed in which the cortically localized *pebble* interacts with the central spindle associated MgcRacGAP/MKlp1 complex, and thereby forms a connection between the cortical ring and the central spindle (Somers and Saint, 2003). In human cells, a ring like Ect2 structure has not been observed, but our observation that overexpressed amino-terminal fragments show a ring like structure at the site of the contractile ring suggests that a similar structure could also be formed in human cells. Moreover, MgcRacGAP and MKlp1 are targeted to this structure, similar to as what has been shown in *Drosophila*. As such a structure can only be observed in human cells upon overexpression of certain amino-terminal fragments, it suggest that either very low levels of Ect2 localize to this site or that under normal conditions this association is very transient in human cells. The cytokinesis defect observed with cells expressing the amino-terminal domain is therefore likely a result of sustained presence of this structure at the contractile ring. The reason why this is only observed with certain amino-terminal

fragments that lack NLS sequences suggest that the formation of this structure is negatively regulated by sequences around this NLS motif.

Our study strengthens the conclusion that Ect2 is a key component of the molecular machinery that brings about cytokinesis. We have identified both interaction partners and regulatory domains within Ect2 and demonstrate that the precise temporal and spatial regulation of this GEF is critical for cleavage furrow formation and ingression as well as abscission. Continued studies of the regulation and function of Ect2 will undoubtedly contribute to a better understanding of the regulatory circuits that control cytokinesis.

4.0 Materials and Methods

4.1 Materials

Chemicals were obtained from Sigma-Aldrich or Merck unless otherwise specified. Cell culture media and sera were obtained from Invitrogen and media for growing bacteria were purchased from DIFCO Laboratories or Merck. DNA primers were synthesized by Thermo-Hybaid and synthetic siRNA duplexes by Dharmacon research, Inc. Restriction enzymes were obtained from New England Biolabs, Inc., reagents for purification of DNA from QIAGEN, the minigel system from Bio-rad, Hoefer Semiphor blotting system from Pharmacia-Biotech and NUPAGE gradient gels from Invitrogen.

4.2 Plasmid constructions and site directed mutagenesis

All cloning procedures were performed according to standard techniques as described in *Molecular Cloning, A Laboratory Manual*, 2nd editition, Sambrook, J.,Fritsch, E.F., Maniatis, T., Cold Spring Harbor Laboratory Press 1989 and *Current Protocols in Molecular Biology*, Wiley, 1999. Restriction enzyme reactions were carried out as specified by the suppliers (NEB). Ligation reactions were done using T_4 DNA Ligase (NEB) or using a Rapid Ligation Kit (Roche) as described by the manufacturer's instructions. Extraction of DNA from agarose gels and preparation of plasmid DNA was performed using kits from QIAGEN according to the manufacturer's instructions. For PCR reactions, the Pfu DNA polymerase PCR System was used as recommended by the manufacturer (Promega) and reactions were carried out in a Perkin Elmer GeneAmp PCR System 9600. All PCR products were checked by sequencing at Medigenomix or Max-Planck In-house DNA sequencing facility. All DNA modifying enzymes including Klenow polymerase fragment, T_4 PNK kinase and calf-intestinal phosphatase were used from NEB according to manufacturer's instructions.

Full-length human Ect2 cDNA was amplified from a HeLa S3 cDNA library (Clonetech Laboratories, Inc.) with primers M1451 (5' GCT GAT TTA GAA GAA TAC

AAA TCA TGG CGT 3') and M1452 (5' TAA GAT TTT GGT AAC GCT TCA TAT CAA ATG 3') using Pfu DNA polymerase. The amplified PCR product was purified and used as a template for primers M1386 (5' CCG GAT CCA TCA TGG CTG AAA ATA GTG TAT TAA C 3') and M1387 (5' CCC TCG AGT CAT ATC AAA TGA GTT GTA GAT CTA C 3') comprising BamHI and XhoI restriction enzymes and cloned into a pBSKS(+) vector. The sequence of the cDNA was confirmed by sequencing. This cDNA was subcloned into a pcDNA3.1/3x-myc-C vector in frame with sequences that encode three amino-terminal myc-tags. In addition, a series of constructs was made with different amino-terminal tags including EGFP (pEGFP-T_7/C_1), GST (pGEX-6P-3), His_6 (pQE-30), FLAG (pcDNA3.1/Flag-C) and HA (pcDNA3.1/HA-C) vectors. For details, see the plasmid list (supplementary table 1). In order to create recombinant baculovirus for expression of GST-tagged Ect2 in Sf9 insect cells, the Ect2 cDNA was subcloned into the pVL13GST93 vector.

Deletion constructs Ect2 1-420, Ect2 1-333, Ect2 320-883, Ect2 414-630 and Ect2 753-883 were made by PCR amplification using the full-length ECT2 cDNA as a template and specific primers containing BamHI (5' end) and XhoI (3' end) sites. These cDNA fragments were then ligated into the pcDNA3.1/3x-myc-C vector. These constructs were verified by sequencing. Truncation construct Ect2 1-388 was made by restriction digestion of the pcDNA3.1/3x-myc-Ect2 with BamHI and EcoRV restriction enzymes and the excised Ect2 cDNA fragment was cloned into the pcDNA3.1/3x-myc-C vector. In addition, this cDNA fragment was cloned into the bacterial expression vector pQE-30 for the production of recombinant His_6-tagged protein for generating antibodies in rabbits. Truncation construct Ect2 1-288 was made by restriction digestion of the pcDNA3.1/3x-myc-Ect2 with KpnI and BglII and the excised Ect2 cDNA fragment was cloned into the pcDNA3.1/3x-myc-C vector. For generating a 3x-myc-NLS-Ect2 1-333 construct, the triple SV40T NLS sequence was excised from pEYFP-Nuc (Clonetech, a gift from Dr. Frauke Melchior) by BglII/BamHI digestion and the excised fragment was cloned into the BamHI site of the pcDNA3.1/3x-myc-Ect2 1-333 construct. The orientation of the fragment was confirmed by sequencing. For the 3x-myc-Ect2 1-333 stable cell line generation, the pcDNA3.1/3x-myc-Ect2 1-333 vector was digested with the AflII restriction enzyme and filled in the 5' overhangs with Klenow fragment

followed by subsequent XhoI restriction digestion. This excised Ect2 cDNA fragment was then cloned into the pcDNA4/TO puromycin vector.

Site directed mutagenesis was performed by PCR using complementary oligonucleotides according to Stratagene's quick change site directed mutagenesis method. For a list of all point mutations see the plasmid list (supplementary table 1). All mutations were confirmed by DNA sequencing.

An EST clone encoding the hWW45 cDNA was obtained from the Image consortium (IMAGp99J155583Q3, Genbank ID ai679398). This cDNA was amplified by PCR with primers M1770 (5' CCG GAT CCA GGA TGC TGT CCC GAC AGA AAC C3') and M1771 (5' CCT CTA GAC TCG AGT CAA AAA TTT TTT CCA TGT TGT TGG GC 3'). The insert was excised using BamHI and XbaI restriction enzymes and cloned into a pBS-SK vector. The cDNA sequence was verified by sequencing and subcloned into pcDNA3.1/3x-myc-C vector using the restriction sites BamHI and XhoI. Wild type and mutant (K82R) Plk1 plasmids have been described before (Meraldi *et al.*, 2002; Smits *et al.*, 2000).

4.3 Antibodies

For generating rabbit polyclonal antibodies against human Ect2, an amino-terminal Ect2 protein fragment (residues 1-388) fused to a polyhistidine tag was used. *Escherichia coli* strain JM109 carrying this plasmid was grown overnight at 37^{o}C in LB medium with Ampicillin and diluted (20 times) next day into 500 ml of pre-warmed LB medium with Ampicillin and grown for three hours at 37^{o}C until the OD_{600} of the culture reached approximately 0.5-0.8. At this density, the expression of the His_6-Ect2 fusion protein was induced with 1 mM IPTG for 3-4 hours. Cells were harvested, resuspended in lysis buffer (150 mM NaCl, 10 mM imidazole, 0.05 % NP40, 1 mM PMSF, 0.1 mM EDTA, 5 mM β-Mercaptoethanol, 20 mM NaH_2PO_4/Na_2HPO_4 (pH 7.8) and 0.5 mg/ml lysozyme) and disrupted using a sonicator at 4°C (Bandelin SONOPLUS homogenisatoren HD2070, HD2200). The lysate was then cleared (centrifuged at 10000 rpm for 10 min) and incubated with one ml of 50% Ni-NTA agarose beads (Qiagen) on a rotating wheel for

one hour at 4°C. Thereafter, the Ni-NTA beads were washed three times with 10 mM imidazole wash buffer (10 mM imidazole, 500 mM NaCl, 0.05 % NP40, 20 mM NaH_2PO_4/Na_2HPO_4 (pH 7.8) and 5 mM β-Mercaptoethanol) followed by two washes with 10 mM imidazole wash buffer containing 5 mM ATP and two washes with 20 mM imidazole wash buffer. The His_6-Ect2 fusion protein was then eluted with three bead-volumes of 250 mM imidazole elution buffer (250 mM imidazole, 500 mM NaCl, 0.05 % NP40, 20 mM NaH_2PO_4/Na_2HPO_4 (pH 7.8) and 5 mM β-Mercaptoethanol). The isolated fusion protein was further purified by a preparative SDS-PAGE gel. For this, the protein in the gel was stained with an ice cold solution of 0.25 M KCl and 1 mM β-mercaptoethanol. The milky white band containing the fusion protein was then cut out of the gel and placed in the dialysis bag. The protein was eluted from the gel by electrophoresis at 100V for three hours in 0.5x SDS buffer in the cold room.

This purified fusion protein fragment was then used for immunization of New Zealand white rabbits (Elevage Scientifique des Dombes, Chatillon sur Chalarone, France). In brief, about 250 μg of the His_6-Ect2 1-388 protein was first injected subcutaneously with Freund's complete adjuvant and three subsequent injections with 200 μg of protein were done intramuscularly. Specific Ect2 antibodies were purified from the serum, using the same antigen as used for immunization, immobilized on a 0.45 μm nitrocellulose membrane (Schleicher & Schuell). The serum was incubated for two hours with the immobilized antigen and unbound antibodies were washed away with PBST (PBS + 0.05% Tween-20). The specifically bound antibodies were then eluted with six volumes of 100 mM Glycine pH 2.8 and the pH of each eluate was immediately adjusted to pH 8.0 by addition of 1/10 volume of 1 M Tris-HCl pH 8.0. The first three eluates containing the highest antibody concentrations were pooled and dialyzed overnight against PBST. Finally, the antibodies were concentrated (using Amicon filters) to 1 μg/μl and frozen as small aliquots at -80°C.

A rabbit polyclonal antibody against human MgcRacGAP was made using a carboxyl-terminal peptide (CSKSKSATNLGRQG N) of human MgcRacGAP coupled to keyhole limpet haemocyanin (Sigma Genosys). For affinity purification, about 167 mg of thiopropyl sepharose powder was added to 500 μl of double distilled water. The slurry was washed twice with water and then with binding buffer (100 mM Tris-HCl pH 7.5,

500 mM NaCl, 1 mM EDTA and 5 mM β-Mercaptoethanol). About one mg of peptide was added to this slurry in 750 µl of total volume and incubated for over night at 4°C on a rotating wheel. The supernatant was removed and the sepharose beads were washed once with the binding buffer and blocked with 200 mM Ethanolamine pH 8.0 in one ml total volume for two hours at 4°C. To isolate peptide specific antibodies, about one ml of serum was incubated for three hours with the peptide bound thiopropyl sepharose beads on a rotating wheel at 4°C. After five washes with 10 mM Tris-HCl pH 7.5, 100 mM NaCl, 0.1% NP40, the bound antibody was eluted with seven times 300 µl of 100 mM Glycine pH 2.8 and the pH of the eluates was subsequently adjusted to pH 8.0 by addition of 1/10 volume of 1 M Tris-HCl pH 8.0. All the eluates were pooled and dialyzed overnight against PBS and concentrated to 1 µg/µl.

Affinity purified rabbit polyclonal antibodies against human MKlp1 and MKlp2 were gifts from Stefan Huemmer and Thomas Mayer (Max Planck Institute of Biochemistry, Martinsried, Germany).

4.4 Binding of antibodies to beads

Polyclonal antibodies were bound to Affiprep protein A beads (Biorad), by adding 15 µg of antibodies to 30 µl beads and incubated for one hour at 4°C on a rotating wheel. For coupling monoclonal antibodies, including anti-myc 9E10, a similar procedure was followed, except that immunopure immobilized protein G (Pierce) resin was used, instead of Affiprep beads. To covalently cross-link antibodies to the used matrix, the beads were washed twice with 500 µl Na Borate (pH 9.0) and then incubated in the same buffer containing 20 mM dimethyl pimelimidate. After incubation for 30 min at room temperature on rotating wheel, the beads were washed once with blocking buffer (0.5 ml of 0.2 M Ethanolamine, pH 8.0) followed by two hours incubation in this buffer on a rotating wheel at room temperature. Finally, the beads were washed with PBS.

To isolate IgGs from pre-immune sera to be used in control experiments, about 100 µl of serum was added to 150 µl of Affiprep protein A beads (Biorad) and incubated on a rotating wheel for 30-60 min at 4°C. The beads were subsequently washed three

times with ice-cold PBS followed by elution with eight times 150 µl of 100 mM Glycine pH 2.8. The pH of the eluates was adjusted to 8.0 by mixing with 1/10 volume of 1 M Tris-HCl pH 8.0. Finally, the fractions (1-3) with the highest antibody concentrations were pooled and dialyzed against PBS and concentrated to 1 µg/µl.

4.5 Generation of recombinant baculo viruses

Baculogold DNA (0.25 µg) was mixed with 2.5 µl of transfer vector (BaculoGold Kit, Pharmingen) and incubated for five min followed by the addition of 500 µl buffer-B. In the mean time, the Sf9 insect cell medium of a 3 cm plate seeded with Sf9 insect cells was replaced with 500 µl buffer-A and the DNA mixture in buffer-B was then slowly added (drop by drop) to these cells. After four hours incubation at 27°C, the cells were washed once with 2.5 ml of insect cell medium and incubated for 2-3 days at 27°C in the same medium. The medium supernatant was then collected and spun for five min at 1000 rpm and 100 µl of this cleared supernatant (Passage 0, P_0) was then used to infect Sf9 cells in a 10 cm dish. After 3-4 days, the medium culture supernatant (P_1) was collected and used for a next amplification round. Finally, the P_3 supernatant culture medium had a sufficient virus titer for the production of recombinant protein.

4.6 Production of GST-Ect2 protein from sf9 insect cells

About 250 µl (depending on the titre) of P_3 amplified recombinant Ect2 baculovirus were used for transfecting Sf9 insect cells in a 15 cm dish. After 36-48 hours of transfection, these cells were collected by centrifugation for five min at 1000 rpm. These cells were washed once with PBS containing 1 mM PMSF and lysed in 500 µl lysis buffer (10 mM HEPES pH 7.7, 20 mM β-Mercaptoethanol, 5 mM EGTA, 150 mM NaCl, 1% NP40, 1 mM PMSF, 5 mM NaF, 10 µg/ml each of Leupeptin, Chymostatin, Aprotinin and 0.1 mM Na-Vandate). Extracts were passed five times through a G27 needle and incubated

for 15 min on ice. The lysate was cleared by centrifugation at 4°C for 15 min at maximum speed in table top centrifuge and about 100 µl of glutathione sepharose beads were then added to the extract and incubated for one hour at 4°C on a rotating wheel. The beads were subsequently washed twice with lysis buffer containing 300 mM NaCl and incubated overnight at 4°C with PreScission protease (Amersham) in cleavage buffer (50 mM Tris HCl pH 7.0, 150 mM NaCl, 1 mM EDTA, 1 mM DTT and 0.01% NP40). Next day, the supernatant containing the soluble Ect2 protein without a tag was collected and concentrated if required.

4.7 siRNA experiments

For siRNA, the following target sequences were used:

Ect2: 5'AAG AGU GGU UCU GGG GAA GCA 3',
5'AAA UAC UGC UGU GAA UCU AUU 3',
5'CAA UUU AUG CAG AGA UUA AUU 3',
5'CAU UUG AUA UGA AGC GUU AUU 3',

MgcRacGAP: 5'AAG UGG CAG AGG ACU GAC CAU 3';

MKlp1: 5'AAG CAG UCU UCC AGG UCA UCU 3';

MKlp2: 5'AAC CAC CUA UGU AAU CUC AUG 3';

Aurora-B: 5'AAG GUG AUG GAG AAU AGC AGU 3'

Citron kinase: 5'CAG GAT ATA CCG TAA CAC GAA 3'
5' ATG GAA GGC ACT ATT TCT CAA 3'

SiRNA duplexes were transfected with oligofectamine (Life Technologies) according to manufacturer's instructions. As a control, the GL-2 duplex targeting the luciferase gene was used (Elbashir *et al.*, 2001).

4.8 Cell culture and generation of stable cell lines

HeLa S3 cells were grown at 37°C under 5 % CO_2 in Dulbecco's modified Eagle's medium (DMEM) (GIBCO) supplemented with 10 % heat-inactivated fetal calf serum (GIBCO-BRL) and penicillin-streptomycin (100 IU/ml and 100 μg/ml, respectively). Sf9 insect cells were grown at 27°C in TC-100 medium (GIBCO-BRL) supplemented with 10% heat inactivated serum (GIBCO-BRL) and penicillin-streptomycin (100 IU/ml and 100 μg/ml, respectively). Transfections of mammalian cells were performed using Fugene 6 reagent (Roche) according to manufacturer's instructions.

For the generation of tetracycline-inducible stable cell lines, about 10 μg of plasmid (pcDNA4T/O puromycin) encoding the myc-tagged Ect2 1-333 protein fragment was transfected using Fugene 6 (Roche) into HeLa S3 cells (15 cm dish) that stably expressed a CMV controlled tetracycline repressor gene together with a blasticidine resistance marker (pcDNA6/TR, Invitrogen). The transfected cell lines were grown in medium containing 5 μg/ml blasticidin and 36 hours after transfection 1.5 μg/ml puromycin was added to select the stably transfected clones. After three days, when small cell colonies were seen, the concentration of puromycin was reduced to 1 μg/ml. About two days later, 48 clones were picked and screened for the inducible expression of myc-Ect2 1-333 protein by addition of 1 μg/ml tetracycline. After 24 hours, cells were fixed with paraformaldehyde and analyzed by immunofluorescence microscopy after staining the cells with anti-myc 9E10 antibodies. The stable inducible cell lines were selected only if the expression of myc-Ect2 1-333 was seen upon induction with tetracycline.

4.9 Cell extracts, immunoprecipitations and western blot analysis

To enrich cells in prometaphase and metaphase stages of the cell cycle, an aphidicolin-nocodazole block/release protocol was used. In brief, HeLa S3 cells were first treated with 1.6 μg/ml aphidicolin for 17 hours, washed three times with PBS to release from the block and fresh medium was added without drugs for another six hours. Cells were then

treated with 50 ng/ml nocodazole for eight hours to arrest cells in a prometaphase like state. Mitotic cells were then collected by a "mitotic shake off", washed three times with PBS and released in fresh medium for about 90 min (spinner culture). The mitotic cell cycle stage of these cells was monitored by indirect immunofluorescence microscopy of cell aliquots stained with 4′, 6-diamidino-2-phenylindole (DAPI). To enrich HeLa S3 cells in metaphase of the cell cycle that transiently express recombinant proteins, cells were transfected with the respective plasmid constructs and simultaneously treated with aphidicolin. Further synchronization procedures were then similar to the one described above.

For making cell extracts, cells were washed with ice cold PBS containing 1 mM phenylmethylsulfonyl fluoride (PMSF) and resuspended in ice cold HEPES lysis buffer (50 mM Hepes pH7.4, 150 mM NaCl, 0.5% Triton X-100) containing 30 μg/ml RNase A, 30 μg/ml DNase, 1 μM Okadaic acid, 2 μg/ml Latrunculin-B and protease and phosphatase inhibitors (Silljé *et al*., 1999). After 15 min incubation on ice, extracts were cleared at 13000 rpm for 15 min at 4°C. Protein concentrations were determined using the Dc protein assay (Bio-Rad). For immunoprecipitations, about 10 μg of polyclonal antibodies coupled to Affi-prep protein A beads (Bio-Rad) were used. For immunoprecipitation of myc-tagged recombinant proteins, anti-myc 9E10 antibodies bound to Immunopure immobilized protein G resin (Pierce) was used. Lysates were incubated for four hours with the respective antibody bound resins and subsequently washed three times with lysis buffer. For immunoblotting, equal protein amounts were separated by SDS-PAGE, followed by transfer onto nitrocellulose membranes (Schleicher & Schuell). Membranes were incubated for one hour in blocking buffer (5% low-fat dry milk in PBST (PBS + 0.1% Tween-20). All antibody incubations were carried out in blocking buffer at 4°C for overnight. Membranes were probed with the following antibodies in PBST containing 5 % milk: affinity-purified rabbit anti-Ect2 (1 μg/ml), chicken anti-MgcRacGAP antibodies (R&D systems, 1 μg/ml), affinity purified rabbit MKlp1 (0.5 μg/ml), rabbit MKlp2 serum (1:1000), monoclonal anti-myc 9E10 (1:10 culture supernatant), monoclonal anti-Plk1 (1:20, PL2), monoclonal anti-α-tubulin (Sigma-Aldrich, 1:3000). Signals were detected by ECL SuperSignal (Pierce Chemical Co.).

4.10 Immunoprecipitation of endogenous Ect2 from HeLa S3 spinner culture cells

Five flasks of HeLa S3 cells (each 175 cm^2) grown to 90% confluence were trypsinized and and inoculated in one litre spinner culture flasks containing 500 ml DMEM + 500 ml RPMI1640 medium and 10% FCS and 1% penicillin-streptomycin. These cells were grown for 3-4 days and the medium was then removed by decanting, leaving the cell clumps at the bottom. These cells were washed once with PBS, trypsinized briefly (10 ml of trypsin was added and incubated at 37°C) to disperse the cell clumps and resuspended in the same medium containing either 1 mM thymidine or 75 ng/ml nocodazole to enrich cells in interphase and mitosis, respectively. Subsequently cells were cultured for another 20 hours in this medium, washed three times with cold PBS and released in fresh medium without drugs. Cells were then harvested, washed with PBS containing 1mM PMSF and resuspended in 10 mM Triethanolamine pH 7.2 buffer containing 150 mM NaCl for 10 min. These cells were centrifuged at 1000 rpm for three min and washed with 10 ml HB buffer (100 mM Sucrose, 25 mM HEPES pH 3.4, 2 mM EGTA, 2 mM $MgCl_2$, 1 mM DTT, 1 mM PMSF, 20 mM NaF, 0.3 mM Na-Vanadate, 1 μM Okadaic acid and 1 μg/ml of Leupeptin, Pepstatin and Aprotinin). Finally, cells were homogenised in HB buffer using a douncer with pestle B. Staining cells with trypan blue monitored the efficiency of homogenization. The extracts were cleared by centrifugation at 10000 rpm for 10 min in a SS34 rotor (Beckman), followed by ultra centrifugation at 90000 rpm in a three ml polycarbonate TLA 100.3 Beckman tube for 15 min at 4°C in a TLA 100.3 rotor (Beckman). The supernatant was collected avoiding the pellet and floating lipid layer, and transferred into a new tube. About 0.1% NP40 was added to these lysates and immunoprecipitations were done by the addition of 100-300 μl of anti-Ect2 antibody beads or pre-immune IgGs beads. After overnight incubations at 4°C on a rotating wheel, these beads were washed three times with HB buffer containing 0.1% NP40 and 150 mM NaCl but without sucrose, leupeptin, pepstatin and aprotinin. Finally the beads were resuspended in 100 μl SDS-PAGE sample buffer and one-third of the immunoprecipitates were separated on a NUPAGE 4-12% gradient gel *(Invitrogen*).

4.11 Cell cycle profile and flow cytometry analysis

Mitotic HeLa S3 cells obtained from eight triple flasks (525 cm^2 each) using the aphidicolin/nocodazole block release protocol as described above, were released in fresh medium without drugs. Cells were then collected at 20 min time intervals for 140 min. For FACS analysis, HeLa S3 cells were fixed in 70% ethanol followed by incubation for 30 min in PBS containing 10 μg/ml RNase A (Sigma-Aldrich) and 5 μg/ml propidium iodide (Sigma-Aldrich). Analysis of the stained cells was performed with a FACScan according to the manufacturer's instructions and Cell Quest Software (Becton Dickinson) was used to analyze the data.

4.12 Immunofluorescence microscopy

Cells grown on HCl treated coverslips were fixed with 3% paraformaldehyde/2% sucrose for 10 min at room temperature and subsequently permeabilized with ice cold 0.5% Triton X-100 for five min. For visualizing RhoA, cells were fixed with 10% TCA (Tri Chloro Acetic Acid) at room temperature for 15 min and permeabilized with 0.5% Triton X-100 for five min. To visualize Ect2 with polyclonal antibodies recognizing the carboxyl-terminus of Ect2 (Santa Cruz), cells were fixed and permeabilized simultaneously with 20 mM PIPES pH 6.8, 4% formaldehyde, 0.2% Triton X-100, 10 mM EGTA, 1 mM $MgCl_2$ for 10 min at room temperature. Afterwards, cells were incubated for 30 min at room temperature in blocking solution (PBS, 1% BSA). All antibody incubations were carried out for one hour at room temperature in a humidified chamber, followed by three washes with PBS. Primary antibodies used were rabbit polyclonal anti-Ect2 (762) (1 μg/ml), rabbit polyclonal anti-Ect2 raised against carboxyl-terminal epitopes (Santacruz, 1:200), rabbit polyclonal anti-MgcRacGAP (1 μg/ml), chicken polyclonal anti-MgcRacGAP (R&D systems, 1 μg/ml), rabbit polyclonal anti-MKlp1 (Santacruz, 1:200), mouse AIM-1 monoclonal anti-Aurora B (Becton Dickinson, 1:200), mouse monoclonal anti-RhoA (Santa Cruz Biotechnology, 1:200), mouse monoclonal anti-Citron kinase (BD Transduction laboratories 1:200), mouse monoclonal

anti-Plk1 (PL2) culture supernatant 1:20, sheep polyclonal anti-MKlp2 (1:1000). Primary antibodies were detected with Alexa-Fluor-488- and Alexa-Fluor-555-conjugated goat anti-mouse or anti-rabbit IgGs (1:1000, Molecular Probes). DNA was stained with DAPI (2 μg/ml). Following three washes with PBS, coverslips were mounted onto slides using mounting medium with 80% glycerol and 3% DABCO (in PBS). Immunofluorescence microscopy was performed using a Zeiss Axioplan II microscope with Apochromat 40x and 63x oil immersion objectives, respectively. Photographs were taken using a Micromax CCD camera (model CCD-1300-Y, Princeton Instruments) and Metaview software (Visitron Systems GmbH, Puchheim, Germany). For high-resolution images, a Deltavision microscope on a Nikon Eclipse TE200 base (Applied Precision) equipped with S Fluor 40x/1.3 and Plan Apo 60x/1.4 oil immersion objectives and a photometrics Cool Snap HQ camera was used for collecting 0.15 μm distanced optical sections in the Z-axis. Images at single focal planes were processed with a deconvolution algorithm and then projected into a single picture using the Softworx software (Applied Precision). Images were cropped in Adobe Photoshop 6.0, and then sized and placed in figures using Adobe Illustrator 10 (Adobe Systems Inc.).

4.13 In vitro *kinase assays*

In vitro kinase reactions were carried out for 30 min at 30°C in buffers supplemented with 10 μM ATP and 2 μCi of [γ^{32}-P]-ATP (Amersham Corp.) For Plk1 kinase assays, recombinant Plk1 WT and Plk1 KD (K82R) proteins produced in insect cells were used and kinase activities were assayed in 20 mM Hepes (pH 7.7), 10 mM $MgCl_2$, 1 mM EGTA, 5 mM NaF and 1 mM DTT with 1 μg/ml each of Leupeptin, Pepstatin and Chymostatin. Recombinant Cdk1/cyclin B complex was also produced in insect cells and kindly provided by Dr.Rudiger Neef. For measuring Cdk1/cyclin B activity, the kinase activities were assayed in buffer containing 50 mM Tris-HCl, pH 7.5, 10 mM $MgCl_2$, 1 mM DTT, 50 mM β-glycerophosphate and 10 mM NaF. GST-Aurora-B kinase WT and KD (K106R) in complex with His_6-INCENP were kind gifts from Dr. Reiko Honda. The Aurora-B kinase activities were assayed in a buffer containing 50 mM Tris-HCl, pH 7.4,

10 mM $MgCl_2$, 1 mM EGTA, 1 mM DTT, 5 mM NaF, 5 mM β-glycerophosphate and 5 mM Na-Vanadate. Substrates used in these kinase assays were recombinant Ect2 (0.2 mg/ml for all kinase assay reactions), 0.5 mg/ml casein (for Plk1), 0.4 mg/ml histone H1 (for Cdk1/cyclin B) and 0.5 mg/ml histone H3 (for Aurora-B). Kinase reactions were terminated by addition of SDS-PAGE sample buffer and heating for five min at 95°C. After separation of the proteins by SDS-PAGE, ^{32}P incorporation was visualized by autoradiography.

4.14 Live-cell imaging

For live-cell imaging, HeLa S3 cells were grown in 35 mm dishes and treated with aphidicolin (1.6 μg/ml) for 16 hours to arrest cells at the G1/S phase boundary. Cells were then washed three times with PBS, released in fresh (drug free) medium and eight hours later the medium was changed into CO_2 independent medium without L-Glutamine (GIBCO). The cell culture dish was then placed on a heated (37°C) sample stage and live-cell imaging was performed with a Zeiss Axiovert-2 microscope with Plan Neofluar 40x objective. Images were captured with 10 milliseconds exposure time at two minute intervals for 16 hours using metaview imaging software. For live-cell imaging of the myc-Ect2 1-333 stable inducible cell line, tetracycline (1 μg/ml) was added upon release from the aphidicolin block. For live-cell imaging of siRNA treated HeLa S3 cells, cells were simultaneously arrested with aphidicolin and transfected with siRNA oligoduplexes and upon release from the aphidicolin block after 16 hours, cells were again transfected with siRNA duplexes.

4.15 Mass spectrometry

Coomassie stained protein bands were excised from SDS-PAGE gels in a dust free environment and in-gel digested (Shevchenko *et al.*, 1996) with trypsin (Promega, sequencing grade). Matrix-assisted laser desorption/ionization (MALDI) time-of-flight

(TOF) mass spectrometry (Brucker Daltonik, Bremen, Germany) was used to identify the phosphorylated peptides. As a matrix, 2,5 dihydroxybenzoic acid (Bruker Daltonik) or α-cyano-4-hydroxycinnamic acid (Bruker Daltonik) were used. Subsequently, the phosphorylation sites were confirmed by post source decay (PSD) (Hoffmann *et al.*, 1999). Peptides showing the typical losses of 98 mass units (Phosphoric acid) and 80 mass units (phosphate group) were considered as phosphopeptides. The exact localization of the phosphorylated residues within the peptides was determined by MS-MS based sequencing using a quadrupole time-of-flight (QTOF) mass spectrometer.

List of Abbreviations

AA	amino acid
ATP	adenosine 5´-triphosphate
BRCT	carboxyl-terminal domain of breast cancer susceptibility protein
BSA	bovine serum albumin
CDK	cyclin-dependent kinase
cDNA	complementary deoxyribonucleic acid
CHAPS	3-[(3-Cholamidopropyl)dimethylammonio]-1-propanesulfonate
Cm	centi-metre
CMV	cytomegalo virus
CO_2	carbon dioxide
DAPI	4´,6-diamidino-2-phenylindole
DNA	deoxyribonucleic acid
DTT	dithiothreitol
ECL	enhanced chemiluminescence
EDTA	ethylene dinitrilo tetraacetic acid
ELISA	enzyme linked immunosorbent assay
FACS	fluorescence activated cell sorter
FCS	fetal calf serum
GDP	guanosine 5'-diphosphate
GEF	guanine nucleotide exchange factor
GFP	green fluorescent protein
GTP	guanosine 5'-triphosphate
HCl	hydrochloric acid
HEPES	N-2-Hydroxyethylpiperazine-N`-2-ethane sulfonic acid
IgG	immunoglobulin G
IP	immunoprecipitation
IPTG	isopropyl-beta-D-thiogalactopyranoside
IU	international unit

KD	catalytically impaired
kDa	kilo-daltons
LB	luria-broth
M	molar
mAb	monoclonal antibody
µCi	micro-curie
µl	micro-litre
µg	micro-gram
MA	mitotic apparatus
MgCl2	magnesium chloride
Min	minutes
Ml	milli-litre
Mm	milli-metre
mM	milli-molar
MT	microtubules
MS	mass spectrometry
MW	molecular weight marker
NaF	sodium fluoride
NaCl	sodium chloride
ng	nano-gram
NLS	nuclear localization signal
OA	okadaic acid
OD	optical density
PBS	phosphate-buffered saline
PCR	polymerase chain reaction
PH	plekstrin homology
PIPES:	1,4-Piperazinediethanesulfonic acid
PMSF	phenylmethylsulfonyl fluoride
RNA	ribonucleic acid
rpm	revolutions per minute
RT	room temperature

SDS-PAGE	sodium-dodecylsulfate polyacrylamid gelelectrophoresis
siRNA	small interference Ribonucleic Acid
SV40T	simian virus large T antigen
V	volts
WT	wild-type

References

Adams, R. R., Wheatley, S. P., Gouldsworthy, A. M., Kandels-Lewis, S. E., Carmena, M., Smythe, C., Gerloff, D. L. and Earnshaw, W. C. (2000). INCENP binds the Aurora-related kinase AIRK2 and is required to target it to chromosomes, the central spindle and cleavage furrow. *Curr.Biol* **10**, 1075-1078.

Aktories, K. and Hall, A. (1989). Botulinum ADP-ribosyltransferase C3: a new tool to study low molecular weight GTP-binding proteins. *Trends Pharmacol.Sci.* **10**, 415-418.

Alsop, G. B. and Zhang, D. (2003). Microtubules are the only structural constituent of the spindle apparatus required for induction of cell cleavage. *J Cell Biol* **162**, 383-390.

Amano, M., Ito, M., Kimura, K., Fukata, Y., Chihara, K., Nakano, T., Matsuura, Y. and Kaibuchi, K. (1996). Phosphorylation and activation of myosin by Rho-associated kinase (Rho-kinase). *J Biol Chem.* **271**, 20246-20249.

Andersen, S. S. (1999). Balanced regulation of microtubule dynamics during the cell cycle: a contemporary view. *Bioessays* **21**, 53-60.

Andrews, P. D., Ovechkina, Y., Morrice, N., Wagenbach, M., Duncan, K., Wordeman, L. and Swedlow, J. R. (2004). Aurora B regulates MCAK at the mitotic centromere. *Dev.Cell* **6**, 253-268.

Asnes, C. F. and Schroeder, T. E. (1979). Cell cleavage. Ultrastructural evidence against equatorial stimulation by aster microtubules. *Exp.Cell Res* **122**, 327-338.

Bahler, J., Steever, A. B., Wheatley, S., Wang, Y., Pringle, J. R., Gould, K. L. and McCollum, D. (1998). Role of polo kinase and Mid1p in determining the site of cell division in fission yeast. *J Cell Biol* **143**, 1603-1616.

Balasubramanian, M. K., Bi, E. and Glotzer, M. (2004). Comparative analysis of cytokinesis in budding yeast, fission yeast and animal cells. *Curr.Biol* **14**, R806-R818.

Balasubramanian, M. K., McCollum, D., Chang, L., Wong, K. C., Naqvi, N. I., He, X., Sazer, S. and Gould, K. L. (1998). Isolation and characterization of new fission yeast cytokinesis mutants. *Genetics* **149**, 1265-1275.

Barr, F. A., Sillje, H. H. and Nigg, E. A. (2004). Polo-like kinases and the orchestration of cell division. *Nat Rev Mol Cell Biol* **5**, 429-440.

Bement, W. M., Benink, H. A. and von Dassow, G. (2005). A microtubule-dependent zone of active RhoA during cleavage plane specification. *J Cell Biol* **170**, 91-101.

Berdnik, D. and Knoblich, J. A. (2002). Drosophila Aurora-A is required for centrosome maturation and actin-dependent asymmetric protein localization during mitosis. *Curr.Biol* **12**, 640-647.

Bishop, J. D. and Schumacher, J. M. (2002). Phosphorylation of the carboxyl terminus of inner centromere protein (INCENP) by the Aurora B Kinase stimulates Aurora B kinase activity. *J Biol Chem.* **277**, 27577-27580.

Blomberg, N., Baraldi, E., Nilges, M. and Saraste, M. (1999). The PH superfold: a structural scaffold for multiple functions. *Trends Biochem.Sci* **24**, 441-445.

Bluemink, J. G. (1971). Cytokinesis and cytochalasin-induced furrow regression in the first-cleavage zygote of Xenopus laevis. *Z.Zellforsch.Mikrosk.Anat.* **121**, 102-126.

Bonaccorsi, S., Giansanti, M. G. and Gatti, M. (1998). Spindle self-organization and cytokinesis during male meiosis in asterless mutants of Drosophila melanogaster. *J Cell Biol* **142**, 751-761.

Bork, P., Hofmann, K., Bucher, P., Neuwald, A. F., Altschul, S. F. and Koonin, E. V. (1997). A superfamily of conserved domains in DNA damage-responsive cell cycle checkpoint proteins. *FASEB J* **11**, 68-76.

Bringmann, H. and Hyman, A. A. (2005). A cytokinesis furrow is positioned by two consecutive signals. *Nature* **436**, 731-734.

Burgess, D. R. (1977). Ultrastructure of meiosis and polar body formation in the egg of the mud snail, Ilyanassa obsoleta. *Prog.Clin.Biol Res* **17:569-79.**, 569-579.

Burgess, D. R. and Chang, F. (2005). Site selection for the cleavage furrow at cytokinesis. *Trends Cell Biol* **15**, 156-162.

Caldecott, K. W. (2003). Cell signaling. The BRCT domain: signaling with friends? *Science* **302**, 579-580.

Callebaut, I. and Mornon, J. P. (1997). From BRCA1 to RAP1: a widespread BRCT module closely associated with DNA repair. *FEBS Lett.* **400**, 25-30.

Canevascini, S., Marti, M., Frohli, E. and Hajnal, A. (2005). The Caenorhabditis elegans homologue of the proto-oncogene ect-2 positively regulates RAS signalling during vulval development. *EMBO Rep.* **6,** 1169-1175.

Canman, J. C., Cameron, L. A., Maddox, P. S., Straight, A., Tirnauer, J. S., Mitchison, T. J., Fang, G., Kapoor, T. M. and Salmon, E. D. (2003). Determining the position of the cell division plane. *Nature* **424**, 1074-1078.

Cao, L. G. and Wang, Y. L. (1996). Signals from the spindle midzone are required for the stimulation of cytokinesis in cultured epithelial cells. *Mol Biol Cell* **7**, 225-232.

Carmena, M. and Earnshaw, W. C. (2003). The cellular geography of aurora kinases. *Nat Rev Mol Cell Biol* **4**, 842-854.

Carmena, M., Riparbelli, M. G., Minestrini, G., Tavares, A. M., Adams, R., Callaini, G. and Glover, D. M. (1998). Drosophila polo kinase is required for cytokinesis. *J Cell Biol* **143**, 659-671.

Casamayor, A. and Snyder, M. (2002). Bud-site selection and cell polarity in budding yeast. *Curr.Opin.Microbiol.* **5**, 179-186.

Casenghi, M., Meraldi, P., Weinhart, U., Duncan, P. I., Korner, R. and Nigg, E. A. (2003). Polo-like kinase 1 regulates Nlp, a centrosome protein involved in microtubule nucleation. *Dev.Cell* **5**, 113-125.

Castrillon, D. H. and Wasserman, S. A. (1994). Diaphanous is required for cytokinesis in Drosophila and shares domains of similarity with the products of the limb deformity gene. *Development* **120**, 3367-3377.

Chan, E. H. Y., Nousiainen, M., Chalamalasetty, R. B., Schafer, A., Nigg, E. A. and Sillje, H. H. W. (2005). The Ste20-like kinase Mst2 activates the human large tumor suppressor kinase Lats1. **24**, 2076-2086.

Chang, F., Drubin, D. and Nurse, P. (1997). cdc12p, a protein required for cytokinesis in fission yeast, is a component of the cell division ring and interacts with profilin. *J Cell Biol* **137**, 169-182.

Chang, F., Woollard, A. and Nurse, P. (1996). Isolation and characterization of fission yeast mutants defective in the assembly and placement of the contractile actin ring. *J Cell Sci* **109**, 131-142.

Chant, J. (1999). Cell polarity in yeast. *Annu.Rev Cell Dev.Biol* **15**, 365-391.

Charras, G. T., Yarrow, J. C., Horton, M. A., Mahadevan, L. and Mitchison, T. J. (2005). Non-equilibration of hydrostatic pressure in blebbing cells. *Nature* **435**, 365-369.

Clapperton, J. A., Manke, I. A., Lowery, D. M., Ho, T., Haire, L. F., Yaffe, M. B. and Smerdon, S. J. (2004). Structure and mechanism of BRCA1 BRCT domain recognition of phosphorylated BACH1 with implications for cancer. *Nat.Struct.Mol.Biol.* **11**, 512-518.

Cohen, P., Holmes, C. F. and Tsukitani, Y. (1990). Okadaic acid: a new probe for the study of cellular regulation. *Trends Biochem.Sci* **15**, 98-102.

Coleman, T. R. and Dunphy, W. G. (1994). Cdc2 regulatory factors. *Curr.Opin.Cell Biol* **6**, 877-882.

Conrad, G. W. and Williams, D. C. (1974). Polar lobe formation and cytokinesis in fertilized eggs of Ilyanassa obsoleta. I. Ultrastructure and effects of cytochalasin B and colchicine. *Dev.Biol* **36**, 363-378.

Cote, J. F. and Vuori, K. (2002). Identification of an evolutionarily conserved superfamily of DOCK180-related proteins with guanine nucleotide exchange activity. *J Cell Sci* **115**, 4901-4913.

Coue, M., Brenner, S. L., Spector, I. and Korn, E. D. (1987). Inhibition of actin polymerization by latrunculin A. *FEBS Lett.* **213**, 316-318.

Cox, D. N., Seyfried, S. A., Jan, L. Y. and Jan, Y. N. (2001). Bazooka and atypical protein kinase C are required to regulate oocyte differentiation in the Drosophila ovary. *Proc.Natl.Acad.Sci U.S.A* **98**, 14475-14480.

Cunto, F. D., Imarisio, S., Camera, P., Boitani, C., Altruda, F. and Silengo, L. (2002). Essential role of citron kinase in cytokinesis of spermatogenic precursors. *J Cell Sci* **115**, 4819-4826.

Daga, R. R. and Chang, F. (2005). Dynamic positioning of the fission yeast cell division plane. *Proc.Natl.Acad.Sci U.S.A* **102**, 8228-8232.

D'Avino, P. P., Savoian, M. S. and Glover, D. M. (2004). Mutations in sticky lead to defective organization of the contractile ring during cytokinesis and are enhanced by Rho and suppressed by Rac. *J Cell Biol* **166**, 61-71.

De Brabander, M., Geuens, G., Nuydens, R., Willebrords, R., Aerts, F. and De Mey, J. (1986). Microtubule dynamics during the cell cycle: the effects of taxol and nocodazole on the microtubule system of Pt K2 cells at different stages of the mitotic cycle. *Int.Rev Cytol.* **101**, 215-274.

Dechant, R. and Glotzer, M. (2003). Centrosome separation and central spindle assembly act in redundant pathways that regulate microtubule density and trigger cleavage furrow formation. *Dev.Cell* **4**, 333-344.

Di Cunto, F., Imarisio, S., Hirsch, E., Broccoli, V., Bulfone, A., Migheli, A., Atzori, C., Turco, E., Triolo, R., Dotto, G. P. *et al.* (2000). Defective neurogenesis in citron kinase knockout mice by altered cytokinesis and massive apoptosis. *Neuron* **28**, 115-127.

Doxsey, S. (2001). Re-evaluating centrosome function. *Nat Rev Mol Cell Biol* **2**, 688-698.

Drubin, D. G. and Nelson, W. J. (1996). Origins of cell polarity. *Cell* **84**, 335-344.

Easton, D. F., Narod, S. A., Ford, D. and Steel, M. (1994). The genetic epidemiology of BRCA1. Breast Cancer Linkage Consortium. *Lancet* **344**, 761.

Echard, A. and O'Farrell, P. H. (2003). The degradation of two mitotic cyclins contributes to the timing of cytokinesis. *Curr.Biol.* **13**, 373-383.

Eda, M., Yonemura, S., Kato, T., Watanabe, N., Ishizaki, T., Madaule, P. and Narumiya, S. (2001). Rho-dependent transfer of Citron-kinase to the cleavage furrow of dividing cells. *J Cell Sci* **114**, 3273-3284.

Edgar, B. A. and Lehner, C. F. (1996). Developmental Control of Cell Cycle Regulators: A Fly's Perspective. *Science* **274**, 1646-1652.

Elbashir, S. M., Harborth, J., Lendeckel, W., Yalcin, A., Weber, K. and Tuschl, T. (2001). Duplexes of 21-nucleotide RNAs mediate RNA interference in cultured mammalian cells. *Nature* **411**, 494-498.

Elia, A. E., Rellos, P., Haire, L. F., Chao, J. W., Ivins, F. J., Hoepker, K., Mohammad, D., Cantley, L. C., Smerdon, S. J. and Yaffe, M. B. (2003). The molecular basis for phosphodependent substrate targeting and regulation of Plks by the Polo-box domain. *Cell* **115**, 83-95.

Endicott, J. A., Nurse, P. and Johnson, L. N. (1994). Mutational analysis supports a structural model for the cell cycle protein kinase p34. *Protein Eng.* **7**, 243-253.

Evangelista, M., Blundell, K., Longtine, M. S., Chow, C. J., Adames, N., Pringle, J. R., Peter, M. and Boone, C. (1997). Bni1p, a yeast formin linking cdc42p and the actin cytoskeleton during polarized morphogenesis. *Science.* **276**, 118-122.

Evans, T., Rosenthal, E. T., Youngblom, J., Distel, D. and Hunt, T. (1983). Cyclin: a protein specified by maternal mRNA in sea urchin eggs that is destroyed at each cleavage division. *Cell* **33**, 389-396.

Flemming, W. (1882). Zellsubstanz, Kern und Zelltheilung. *(F. C. W. Vogel, Leipzig)*

Fujiwara, K. and Pollard, T. D. (1976). Fluorescent antibody localization of myosin in the cytoplasm, cleavage furrow, and mitotic spindle of human cells. *J Cell Biol* **71**, 848-875.

Gassmann, R., Carvalho, A., Henzing, A. J., Ruchaud, S., Hudson, D. F., Honda, R., Nigg, E. A., Gerloff, D. L. and Earnshaw, W. C. (2004). Borealin: a novel chromosomal passenger required for stability of the bipolar mitotic spindle. *J Cell Biol* **166**, 179-191.

Giet, R. and Glover, D. M. (2001). Drosophila aurora B kinase is required for histone H3 phosphorylation and condensin recruitment during chromosome condensation and to organize the central spindle during cytokinesis. *J Cell Biol* **152**, 669-682.

Giet, R., McLean, D., Descamps, S., Lee, M. J., Raff, J. W., Prigent, C. and Glover, D. M. (2002). Drosophila Aurora A kinase is required to localize D-TACC to centrosomes and to regulate astral microtubules. *J Cell Biol* **156**, 437-451.

Giet, R., Petretti, C. and Prigent, C. (2005). Aurora kinases, aneuploidy and cancer, a coincidence or a real link? *Trends Cell Biol* **15**, 241-250.

Gladfelter, A. S., Pringle, J. R. and Lew, D. J. (2001). The septin cortex at the yeast mother-bud neck. *Curr.Opin.Microbiol.* **4**, 681-689.

Glotzer, M. (2001). Animal cell cytokinesis. *Annu.Rev Cell Dev.Biol* **17**, 351-386.

Glotzer, M. (2005). The molecular requirements for cytokinesis. *Science* **307**, 1735-1739.

Gould, K. L. and Nurse, P. (1989). Tyrosine phosphorylation of the fission yeast cdc2+ protein kinase regulates entry into mitosis. *Nature.* **342**, 39-45.

Gruneberg, U., Neef, R., Honda, R., Nigg, E. A. and Barr, F. A. (2004). Relocation of Aurora B from centromeres to the central spindle at the metaphase to anaphase transition requires MKlp2. *J.Cell Biol.* **166**, 167-172.

Guertin, D. A., Trautmann, S. and McCollum, D. (2002). Cytokinesis in Eukaryotes. *Microbiol. Mol. Biol. Rev.* **66**, 155-178.

Guo, S. and Kemphues, K. J. (1996). A non-muscle myosin required for embryonic polarity in Caenorhabditis elegans. *Nature* **382**, 455-458.

Guse, A., Mishima, M. and Glotzer, M. (2005). Phosphorylation of ZEN-4/MKLP1 by aurora B regulates completion of cytokinesis. *Curr.Biol* **15**, 778-786.

Hagstrom, K. A. and Meyer, B. J. (2003). CONDENSIN AND COHESIN: MORE THAN CHROMOSOME COMPACTOR AND GLUE. *Nature Reviews Genetics* **4**, 520-534.

Hanisch, A., Wehner, A., Nigg, E. A. and Sillje, H. H. W. (2005). Different Plk1 Functions Show Distinct Dependencies on Polo-Box Domain-mediated Targeting. *Mol. Biol. Cell*, E05-08-0801.

Hannak, E., Kirkham, M., Hyman, A. A. and Oegema, K. (2001). Aurora-A kinase is required for centrosome maturation in Caenorhabditis elegans. *J Cell Biol* **155**, 1109-1116.

Hara, T., Abe, M., Inoue, H., Yu, L.-R., Veenstra, T. D., Kang, Y. H., Lee, K. S. and Miki, T. (2006) Cytokinesis regulator ECT2 changes its conformation through phosphorylation at Thr-341 in G2//M phase. *J Biol Chem.* **25,** 566-578.

Harkins, H. A., Page, N., Schenkman, L. R., De Virgilio, C., Shaw, S., Bussey, H. and Pringle, J. R. (2001). Bud8p and Bud9p, proteins that may mark the sites for bipolar budding in yeast. *Mol Biol Cell* **12**, 2497-2518.

Harper, J. W. and Adams, P. D. (2001). Cyclin-dependent kinases. *Chem.Rev* **101**, 2511-2526.

Harris, S. D., Hamer, L., Sharpless, K. E. and Hamer, J. E. (1997). The Aspergillus nidulans sepA gene encodes an FH1/2 protein involved in cytokinesis and the maintenance of cellular polarity. *EMBO J* **16**, 3474-3483.

Hauf, S., Waizenegger, I. C. and Peters, J. M. (2001). Cohesin cleavage by separase required for anaphase and cytokinesis in human cells. *Science* **293**, 1320-1323.

Heintz, N., Sive, H. L. and Roeder, R. G. (1983). Regulation of human histone gene expression: kinetics of accumulation and changes in the rate of synthesis and in the half-lives of individual histone mRNAs during the HeLa cell cycle. *Mol Cell Biol* **3**, 539-550.

Hill, E., Clarke, M. and Barr, F. A. (2000). The Rab6-binding kinesin, Rab6-KIFL, is required for cytokinesis. *EMBO J* **19**, 5711-5719.

Hirose, K., Kawashima, T., Iwamoto, I., Nosaka, T. and Kitamura, T. (2001). MgcRacGAP is involved in cytokinesis through associating with mitotic spindle and midbody. *J Biol Chem.* **276**, 5821-5828.

Hoffmann, R., Metzger, S., Spengler, B. and Otvos, L., Jr. (1999). Sequencing of peptides phosphorylated on serines and threonines by post-source decay in matrix-assisted laser desorption/ionization time-of-flight mass spectrometry. *J Mass Spectrom.* **34**, 1195-1204.

Honda, R., Korner, R. and Nigg, E. A. (2003). Exploring the functional interactions between Aurora B, INCENP, and survivin in mitosis. *Mol Biol Cell* **14**, 3325-3341.

Hunt, T. (1991). Cyclins and their partners: from a simple idea to complicated reality. *Semin.Cell Biol* **2**, 213-222.

Hyvonen, M., Macias, M. J., Nilges, M., Oschkinat, H., Saraste, M. and Wilmanns, M. (1995). Structure of the binding site for inositol phosphates in a PH domain. *EMBO J* **14**, 4676-4685.

Jackman, M., Lindon, C., Nigg, E. A. and Pines, J. (2003). Active cyclin B1-Cdk1 first appears on centrosomes in prophase. *Nat Cell Biol* **5**, 143-148.

Jiang, W., Jimenez, G., Wells, N. J., Hope, T. J., Wahl, G. M., Hunter, T. and Fukunaga, R. (1998). PRC1: a human mitotic spindle-associated CDK substrate protein required for cytokinesis. *Mol Cell* **2**, 877-885.

Jurgens, G. (2005). Plant cytokinesis: fission by fusion. *Trends Cell Biol* **15**, 277-283.

Kaitna, S., Mendoza, M., Jantsch-Plunger, V. and Glotzer, M. (2000). Incenp and an aurora-like kinase form a complex essential for chromosome segregation and efficient completion of cytokinesis. *Curr.Biol* **10**, 1172-1181.

Kawano, Y., Fukata, Y., Oshiro, N., Amano, M., Nakamura, T., Ito, M., Matsumura, F., Inagaki, M. and Kaibuchi, K. (1999). Phosphorylation of myosin-binding subunit (MBS) of myosin phosphatase by Rho-kinase *in vivo*. *J Cell Biol* **147**, 1023-1038.

Kemp, C. A., Kopish, K. R., Zipperlen, P., Ahringer, J. and O'Connell, K. F. (2004). Centrosome maturation and duplication in C. elegans require the coiled-coil protein SPD-2. *Dev.Cell* **6**, 511-523.

Kim, J. E., Billadeau, D. D. and Chen, J. (2005).The tandem BRCT domains of Ect2 are required for both negative and positive regulation of Ect2 in cytokinesis. *J.Biol.Chem.* **280**, 5733-5739.

Kimura, K., Hirano, M., Kobayashi, R. and Hirano, T. (1998). Phosphorylation and activation of 13S condensin by Cdc2 *in vitro*. *Science* **282**, 487-490.

Kimura, K., Tsuji, T., Takada, Y., Miki, T. and Narumiya, S. (2000). Accumulation of GTP-bound RhoA during cytokinesis and a critical role of ECT2 in this accumulation. *J.Biol.Chem.* **275**, 17233-17236.

King, R. W., Deshaies, R. J., Peters, J.-M. and Kirschner, M. W. (1996). How Proteolysis Drives the Cell Cycle. *Science* **274**, 1652-1659.

Kishi, K., Sasaki, T., Kuroda, S., Itoh, T. and Takai, Y. (1993). Regulation of cytoplasmic division of Xenopus embryo by rho p21 and its inhibitory GDP/GTP exchange protein (rho GDI). *J. Cell Biol.* **120**, 1187-1195.

Kitamura, T., Kawashima, T., Minoshima, Y., Tonozuka, Y., Hirose, K. and Nosaka, T. (2001). Role of MgcRacGAP/Cyk4 as a regulator of the small GTPase Rho family in cytokinesis and cell differentiation. *Cell Struct.Funct.* **26**, 645-651.

Kitayama, C., Sugimoto, A. and Yamamoto, M. (1997). Type II myosin heavy chain encoded by the myo2 gene composes the contractile ring during cytokinesis in Schizosaccharomyces pombe. *J Cell Biol* **137**, 1309-1319.

Komatsu, S., Yano, T., Shibata, M., Tuft, R. A. and Ikebe, M. (2000). Effects of the regulatory light chain phosphorylation of myosin II on mitosis and cytokinesis of mammalian cells. *J Biol Chem.* **275**, 34512-34520.

Koonin, E. V., Altschul, S. F. and Bork, P. (1996). BRCA1 protein products ... Functional motifs.. *Nat Genet.* **13**, 266-268.

Kosako, H., Yoshida, T., Matsumura, F., Ishizaki, T., Narumiya, S. and Inagaki, M. (2000). Rho-kinase/ROCK is involved in cytokinesis through the phosphorylation of myosin light chain and not ezrin/radixin/moesin proteins at the cleavage furrow. *Oncogene* **19**, 6059-6064.

Kurasawa, Y., Earnshaw, W. C., Mochizuki, Y., Dohmae, N. and Todokoro, K. (2004). Essential roles of KIF4 and its binding partner PRC1 in organized central spindle midzone formation. *EMBO J* **23**, 3237-3248.

Kuriyama, R., Gustus, C., Terada, Y., Uetake, Y. and Matuliene, J. (2002). CHO1, a mammalian kinesin-like protein, interacts with F-actin and is involved in the terminal phase of cytokinesis. *J.Cell Biol.* **156**, 783-790.

Lan, W., Zhang, X., Kline-Smith, S. L., Rosasco, S. E., Barrett-Wilt, G. A., Shabanowitz, J., Hunt, D. F., Walczak, C. E. and Stukenberg, P. T. (2004). Aurora B phosphorylates centromeric MCAK and regulates its localization and microtubule depolymerization activity. *Curr.Biol* **14**, 273-286.

Lane, H. A. and Nigg, E. A. (1996). Antibody microinjection reveals an essential role for human polo-like kinase 1 (Plk1) in the functional maturation of mitotic centrosomes. *J Cell Biol* **135**, 1701-1713.

Lee, Y. M. and Kim, W. (2004). Kinesin superfamily protein member 4 (KIF4) is localized to midzone and midbody in dividing cells. *Exp.Mol Med.* **36**, 93-97.

Lehner, C. F. (1992). The pebble gene is required for cytokinesis in Drosophila. *J.Cell Sci.* **103**, 1021-1030.

Lemmon, M. A. (2004). Pleckstrin homology domains: not just for phosphoinositides. *Biochem.Soc.Trans.* **32**, 707-711.

Liu, X., Wang, H., Eberstadt, M., Schnuchel, A., Olejniczak, E. T., Meadows, R. P., Schkeryantz, J. M., Janowick, D. A., Harlan, J. E., Harris, E. A. *et al.* (1998). NMR structure and mutagenesis of the N-terminal Dbl homology domain of the nucleotide exchange factor Trio. *Cell* **95**, 269-277.

Liu, X. F., Ishida, H., Raziuddin, R. and Miki, T. (2004). Nucleotide exchange factor ECT2 interacts with the polarity protein complex Par6/Par3/protein kinase Czeta (PKCzeta) and regulates PKCzeta activity. *Mol Cell Biol* **24**, 6665-6675.

Lloyd, C. and Hussey, P. (2001). Microtubule-associated proteins in plants--why we need a MAP. *Nat Rev Mol Cell Biol* **2**, 40-47.

Longtine, M. S. and Bi, E. (2003). Regulation of septin organization and function in yeast. *Trends Cell Biol* **13**, 403-409.

Lord, M., Inose, F., Hiroko, T., Hata, T., Fujita, A. and Chant, J. (2002). Subcellular localization of Axl1, the cell type-specific regulator of polarity. *Curr.Biol* **12**, 1347-1352.

Lowe, M., Rabouille, C., Nakamura, N., Watson, R., Jackman, M., Jamsa, E., Rahman, D., Pappin, D. J. and Warren, G. (1998). Cdc2 kinase directly phosphorylates the cis-Golgi matrix protein GM130 and is required for Golgi fragmentation in mitosis. *Cell.* **94**, 783-793.

Mabuchi, I., Hamaguchi, Y., Fujimoto, H., Morii, N., Mishima, M. and Narumiya, S. (1993). A rho-like protein is involved in the organisation of the contractile ring in dividing sand dollar eggs. *Zygote.* **1**, 325-331.

Mabuchi, I. and Okuno, M. (1977). The effect of myosin antibody on the division of starfish blastomeres. *J Cell Biol* **74**, 251-263.

Madaule, P., Eda, M., Watanabe, N., Fujisawa, K., Matsuoka, T., Bito, H., Ishizaki, T. and Narumiya, S. (1998). Role of citron kinase as a target of the small GTPase Rho in cytokinesis. *Nature* **394**, 491-494.

Manke, I. A., Lowery, D. M., Nguyen, A. and Yaffe, M. B. (2003). BRCT repeats as phosphopeptide-binding modules involved in protein targeting. *Science* **302**, 636-639.

Matuliene, J. and Kuriyama, R. (2002). Kinesin-like protein CHO1 is required for the formation of midbody matrix and the completion of cytokinesis in mammalian cells. *Mol Biol Cell* **13**, 1832-1845.

Meraldi, P., Honda, R. and Nigg, E. A. (2002). Aurora-A overexpression reveals tetraploidization as a major route to centrosome amplification in p53-/- cells. *EMBO J.* **21**, 483-492.

Meraldi, P. and Nigg, E. A. (2002). The centrosome cycle. *FEBS Lett.* **521**, 9-13.

Miki, T., Smith, C. L., Long, J. E., Eva, A. and Fleming, T. P. (1993). Oncogene ect2 is related to regulators of small GTP-binding proteins. *Nature* **362**, 462-465.

Minoshima, Y., Kawashima, T., Hirose, K., Tonozuka, Y., Kawajiri, A., Bao, Y. C., Deng, X., Tatsuka, M., Narumiya, S., May, W. S., Jr. *et al.* (2003). Phosphorylation by aurora B converts MgcRacGAP to a RhoGAP during cytokinesis. *Dev.Cell* **4**, 549-560.

Mishima, M., Kaitna, S. and Glotzer, M. (2002). Central spindle assembly and cytokinesis require a kinesin-like protein/RhoGAP complex with microtubule bundling activity. *Dev.Cell* **2**, 41-54.

Mishima, M., Pavicic, V., Gruneberg, U., Nigg, E. A. and Glotzer, M. (2004). Cell cycle regulation of central spindle assembly. *Nature* **430**, 908-913.

Mollinari, C., Kleman, J. P., Jiang, W., Schoehn, G., Hunter, T. and Margolis, R. L. (2002). PRC1 is a microtubule binding and bundling protein essential to maintain the mitotic spindle midzone. *J Cell Biol* **157**, 1175-1186.

Mollinari, C., Kleman, J. P., Saoudi, Y., Jablonski, S. A., Perard, J., Yen, T. J. and Margolis, R. L. (2005). Ablation of PRC1 by small interfering RNA demonstrates that cytokinetic abscission requires a central spindle bundle in mammalian cells, whereas completion of furrowing does not. *Mol Biol Cell* **16**, 1043-1055.

Morgan, D. O. (1997). Cyclin-dependent kinases: engines, clocks, and microprocessors. *Annu.Rev Cell Dev.Biol* **13:261-91.**, 261-291.

Motegi, F., Mishra, M., Balasubramanian, M. K. and Mabuchi, I. (2004). Myosin-II reorganization during mitosis is controlled temporally by its dephosphorylation and spatially by Mid1 in fission yeast. *J Cell Biol* **165**, 685-695.

Mulvihill, D. P., Win, T. Z., Pack, T. P. and Hyams, J. S. (2000). Cytokinesis in fission yeast: a myosin pas de deux. *Microsc.Res Tech.* **49**, 152-160.

Mundt, K. E., Golsteyn, R. M., Lane, H. A. and Nigg, E. A. (1997). On the regulation and function of human polo-like kinase 1 (PLK1): effects of overexpression on cell cycle progression. *Biochem.Biophys.Res Commun.* **239**, 377-385.

Murray, A. W. (2004). Recycling the cell cycle: cyclins revisited. *Cell* **116**, 221-234.

Naim, V., Imarisio, S., Di Cunto, F., Gatti, M. and Bonaccorsi, S. (2004). Drosophila citron kinase is required for the final steps of cytokinesis. *Mol Biol Cell* **15**, 5053-5063.

Neef, R., Preisinger, C., Sutcliffe, J., Kopajtich, R., Nigg, E. A., Mayer, T. U. and Barr, F. A. (2003). Phosphorylation of mitotic kinesin-like protein 2 by polo-like kinase 1 is required for cytokinesis. *J Cell Biol* **162**, 863-875.

Nigg, E. A. (1995). Cyclin-dependent protein kinases: key regulators of the eukaryotic cell cycle. *Bioessays* **17**, 471-480.

Nigg, E. A. (1996). Cyclin-dependent kinase 7: at the cross-roads of transcription, DNA repair and cell cycle control? *Curr.Opin.Cell Biol* **8**, 312-317.

Nigg, E. A. (2001). Mitotic kinases as regulators of cell division and its checkpoints. *Nat Rev Mol Cell Biol* **2**, 21-32.

Niiya, F., Xie, X., Lee, K. S., Inoue, H. and Miki, T. (2005). Inhibition of Cdk1 induces cytokinesis without chromosome segregation in an ECT2 and MgcRacGAP-dependent manner. *J Biol Chem.* **280**, 36502-36509.

Oceguera-Yanez, F., Kimura, K., Yasuda, S., Higashida, C., Kitamura, T., Hiraoka, Y., Haraguchi, T. and Narumiya, S. (2005). Ect2 and MgcRacGAP regulate the activation and function of Cdc42 in mitosis. *J Cell Biol* **168**, 221-232.

Oegema, K., Savoian, M. S., Mitchison, T. J. and Field, C. M. (2000). Functional analysis of a human homologue of the Drosophila actin binding protein anillin suggests a role in cytokinesis. *J Cell Biol* **150**, 539-552.

Ohkura, H., Hagan, I. M. and Glover, D. M. (1995). The conserved Schizosaccharomyces pombe kinase plo1, required to form a bipolar spindle, the actin ring, and septum, can drive septum formation in G1 and G2 cells. *Genes Dev.* **9**, 1059-1073.

Otegui, M. S., Mastronarde, D. N., Kang, B. H., Bednarek, S. Y. and Staehelin, L. A. (2001). Three-dimensional analysis of syncytial-type cell plates during endosperm cellularization visualized by high resolution electron tomography. *Plant Cell* **13**, 2033-2051.

Page, A. M. and Hieter, P. (1999). The anaphase-promoting complex: new subunits and regulators. *Annu.Rev Biochem.* **68**, 583-609.

Paoletti, A. and Bornens, M. (1997). Organisation and functional regulation of the centrosome in animal cells. *Prog.Cell Cycle Res* **3**, 285-299.

Paoletti, A. and Chang, F. (2000). Analysis of mid1p, a protein required for placement of the cell division site, reveals a link between the nucleus and the cell surface in fission yeast. *Mol Biol Cell* **11**, 2757-2773.

Paweletz, N. (2001). Walther Flemming: pioneer of mitosis research. *Nat Rev Mol Cell Biol* **2**, 72-75.

Perry, M. M., John, H. A. and Thomas, N. S. (1971). Actin-like filaments in the cleavage furrow of newt egg. *Exp.Cell Res* **65**, 249-253.

Peters, J. M. (2002). The anaphase-promoting complex: proteolysis in mitosis and beyond. *Mol Cell* **9**, 931-943.

Pines, J. (1993a). Cyclins and cyclin-dependent kinases: take your partners. *Trends Biochem.Sci* **18**, 195-197.

Pines, J. (1993b). Cyclins and their associated cyclin-dependent kinases in the human cell cycle. *Biochem.Soc.Trans.* **21**, 921-925.

Prokopenko, S. N., Brumby, A., O'Keefe, L., Prior, L., He, Y., Saint, R. and Bellen, H. J. (1999). A putative exchange factor for Rho1 GTPase is required for initiation of cytokinesis in Drosophila. *Genes Dev.* **13**, 2301-2314.

Rajagopalan, S., Wachtler, V. and Balasubramanian, M. (2003). Cytokinesis in fission yeast: a story of rings, rafts and walls. *Trends Genet.* **19**, 403-408.

Rappaport, R. (1968). [Geometrical relations of the cleavage stimulus in flattened, perforated sea urchin eggs]. *Embryologia.(Nagoya)* **10**, 89-104.

Rappaport, R. (1982). Cytokinesis: the effect of initial distance between mitotic apparatus and surface on the rate of subsequent cleavage furrow progress. *J Exp.Zool.* **221**, 399-403.

Rieder, C., Cole, R., Khodjakov, A. and Sluder, G. (1995). The checkpoint delaying anaphase in response to chromosome monoorientation is mediated by an inhibitory signal produced by unattached kinetochores. *J. Cell Biol.* **130**, 941-948.

Robbins, J., Dilworth, S. M., Laskey, R. A. and Dingwall, C. (1991). Two interdependent basic domains in nucleoplasmin nuclear targeting sequence: identification of a class of bipartite nuclear targeting sequence. *Cell* **64**, 615-623.

Rodriguez, M., Yu, X., Chen, J. and Songyang, Z. (2003). Phosphopeptide Binding Specificities of BRCA1 COOH-terminal (BRCT) Domains. *J. Biol. Chem.* **278**, 52914-52918.

Rudner, A. D. and Murray, A. W. (1996). The spindle assembly checkpoint. *Curr.Opin.Cell Biol* **8**, 773-780.

Rudolph, M. G., Weise, C., Mirold, S., Hillenbrand, B., Bader, B., Wittinghofer, A. and Hardt, W. D. (1999). Biochemical analysis of SopE from Salmonella typhimurium, a highly efficient guanosine nucleotide exchange factor for RhoGTPases. *J Biol Chem.* **274**, 30501-30509.

Russo, A. A., Jeffrey, P. D. and Pavletich, N. P. (1996). Structural basis of cyclin-dependent kinase activation by phosphorylation. *Nat Struct.Biol.* **3**, 696-700.

Saito, S., Liu, X. F., Kamijo, K., Raziuddin, R., Tatsumoto, T., Okamoto, I., Chen, X., Lee, C. C., Lorenzi, M. V., Ohara, N. *et al.* (2004). Deregulation and mislocalization of the cytokinesis regulator ECT2 activate the Rho signaling pathways leading to malignant transformation. *J.Biol.Chem.* **279**, 7169-7179.

Sampath, S. C., Ohi, R., Leismann, O., Salic, A., Pozniakovski, A. and Funabiki, H. (2004). The chromosomal passenger complex is required for chromatin-induced microtubule stabilization and spindle assembly. *Cell* **118**, 187-202.

Sanders, S. L. and Field, C. M. (1994). Cell division. Septins in common? *Curr.Biol* **4**, 907-910.

Sarkisian, M. R., Li, W., Di Cunto, F., D'Mello, S. R. and LoTurco, J. J. (2002). Citron-kinase, a protein essential to cytokinesis in neuronal progenitors, is deleted in the flathead mutant rat. *J Neurosci.* **22**, RC217.

Sawai, T. and Yomota, A. (1990). Cleavage plane determination in amphibian eggs. *Ann.N.Y.Acad.Sci* **582**, 40-49.

Schroeder, T. E. (1978). Cytochalasin B, cytokinesis, and the contractile ring. *Front Biol* **46**, 91-112.

Schroeder, T. E. (1987). Fourth cleavage of sea urchin blastomeres: microtubule patterns and myosin localization in equal and unequal cell divisions. *Dev.Biol* **124**, 9-22.

Segui-Simarro, J. M., Austin, J. R., White, E. A. and Staehelin, L. A. (2004). Electron tomographic analysis of somatic cell plate formation in meristematic cells of Arabidopsis preserved by high-pressure freezing. *Plant Cell* **16**, 836-856.

Seong, Y.-S., Kamijo, K., Lee, J.-S., Fernandez, E., Kuriyama, R., Miki, T. and Lee, K. S. (2002). A Spindle Checkpoint Arrest and a Cytokinesis Failure by the Dominant-negative Polo-box Domain of Plk1 in U-2 OS Cells. jbc.M202602200. *J. Biol. Chem.* **277**, 32282-32293.

Shandala, T., Gregory, S. L., Dalton, H. E., Smallhorn, M. and Saint, R. (2004). Citron kinase is an essential effector of the Pbl-activated Rho signalling pathway in Drosophila melanogaster. *Development* **131**, 5053-5063.

Shevchenko, A., Wilm, M., Vorm, O. and Mann, M. (1996). Mass spectrometric sequencing of proteins silver-stained polyacrylamide gels. *Anal.Chem.* **68**, 850-858.

Shimizu, Y., Thumkeo, D., Keel, J., Ishizaki, T., Oshima, H., Oshima, M., Noda, Y., Matsumura, F., Taketo, M. M. and Narumiya, S. (2005). ROCK-I regulates closure of the eyelids and ventral body wall by inducing assembly of actomyosin bundles. *J Cell Biol* **168**, 941-953.

Sillje, H. H., Takahashi, K., Tanaka, K., Van Houwe, G. and Nigg, E. A. (1999). Mammalian homologues of the plant Tousled gene code for cell-cycle-regulated kinases with maximal activities linked to ongoing DNA replication. *EMBO J* **18**, 5691-5702.

Smits, V. A. J., Klompmaker, R., Arnaud, L., Rijksen, G., Nigg, E. A. and Medema, R. H. (2000). Polo-like kinase-1 is a target of the DNA damage checkpoint. **2**, 672-676.

Sohrmann, M., Fankhauser, C., Brodbeck, C. and Simanis, V. (1996). The dmf1/mid1 gene is essential for correct positioning of the division septum in fission yeast. *Genes Dev.* **10**, 2707-2719.

Solski, P. A., Wilder, R. S., Rossman, K. L., Sondek, J., Cox, A. D., Campbell, S. L. and Der, C. J. (2004). Requirement for C-terminal sequences in regulation of Ect2 guanine nucleotide exchange specificity and transformation. *J.Biol.Chem.* **279**, 25226-25233.

Somers, W. G. and Saint, R. (2003). A RhoGEF and Rho family GTPase-activating protein complex links the contractile ring to cortical microtubules at the onset of cytokinesis. *Dev.Cell* **4**, 29-39.

Song, S. and Lee, K. S. (2001). A novel function of Saccharomyces cerevisiae CDC5 in cytokinesis. *J Cell Biol* **152**, 451-469.

Srivastava, S. K., Wheelock, R. H., Aaronson, S. A. and Eva, A. (1986). Identification of the protein encoded by the human diffuse B-cell lymphoma (dbl) oncogene. *Proc.Natl.Acad.Sci U.S.A* **83**, 8868-8872.

Steinborn, K., Maulbetsch, C., Priester, B., Trautmann, S., Pacher, T., Geiges, B., Kuttner, F., Lepiniec, L., Stierhof, Y. D., Schwarz, H. *et al.* (2002). The Arabidopsis PILZ group genes encode tubulin-folding cofactor orthologs required for cell division but not cell growth. *Genes Dev.* **16**, 959-971.

Straight, A. F., Field, C. M. and Mitchison, T. J. (2005). Anillin binds nonmuscle myosin II and regulates the contractile ring. *Mol Biol Cell* **16**, 193-201.

Swan, K. A., Severson, A. F., Carter, J. C., Martin, P. R., Schnabel, H., Schnabel, R. and Bowerman, B. (1998). cyk-1: a C. elegans FH gene required for a late step in embryonic cytokinesis. *J Cell Sci* **111**, 2017-2027.

Tabata, S. (2000). Sequence and analysis of chromosome 5 of the plant Arabidopsis thaliana. *Nature* **408**, 823-826.

Tatsumoto, T., Sakata, H., Dasso, M. and Miki, T. (2003). Potential roles of the nucleotide exchange factor ECT2 and Cdc42 GTPase in spindle assembly in Xenopus egg cell-free extracts. *J Cell Biochem.* **90**, 892-900.

Tatsumoto, T., Xie, X., Blumenthal, R., Okamoto, I. and Miki, T. (1999). Human ECT2 is an exchange factor for Rho GTPases, phosphorylated in G2/M phases, and involved in cytokinesis. *J.Cell Biol.* **147**, 921-928.

Terada, Y., Tatsuka, M., Suzuki, F., Yasuda, Y., Fujita, S. and Otsu, M. (1998). AIM-1: a mammalian midbody-associated protein required for cytokinesis. *EMBO J* **17**, 667-676.

Terada, Y., Uetake, Y. and Kuriyama, R. (2003). Interaction of Aurora-A and centrosomin at the microtubule-nucleating site in Drosophila and mammalian cells. *J Cell Biol* **162**, 757-763.

Thumkeo, D., Keel, J., Ishizaki, T., Hirose, M., Nonomura, K., Oshima, H., Oshima, M., Taketo, M. M. and Narumiya, S. (2003). Targeted disruption of the mouse rho-associated kinase 2 gene results in intrauterine growth retardation and fetal death. *Mol Cell Biol* **23**, 5043-5055.

Tominaga, T., Sahai, E., Chardin, P., McCormick, F., Courtneidge, S. A. and Alberts, A. S. (2000). Diaphanous-related formins bridge Rho GTPase and Src tyrosine kinase signaling. *Mol Cell* **5**, 13-25.

Trimble, W. S. (1999). Septins: a highly conserved family of membrane-associated GTPases with functions in cell division and beyond. *J Membr.Biol* **169**, 75-81.

Trotter, J. A. and Adelstein, R. S. (1979). Macrophage myosin. Regulation of actin-activated ATPase, activity by phosphorylation of the 20,000-dalton light chain. *J Biol Chem.* **254**, 8781-8785.

Tyers, M., Rachubinski, R. A., Stewart, M. I., Varrichio, A. M., Shorr, R. G., Haslam, R. J. and Harley, C. B. (1988). Molecular cloning and expression of the major protein kinase C substrate of platelets. *Nature* **333**, 470-473.

Valverde, P. (2000). Cloning, expression, and mapping of hWW45, a novel human WW domain-containing gene. *Biochem.Biophys.Res Commun.* **276**, 990-998.

van Vugt, M. A. T. M., van de Weerdt, B. C. M., Vader, G., Janssen, H., Calafat, J., Klompmaker, R., Wolthuis, R. M. F. and Medema, R. H. (2004). Polo-like Kinase-1 Is Required for Bipolar Spindle Formation but Is Dispensable for Anaphase Promoting Complex/Cdc20 Activation and Initiation of Cytokinesis *J. Biol. Chem.* **279**, 36841-36854.

Virchow, R. (1854). Zellularpathologie. *Archiv für pathologische Anatomie.* **Bd. VIII.**

Wasserman, S. (1998). FH proteins as cytoskeletal organizers. *Trends Cell Biol* **8**, 111-115.

Watanabe, N. and Higashida, C. (2004). Formins: processive cappers of growing actin filaments. *Exp.Cell Res.* **301**, 16-22.

Watanabe, N., Madaule, P., Reid, T., Ishizaki, T., Watanabe, G., Kakizuka, A., Saito, Y., Nakao, K., Jockusch, B. M. and Narumiya, S. (1997). p140mDia, a mammalian homolog of Drosophila diaphanous, is a target protein for Rho small GTPase and is a ligand for profilin. *EMBO J* **16**, 3044-3056.

Wells, W. A. (1996). The spindle-assembly checkpoint: aiming for a perfect mitosis, every time. *Trends Cell Biol* **6**, 228-234.

Wheatley, S. P. and Wang, Y. (1996). Midzone microtubule bundles are continuously required for cytokinesis in cultured epithelial cells. *J Cell Biol* **135**, 981-989.

White, J. G. and Borisy, G. G. (1983). On the mechanisms of cytokinesis in animal cells. *J Theor.Biol* **101**, 289-316.

Williams, R. S., Lee, M. S., Hau, D. D. and Glover, J. N. (2004). Structural basis of phosphopeptide recognition by the BRCT domain of BRCA1. *Nat.Struct.Mol.Biol.* **11**, 519-525.

Winter, C. G., Wang, B., Ballew, A., Royou, A., Karess, R., Axelrod, J. D. and Luo, L. (2001). Drosophila Rho-associated kinase (Drok) links Frizzled-mediated planar cell polarity signaling to the actin cytoskeleton. *Cell* **105**, 81-91.

Worthylake, D. K., Rossman, K. L. and Sondek, J. (2000). Crystal structure of Rac1 in complex with the guanine nucleotide exchange region of Tiam1. *Nature* **408**, 682-688.

Wu, J. Q., Kuhn, J. R., Kovar, D. R. and Pollard, T. D. (2003). Spatial and temporal pathway for assembly and constriction of the contractile ring in fission yeast cytokinesis. *Dev.Cell* **5**, 723-734.

Wu, J. W., Hu, M., Chai, J., Seoane, J., Huse, M., Li, C., Rigotti, D. J., Kyin, S., Muir, T. W., Fairman, R. *et al.* (2001). Crystal structure of a phosphorylated Smad2. Recognition of phosphoserine by the MH2 domain and insights on Smad function in TGF-beta signaling. *Mol Cell* **8**, 1277-1289.

Yaffe, M. B. and Elia, A. E. (2001). Phosphoserine/threonine-binding domains. *Curr.Opin.Cell Biol* **13**, 131-138.

Yaffe, M. B. and Smerdon, S. J. (2001). PhosphoSerine/threonine binding domains: you can't pSERious? *Structure.(Camb.)* **9**, R33-R38.

Yamakita, Y., Yamashiro, S. and Matsumura, F. (1994). In vivo phosphorylation of regulatory light chain of myosin II during mitosis of cultured cells. *J Cell Biol* **124**, 129-137.

Yamashiro, S., Totsukawa, G., Yamakita, Y., Sasaki, Y., Madaule, P., Ishizaki, T., Narumiya, S. and Matsumura, F. (2003). Citron kinase, a Rho-dependent kinase, induces di-phosphorylation of regulatory light chain of myosin II. *Mol Biol Cell* **14**, 1745-1756.

Yasuda, S., Oceguera-Yanez, F., Kato, T., Okamoto, M., Yonemura, S., Terada, Y., Ishizaki, T. and Narumiya, S. (2004). Cdc42 and mDia3 regulate microtubule attachment to kinetochores. *Nature* **428**, 767-771.

Yasui, Y., Urano, T., Kawajiri, A., Nagata, K., Tatsuka, M., Saya, H., Furukawa, K., Takahashi, T., Izawa, I. and Inagaki, M. (2004). Autophosphorylation of a newly identified site of Aurora-B is indispensable for cytokinesis. *J Biol Chem.* **279**, 12997-13003.

Yoshigaki, T. (2003). Theoretical evidence that more microtubules reach the cortex at the pole than at the equator during anaphase in sea urchin eggs. *Acta Biotheor.* **51**, 43-53.

Young, P. E., Richman, A. M., Ketchum, A. S. and Kiehart, D. P. (1993). Morphogenesis in Drosophila requires nonmuscle myosin heavy chain function. *Genes Dev.* **7**, 29-41.

Yu, X., Chini, C. C., He, M., Mer, G. and Chen, J. (2003). The BRCT domain is a phospho-protein binding domain. *Science* **302**, 639-642.

Yuce, O., Piekny, A. and Glotzer, M. (2005). An ECT2-centralspindlin complex regulates the localization and function of RhoA. *J Cell Biol* **170**, 571-582.

Zeitlin, S. G., Shelby, R. D. and Sullivan, K. F. (2001). CENP-A is phosphorylated by Aurora B kinase and plays an unexpected role in completion of cytokinesis 10.1083/jcb.200108125. *J. Cell Biol.* **155**, 1147-1158.

Zheng, Y. (2001). Dbl family guanine nucleotide exchange factors. *Trends Biochem.Sci* **26**, 724-732.

Appendix-List of plasmids

name	*tag*	*gene*	*insert*	*species*	*vector*
RB 1		**hww45**	Full length hww45	human	pCMV-Sport6
RB 2		**hww45**	Full length hww45	human	pBS SK
RB 3	myc	**hww45**	Full length hww45	human	pcDNA3.1
RB 4	BD	**hww45**	Full length hww45	human	pGBD-C1
RB 5	His6	**hww45**	Full length hww45	human	pQE-30
RB 6	GFP	**hww45**	Full length hww45	human	pEGFP-T7/C1
RB 7	His6	**hww45**	aa 1-174	human	pQE-30
RB 8	AD	**hww45**	Full length hww45	human	pGAD-C1
RB 9	YFP		pEYFP-N1	human	
RB 10	YFP	**α-tub**		human	pEYFP-Tub
RB 11	CFP			human	pECFP-N1
RB 12	CFP	**H2B**		human	pBOS
RB 13		**Ect2**	Full length Ect2	human	pBS KS
RB 14	myc	**Ect2**	Full length Ect2	human	pcDNA3.1
RB 15	GFP	**Ect2**	Full length Ect2	human	pEGFP-T7/C1
RB 16	His6	**Ect2**	Full length Ect2	human	pQE-30
RB 17	GST	**Ect2**	Full length Ect2	human	pGEX-6P-3
RB 18	myc	**Ect2**	Ect2 aa 1-387	human	pcDNA3.1
RB 19	myc	**Ect2**	Ect2 aa 1-288	human	pcDNA3.1
RB 20		**Ect2**	Ect2 aa 1-214	human	pBSKS
RB 21	myc	**Ect2**	Ect2 aa 476-883	human	pcDNA3.1
RB 22	myc	**Ect2**	Ect2 aa 1-214	human	pcDNA3.1
RB 23	His6	**Ect2**	Ect2 aa 1-387	human	pQE-30
RB 24	His6	**Ect2**	Full length Ect2	human	pVL1393
RB 25		**RhoA**	Full length RhoA EST	human	pCMV Sport6
RB 26	GST	**RhoA**	Full length RhoA	human	pGEX-6P-3
RB 27	His6	**Ect2**	Ect2 aa 476-884	human	pQE-81L
RB 28	GFP	**Ect2**	Ect2 aa 1-387	human	pEGFP-T7/C1
RB 29	GFP	**Ect2**	Ect2 aa 1-214	human	pEGFP-T7/C1
RB 30	GFP	**Ect2**	Ect2 aa 476-883	human	pEGFP-C3

RB 31	His6 **Ect2**	Ect2 aa 476-883	human	pQE-31
RB 32	**Ect2**	Ect2 E428A	human	pBS KS
RB 33	GST **Ect2**	Full length Ect2	human	pVL13GST93
RB 34	myc **Ect2**	Ect2 E428A	human	pCDNA3.1
RB 35	GST **Ect2**	Ect2 E428A	human	pVL13GST93
RB 36	His6 **Ect2**	Ect2 E428A	human	pVL1393
RB 37	BD **Ect2**	Ect2	human	pGBD-C3
RB 38	myc **Ect2**	Full length Ect2	human	pcDNA4/TO/myc
RB 39	myc **Ect2**	Full length Ect2	human	pcDNA4/TO/myc
RB 40	**Ect2**	Full length Ect2	human	pBSKS+
RB 41	myc **Ect2**	Full length V566D	human	pcDNA 3.1
RB 42	GST **Ect2**	Full length V566D	human	pVL1393
RB 44	BD **Ect2**	Ect2 1-387	human	pGBDΩ-C(1)
RB 45	BD **Ect2**	Ect2 476-883	human	pGBDΩ-C(1)
RB 46	AD **Ect2**	Ect2 1-387	human	pGAD-C(1)
RB 47	AD **Ect2**	Ect2 476-883	human	pGAD-C(1)
RB 48	myc **RhoA**	Full length RhoA	human	pcDNA 3.1
RB 49	myc **Ect2**	Ect2 S40A(undesired point mutation)	human	pcDNA 3.1
RB 50	myc **Ect2**	Ect2S40A	human	pcDNA 3.1
RB 51	myc **Ect2**	Ect2 S40D	human	pcDNA 3.1
RB 52	myc **Ect2**	Ect2 T815A	human	pcDNA 3.1
RB 53	myc **Ect2**	Ect2 T815D	human	pcDNA 3.1
RB 55	GST **Myc1 Rac1**	Full length Rac1	human	pGEX-2T
RB 56	GST **Myc1 Cdc42**	Full length Cdc42	human	pGEX-2T
RB 57	GST **Rhotekin RBD**	Rhotekin RBD		pGEX-2T
RB 58	GST **SopE**	SopE 78-240	bacteria	pGEX-2T
RB 59	myc **Ect2**	Ect2 1-333	human	pcDNA3.1
RB 60	myc **Ect2**	Ect2 T815A	human	pcDNA3.1
RB 61	myc **Ect2**	Ect2 T815D	human	pcDNA3.1
RB 62	GST **Ect2**	Ect2 BRCT domains (113-342)	human	pGEX-6P-3
RB 63	GST **Ect2**	Ect2 BRCT domains w211R (113-342)	human	pGEX-6P-3
RB 64	GFP **Ect2**	Ect2 BRCT domains (113-342)	human	pEGFP-T7/C1
RB 65	GFP **Ect2**	Ect2 BRCT domains w211R (113-342)	human	pEGFP-T7/C1
RB 66	myc **Ect2**	Ect2 BRCT domains (113-342)	human	pcDNA3.1
RB 67	myc **Ect2**	Ect2 BRCT domains w211R (113-342)	human	pcDNA3.1
RB 68	His **Ect2**	Ect2 BRCTdomains (113-342)	human	pQE-30
RB 69	His **Ect2**	Ect2 BRCT domains w211R (113-342)	human	pQE-30

RB 70	GFP	**Ect2**	Ect2 s40A	human	pcDNA3.1
RB 71	GFP	**Ect2**	Ect2 S40D	human	pEGFP-T7/C1
RB 72	myc	**Ect2**	Ect2 1-360	human	pcDNA3.1
RB 73	myc	**MKlp1**	Full length	human	pcDNA3.1
RB 74	GFP	**Ect2**	Ect2 V566D	human	pEGFP-T7/C1
RB 75	GFP	**Ect2**	Ect2 E428A	human	pEGFP-T7/C1
RB 76			Cdc42BPB (Kiaa1124)	human	pBSSK+
RB 77			Trim56 (IMAGp958P2343)	human	poTB7
RB 78	GST	**Trim56**	Trim56	human	pGEX-6P-3
RB 79	myc	**Trim56**	Trim56	human	pcDNA3.1
RB 80	His	**Ect2**	Ect2 349-639	human	pQE-82L
RB 81	myc	**Ect2**	Ect2 S20A	human	pcDNA3.1
RB 82	myc	**Ect2**	Ect2 S366A (undesired point mutations)	human	pcDNA3.1
RB 83	myc	**Ect2**	Ect2 S685A	human	pcDNA3.1
RB 84	myc	**Ect2**	Ect2 S336A	human	pcDNA3.1
RB 85	myc	**Ect2**	Ect2 S366A	human	pcDNA3.1
RB 86	myc	**Ect2**	Ect2 S20A, S685A	human	pcDNA3.1
RB 87	myc	**Ect2**	Ect2 S811A	human	pcDNA3.1
RB 88	myc	**Ect2**	Ect2 S20A, S366A, S685A	human	pcDNA3.1
RB 89	myc	**Ect2**	Ect2 S20D	human	pcDNA3.1
RB 90	myc	**Ect2**	Ect2 S366D	human	pcDNA3.1
RB 91	myc	**Ect2**	Ect2 S685D	human	pcDNA3.1
RB 92	myc	**Ect2**	Ect2 S811D	human	pcDNA3.1
RB 93	Flag	**Ect2 WT**	Ect2	human	pcDNA3.1/Flag-C
RB 94	HA	**Ect2 WT**	Ect2	human	pcDNA3.1/HA-C
RB 95	GFP	**Ect2**	Ect2 T815A	human	pEGFP-T7/C1
RB 96	GFP	**Ect2**	Ect2 T815D	human	pEGFP-T7/C1
RB 97	GFP	**Ect2**	Ect2 S20A	human	pEGFP-T7/C1
RB 98	GFP	**Ect2**	Ect2 S336A	human	pEGFP-T7/C1
RB 99	GFP	**Ect2**	Ect2 S366A	human	pEGFP-T7/C1
RB100	myc	**Ect2**	Ect2 1-333 S20A	human	pcDNA 3.1
RB101	myc	**Ect2**	Ect2 1-333 S40A	human	pcDNA 3.1
RB102	myc	**Ect2**	Ect2 1-333 S20D	human	pcDNA 3.1
RB103	myc	**Ect2**	Ect2 1-333 S40D	human	pcDNA 3.1
RB104	myc	**Ect2**	Ect2 1-333 S20A S40A	human	pcDNA 3.1

RB105	myc **Ect2**	Ect2 1-333 S20D S40D	human	pcDNA 3.1
RB106	YFP	3X-SV40NLS	SV40virus	pEYFP-Nuc
RB107	myc **Ect2**	3XSV40-NLS-Ect2 1-333	human	pcDNA 3.1
RB108	myc	3XSV40-NLS	SV40virus	pcDNA 3.1
RB109	myc **Ect2**	Ect2 KRR→NQQ	human	pcDNA 3.1
RB110	myc **Ect2**	Ect2 RKR→QNQ	human	pcDNA 3.1
RB111	myc **Ect2**	Ect2 KRR→NQQ,RKR→QNQ	human	pcDNA 3.1
RB112	AD **Ect2**	Ect2 1-333	human	pGAD-c(1)
RB113	BD **Ect2**	Ect2 1-333	human	pGBDΩ-C(1)
RB114	HA-C **Ect2**	Ect2 1-333	human	pcDNA3.1/HA-C
RB115	HA-C **Ect2**	Ect2 1-360	human	pcDNA3.1/HA-C
RB116	Flag-C **Ect2**	Ect2 1-333	human	pcDNA3.1/Flag-C
RB117	Flag-C **Ect2**	Ect2 1-360	human	pcDNA3.1/Flag-C
RB118	myc **Ect2**	Ect2 1-333	human	pcDNA4/TO
RB119	myc **Ect2**	Ect2 1-360	human	pcDNA4/TO
RB120	myc **Ect2**	Ect2 336-883	human	pcDNA 3.1
RB121	myc **Ect2**	Ect2 355-883	human	pcDNA 3.1
RB122	Flag-C **Ect2**	Ect2 414-883	human	pcDNA3.1/Flag-C
RB123	myc **Ect2**	Ect2 414-630	human	pcDNA 3.1
RB124	myc **Ect2**	Ect2 753-883	human	pcDNA 3.1
RB125	myc **Cyk4**	Full length Human Cyk4 (MgcRacGap)	human	pcDNA3.1
RB126	GFP **Cyk4**	Full length Human Cyk4 (MgcRacGap)	human	
RB127	myc **Ect2**	Ect2 S20A,S366A,S685A,S811A	human	pcDNA 3.1
RB128	myc **Ect2**	Ect2 S20A,S336A,S366A,S685A,S811A	human	pcDNA 3.1
RB129	myc **Ect2**	Ect2 S685D,S811D	human	pcDNA 3.1
RB130	myc **Ect2**	Ect2 S20D,S40D	human	pcDNA 3.1
RB131	myc **Ect2**	Ect2 S20D,S40D,S685D,S811D	human	pcDNA 3.1
RB132	myc **Ect2**	Ect2 S336D,S366D	human	pcDNA 3.1
RB133	myc **Ect2**	Ect2 S20D,S40D,S336D,S366D,S685D,S811D	human	pcDNA 3.1
RB134	myc **Ect2**	Ect21-388 KRR→NQQ,RKR→QNQ	human	pcDNA 3.1
RB135	myc **Ect2**	Ect21-477 KRR→NQQ,RKR→QNQ	human	pcDNA 3.1
RB136	myc **Ect2**	Ect21-569 KRR→NQQ,RKR→QNQ	human	pcDNA 3.1
RB137	myc **Ect2**	Ect2 414-883	human	pcDNA 3.1
RB138	HA-C **Ect2**	Ect2 414-883	human	pcDNA3.1/HA-C
RB139	Flag-C **Ect2**	Ect2 414-630	human	pcDNA3.1/Flag-C
RB140	HA-C **Ect2**	Ect2 414-630	human	pcDNA3.1/HA-C

RB141	Flag-A	**Cyk4**	Human Cyk4	human	pcDNA3.1/Flag-A
RB142	myc-c	**Ect2**	Ect2 1-370	human	pcDNA3.1
RB143	myc-c	**Ect2**	Ect2 1-370 KRR→NQQ	human	pcDNA3.1
RB144	myc-c	**Ect2**	Ect2 5S→5A,KRR→NQQ	human	pcDNA3.1
RB145	myc-c	**Ect2**	Ect2 1-370 S366A	human	pcDNA3.1
RB146	myc-c	**Ect2**	Ect2 1-370 S366D	human	pcDNA3.1
RB147	myc-c	**Ect2**	Ect2 41-333	human	pcDNA3.1
RB148	myc-c	**Ect2**	Ect2 320-370	human	pcDNA3.1
RB149	myc-c	**Ect2**	Ect2 320-388	human	pcDNA3.1
RB150	GFP	**Ect2**	Ect2 1-333	human	pEGFP-T7/C1
RB151	myc-c	**Ect2**	Ect2 1-333 K195A	human	pcDNA3.1
RB152	His	**Ect2**	Ect2 1-333	human	pQE30
RB153	GST	**Ect2**	Ect2 1-333	human	pGEX-6P-3
RB154	GST	**Ect2**	Ect2 1-333 K195A	human	pGEX-6P-3
RB155		**Ect2**	3x-myc-Ect2 1-333 K195A	human	pcDNA4/TO
RB156	GFP	**Ect2**	Ect2 1-333 K195A	human	pEGFP-T7/C1
RB157	AD	**Ect2**	Ect2 414-883	human	pGAD-C1
RB158	AD	**Ect2**	Ect2 414-630	human	pGAD-C1
RB159	BD	**Human Cyk4**	Human Cyk4	human	pGBD omega C1
RB160	myc	**Ect2**	Nterm 1-333+peptide	human	pcDNA3.1
RB161	myc	**Ect2**	Full length	human	pcDNA3.1
RB162	myc	**Ect2**	Nterm 1-333 T153A,K195A	human	pcDNA3.1
RB163	myc	**Ect2**	Ect2 5S →5A	human	pcDNA3.1
RB164	myc	**Ect2**	Ect2 6S →6D	human	pcDNA3.1
RB166	myc	**Ect2**	Ect2 7S→7A	human	pcDNA3.1
RB167	myc	**Ect2**	Ect2 8S→8D	human	pcDNA3.1
RB168	myc	**Ect2**	Ect2 1-420	human	pcDNA3.1
RB169	myc	**Ect2**	Ect2 2S→2D	human	pcDNA3.1
RB170	BD	**Ect2**	Ect2 414-883	human	pGBDΩ-C1
RB171	myc	**Ect2**	N-term 1-333 T153A,K195A,Q192A	human	pcDNA3.1
RB172	myc	**Ect2**	Nterm 1-333 T153A,K195A,V281F	human	pcDNA3.1
RB173	Flag-c	**Ect2**	Nterm 1-333 T153A,K195A	human	pcDNA3.1/Flag-c
RB174	Flag-c	**Ect2**	Nterm 1-333 T153A,K195A,Q192A	human	pcDNA3.1/Flag-c
RB175	Flag-c	**Ect2**	Nterm 1-333 T153A,K195A,V281F	human	pcDNA3.1/Flag-c
RB176	GST	**Ect2**	Ect2 1-333 T153A,K195A	human	pGEX-6P-3

RB 177	GST	**Ect2**	Ect2 1-333 T153A,K195A,Q192A	human	pGEX-6P-3
RB178	GST	**Ect2**	Ect2 1-333 T153A,K195A,V192F	human	pGEX-6P-3
RB179	GST	**Ect2**	Ect2 414-630	human	pGEX-6P-3
RB180	His	**Ect2**	Ect2 1-333 T153A,K195A	human	pQE-30
RB181	GFP	**Ect2**	Ect2 1-333 T153A,K195A	human	pEGFP-t7/C1
RB182	GFP	**Actin**	Actin	human	pAcGFP1
RB183	myc	**Ect2**	Ect2 320-883	human	pcDNA3.1
RB184	myc-HisA	**MKlp1**	Full length	human	pcDNA4/TO/myc
RB185	myc	**Ect2**	Ect2 all Alanine mutant+siRNA	human	pcDNA3.1/3x
RB186	myc	**Ect2**	Ect2 1-333 T328A	human	pcDNA3.1
RB187	myc	**RhoA**	wildtype	human	pRK5myc
RB188	myc	**Rac1**	wildtype	human	pRK5myc
RB189	myc	**Cdc42**	wildtype	human	pRK5myc
RB190	myc	**N19RhoA**	Dominant negative	human	pRK5myc
RB191	myc	**N17Rac1**	Dominant negative	human	pRK5myc
RB192	myc	**N17Cdc42**	Dominant negative	human	pRK5myc
RB193	myc	**MKlp2**	Dominant negative	human	pcDNA3.1/myc

Resume

Name: Ravindra B. Chalamalasetty

Corresponding address:

Ravindra Babu Chalamalasetty

Dept of Cell Biology,

C/o Prof. Dr. Erich Nigg,

Max Planck Institute for Biochemistry,

Am Klopferspitz 18a,

Martinsried, D-82152,

Munich.

Tel: +49 89 8578 3113

Fax: +49 89 8578 3102

Mobile: 0049 17629836795

Lab home page: http://www.biochem.mpg.de/nigg/sillje/sillje_home.html

E-mail: ravindra@biochem.mpg.de

ravindrababu100@gmail.com

Personal:

Indian, Male, Unmarried, 27 years (DOB: 13 May 1978)

Languages known:

Could communicate in English very well.

Education:

PhD thesis (From Aug 2002 onwards-) at the Department of Cell Biology, Max Planck Institute for Biochemistry, Munich.

Project assistant (Aug 2001-June 2002)

I was pursuing as a project assistant for one year in Prof. Raghavan Varadarajan's lab at the Indian Institute of Scineces, Bangalore, India.

Masters degree (Aug1999-may2001):

Completed Master of Science in Biotechnology at the Madurai Kamaraj University, India in April 2001. I scored 76.4% in my master's degree.

Under graduation (1996-1999):

Bachelor of Science in Biochemistry, Microbiology, Aquaculture from

P. B. Siddhartha College of Arts and Science, Nagarjuna University, India. I scored 85% in my under graduation.

Honours, Scholarships, Ranks and Prizes:

1) In **class X**, I was ranked 2nd and received Rs. 300/- as prize money.

2) For **Intermediate course (1993-1995)**, I was selected for the Andhra Pradesh Residential Junior College, Nagarjuna Sagar, India through the entrance test conducted by the Andhra Pradesh State Government.

3) I was selected to the **MSc Biotechnology** course by All India Entrance (Rank-36) conducted by the Jawaharlal Nehru University affiliated to 20 other universities all over India. Receiving a monthly studentship of Rs.400/-, this studentship is established and maintained by the Department of Biotechnology (DBT), Government of India.

4) Apart from this, I was also selected for following universities for the Master's degree program. The selection process is based on competitive written exams.
   Jawaharlal Nehru University, New Delhi in Life Sciences,
   Hyderabad Central University -3rd rank *in Biochemistry,*
   Andhra University, Vizag - 1st *in Biochemistry,*
   Nagarjuna University, Vijayawada - 3rd *in Microbiology.*

5) In **GATE 2001** exam (Graduate Aptitude Test in Engineering), I scored 94% percentile in biological sciences exam. This is an All India entrance exam conducted to assess the knowledge of students for further studies like PhD's and M.Tech (Master of Technology) courses.

6) **JRF-CSIR fellowship MAY-2001**.

I was selected for the award, which would include a package of approximately 50,000 rupees (as of 2001) as a yearly grant for a period of 5 years for pursuing Ph.D. in India. The Universities Grant Commission, India (UGC) and the Council of Scientific and Industrial research (CSIR) are the key agencies to fund the Ph.D. students in India. The students for the award of fellowships are selected by a highly competitive National Eligibility Test (NET) examination. This examination is held twice during the year for selection for the award of Junior Research Fellowships (JRF). Nearly 50,000 applications are received annually for the two NET examinations of which nearly 30,000 candidates take the examination and a total of 1,000 are normally selected for the grant of fellowship both from CSIR and UGC. I was among top 20% of the candidates qualified for Junior Research Fellow under CSIR in the year Dec 2000.

But, as I had the opportunity to pursue my PhD studies at Max Planck Institute for Biochemistry in the Department of Cell Biology, I came over here to be part of wonderful international scientific atmosphere in the department of Prof. Erich Nigg.

Publications:

1. Chalamalasetty RB, Hummer S, Nigg EA, Sillje HH

Interference with Ect2 function blocks cytokinesis by impairing both cleavage furrow formation and abscission (Submitted to Journal of cell science)

2. Gruneberg U, Neef R, Li X, Chan EH, Chalamalasetty RB, Nigg EA, Barr FA.

Kif14 and citron kinase act together to promote efficient cytokinesis. *J Cell Biol. 2006, Jan 30; 172 (3): 363-372.*

3. Chan EH, Nousiainen M, Chalamalasetty RB, Schafer A, Nigg EA, Sillje HH.

Ste20-like kinase Mst2 activates the human large tumor suppressor kinase Lats1. *Oncogene. 2005 Mar 17; 24 (12):2076-86.*

From Indian Institute of Science:

4. Chakshusmathi G, Mondal K, Lakshmi GS, Singh G, Roy A, Ch RB, Madhusudhanan S, Varadarajan R.

Design of temperature-sensitive mutants solely from amino acid sequence. *Proc Natl Acad Sci U S A. 2004 May 25;101 (21):7925-30*

References:

1. **Prof.Erich A.Nigg,**
   Department of Cell Biology,
   Max Planck Institute for Biochemistry,
   Am klopferspitz 18a,
   Martinsried,
   Munich.

2. **Dr.Herman Sillje,**
   Department of Cell Biology,
   Max Planck Institute for Biochemistry,
   Am klopferspitz 18a,
   Martinsried,
   Munich.